UNIVERSITY OF OKLAHOMA

GRADUATE COLLEGE

APPLICATION OF IN SITU CO_2 ENHANCED OIL RECOVERY IN LIQUID-RICH SHALE AND LOW-TEMPERATURE RESERVOIRS

A DISSERTATION

SUBMITTED TO THE GRADUATE FACULTY

in partial fulfillment of the requirements for the

Degree of

DOCTOR OF PHILOSOPHY

By

ONYEKACHI OGBONNAYA

Norman, Oklahoma

2023

APPLICATION OF IN-SITU CO_2 ENHANCED OIL RECOVERY IN LIQUID-RICH SHALE AND LOW-TEMPERATURE RESERVOIRS

A DISSERTATION APPROVED FOR THE

MEWBOURNE SCHOOL OF PETROLEUM AND GEOLOGICAL ENGINEERING

BY THE COMMITTEE CONSISTING OF

Dr. Bor-Jier (Ben) Shiau, Chair

Dr. Jeffrey H. Harwell

Dr. Reza Foudazi

Dr. Chandra Rai

Dr. Rouzbeh Moghanloo

Acknowledgements

I would like to express my heartfelt gratitude to my advisors Dr Bor-Jier (Ben) Shiau and Dr Jeffrey H. Harwell for their unwavering support, invaluable guidance and constant encouragement throughout my PhD journey. Under their mentorship, my knowledge in the field of surfactants and enhanced oil recovery has greatly expanded. I would not have accomplished this study without their invaluable advice and constructive criticism.

I extend my sincere appreciation to the members of my committee, Dr Chandra Rai, Dr Reza Foudazi, and Dr Rouzbeh Moghanloo, for generously sharing their time and offering insightful suggestions during the course of this dissertation. Special gratitude goes to Dr Rai for graciously allowing me to utilize equipment in the IC3 lab for some of my experiments.

I deeply appreciate the help from the team at the Applied Surfactant Laboratory at OU especially Dr Michael Warren, Dr Shuoshi Wang, Dr Changlong Chen, Dr Parichat Phaodee, Na Yuan, Heba Aladwani and Dr Sangho Bang, for their invaluable contributions, scientific discussions, and guidance. I also appreciate the support and knowledge-sharing from the IC3 team, including Dr Ali Tinni, Dr Son Dang, Sidi Mamoudou, Felipe Cruz and Micaela Langevin. Additionally, I am grateful to Dr Mashhad Fahes for her encouragement and for letting me use the equipment in her lab.

Special thanks to the faculty and staff of the Mewbourne School of Petroleum and Geological Engineering, especially Gary Stowe, Sonya Grant, Katie Shapiro and Danika Hines-Barnett for their kindness and willingness to help.

None of this work would have been possible without the unconditional love, prayers and relentless support of my beloved wife, Adaeze, as well as my parents Iroakazi and Comfort Ogbonnaya and the rest of my family and friends. Also, thank you to Lisa, Jorge and Gio Morales for making my time at the University of Oklahoma excitingly memorable.

Above all, I thank God for His love and countless blessings in my life.

Table of Contents

List of Tables

List of Figures

Abstract

The injection of CO_2 presents significant potential for enhancing oil production while minimizing environmental impact by storing CO_2 within the oil reservoir. However, the realization of this potential is hindered by factors such as limited inexpensive CO_2 sources, lack of infrastructure for CO_2 transportation, early gas breakthrough, gravity segregation, viscous fingering, low solubility of CO_2 in water, and asphaltene deposition, among others. To address these challenges, alternative methods to deliver CO_2 to the target oil reservoir through in-situ generation of CO_2 are explored. Specifically, we used aqueous solutions of urea as the CO_2 gas generating agent due to its low cost, availability, ease of handling, high solubility in aqueous solutions, tolerance to high salinity conditions and high yield of CO_2.

This dissertation comprises of two major topics. The first topic focused on the development of effective in-situ CO_2 enhanced oil recovery (ICE) formulations for liquid-rich shale reservoirs while the second topic focused on the application of ICE in low-temperature reservoirs. The first study was conducted in two phases. In the first phase we used dodecane as the oil phase, while crude oil was used in the second phase. We study the synergistic effects of coupling urea with a thermally stable anionic surfactant to further improve oil recovery performance from low-permeability shale formations. We designed the oil recovery experimental procedures to simulate the huff-n-puff technique. Imbibition tests were carried out with oil-saturated Woodford outcrop shale cores for different soaking periods. To assess recovery performance and mechanisms, tests were conducted with four different formulations: brine only, urea in brine, thermostable anionic surfactant in brine, and a blend of urea and surfactant in brine. Surfactant stability at the test temperature was investigated. Furthermore, interfacial tension (IFT) and

wettability alteration tests were conducted to understand their effect on total recovery. In addition, the oil recovery experiments were tested at below and above MMP conditions to help decipher the principal recovery mechanism. Results revealed that the selected enhanced oil recovery (EOR) recipes are stable at reservoir conditions and compatible with the oil samples. There was no significant difference in oil recovery when the test pressure was below or above MMP, which suggests that the oil recovery process involved immiscible CO_2 mechanism. Furthermore, we observed that both IFT reduction and wettability alteration play critical roles in improving oil recovery. For the tests performed with dodecane-saturated shale cores, combining the surfactant with urea did not have any synergistic benefits. This was attributed to the strong water wetness of the dodecane-saturated shale core samples. Moreover, the urea-only case could recover up to 24% of the original oil in place (OOIP) compared to about 6% for the brine-only case, 21% for the surfactant-only case and 22% for the ternary urea/surfactant/brine mixture. For the tests performed with crude oil-saturated shale cores, aging the shale cores in crude oil changed the wettability of the cores from water-wet to oil-wet. We observed a favorable synergistic effect when we combined the surfactant with urea, leading to higher oil recovery after a 14-day soaking period. The oil recovered in the case of 14-days soaking time for the brine only, binary brine/urea, binary brine/surfactant, and ternary urea/surfactant/brine mixture was 7%, 9%, 5%, and 18% of the OOIP, respectively.

The second topic of this research focused on the application of ICE in low-temperature reservoirs. We used a naturally occurring enzyme (urease) to catalyze the generation of in-situ CO_2 under low-temperature reservoir conditions. This study was conducted in two phases. The first phase was conducted with highly purified commercially available urease and deionized (DI) water was

used as the aqueous phase, while the second phase was conducted with crude urease extracts from jack beans and artificial sea water (ASW) was used as the aqueous phase. We conducted batch tests to study the kinetics of the urease-catalyzed hydrolysis of urea at different temperatures and concentrations of urea and urease. Adsorption tests were conducted to study the adsorption of the enzyme on porous media. The extent of wettability alteration and the recovery mechanism for different lithologies was determined through core sample imbibition experiments and contact angle measurements. One-dimensional sand pack flowthrough experiments were conducted with different lithologies at 50 °C in the first phase and at 50 and 70 °C in the second phase, to evaluate the tertiary oil recovery potential of low-temperature ICE using the modified formulations. From the experimental results, urease-catalyzed urea hydrolysis is proven to be effective in generating CO_2 at the test temperatures with urea conversion rate of up to 95 % at 50 °C for the crude urease extracts. The adsorption tests show that urease was significantly adsorbed on limestone surfaces while the adsorption on sandstone was insignificant. Imbibition tests of this improved formulation with various porous media show distinct wettability reversal trends towards a more water-wet state post-imbibition. For the tests with highly purified urease and DI water, the tertiary oil recovery was up to 31.3 % for sandstone at 50 °C. Meanwhile, for the tests with jack bean extracts and ASW, the tertiary oil recovery was up to 28.0 % for limestone at 50 °C. These results were better than the corresponding high temperature (120 °C) cases. Moreover, the tertiary oil recovery for the limestone and sandstone tests were lower at 70 °C compared to 50 °C. This was attributed to the higher solubility of CO_2 in oil at lower temperatures. Overall, the simplicity of the technique used to produce the crude urease extract

from jack beans will significantly reduce the cost of enzyme-catalyzed low-temperature ICE, thus overcoming a major barrier and enabling practical applications in the oilfield.

Chapter 1 Overview

The global demand for energy is forecast to grow as the world population increases and liquid fuels including petroleum and biofuels will remain the largest source of energy, according to the Energy Information Administration's Reference case projection [1]. Based on the projections from *Figure 1-1*, petroleum and biofuels will contribute about 28 % of global energy consumption by 2050 while renewables will contribute about 27 %. Moreover, the global consumption of petroleum liquids and biofuels will increase from 182 quadrillion Btus in 2020 to 249 quadrillion Btus in 2050, an increase of about 37 %.

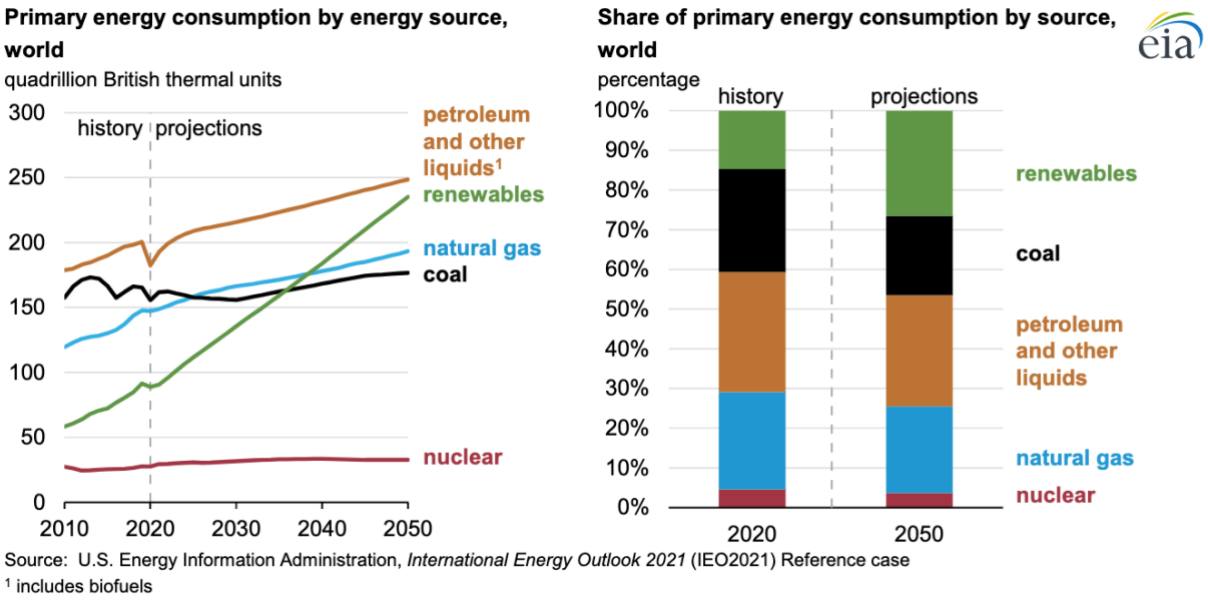

Figure 1-1 World primary energy consumption and share of primary energy consumption by source (from [1])

EOR will play a crucial role in meeting the future demand for oil and gas. The demand for EOR is expected to grow due to an increasing number of aged wells and declining production from existing oilfields. *Figure 1-2* shows the International Energy Agency's (IEA) projected global oil

production from EOR. According to the projections by the IEA, global oil production from EOR will increase by about 120 % from 2015 to 2040 [2]. Additionally, the contribution of CO_2 EOR to the total oil production from EOR is projected to grow from 21 % in 2015 to 35 % in 2040.

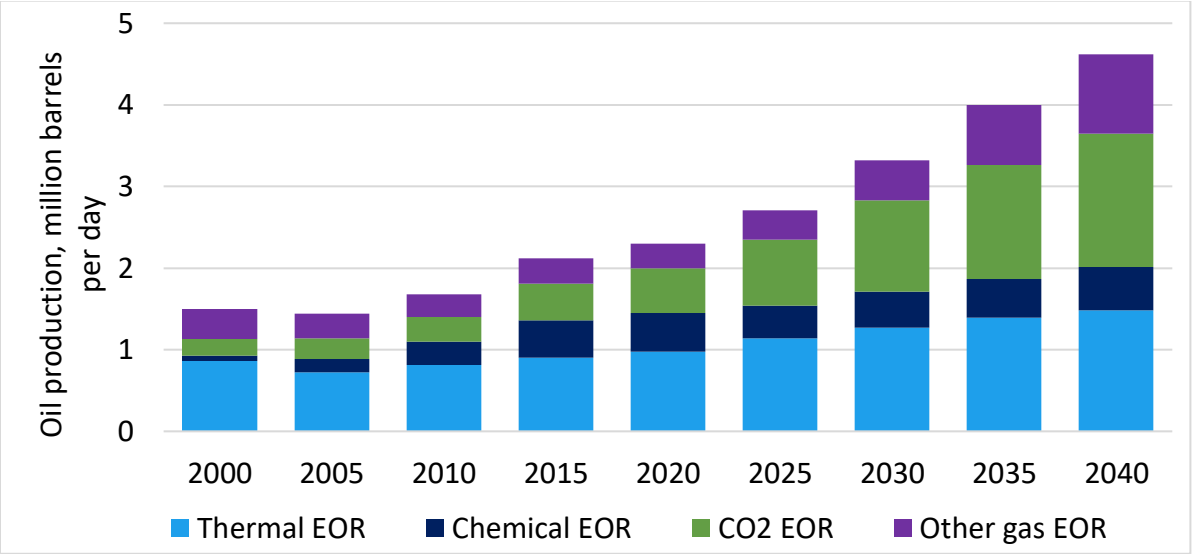

Figure 1-2 Global EOR oil production in the International Energy Agency's New Policies Scenario (adapted from *[2]*)

Figure 1-3 shows the regional mean estimates by the US Geological Survey of the oil volumes that are technically recoverable and the amount of CO_2 that will remain in the reservoir with the application of miscible CO_2 EOR in over 3500 conventional reservoir candidates in the US *[3]*. The results show that an average of 29,000 million barrels (MMbbl) of oil could be technically recoverable from the screened reservoirs. This is equivalent to about 6.7 years of crude oil production at 2022 average US crude oil production rates *[4]*. The results also show that an average of 8400 million metric tons (Mt) of CO_2 could be retained in the screened reservoirs as a result of CO_2 EOR. This represents about 1.3 times the total US greenhouse gas emissions in 2021 *[5]*. The West Texas and Eastern New Mexico regions, which are primarily represented by the Permian Basin, and the Gulf Coast region together account for 60 % of the mean assessed crude

oil production from CO_2 EOR and 61 % of the mean assessed CO_2 geological sequestration in the US. These estimates apply only to the application of miscible CO_2 EOR in conventional reservoirs and does not account for the application of CO_2 EOR in unconventional reservoirs or the use of immiscible CO_2 EOR in both conventional and unconventional reservoirs. Therefore, there is a significant potential to both increase the production of crude oil and sequestrate anthropogenic CO_2 using CO_2 EOR.

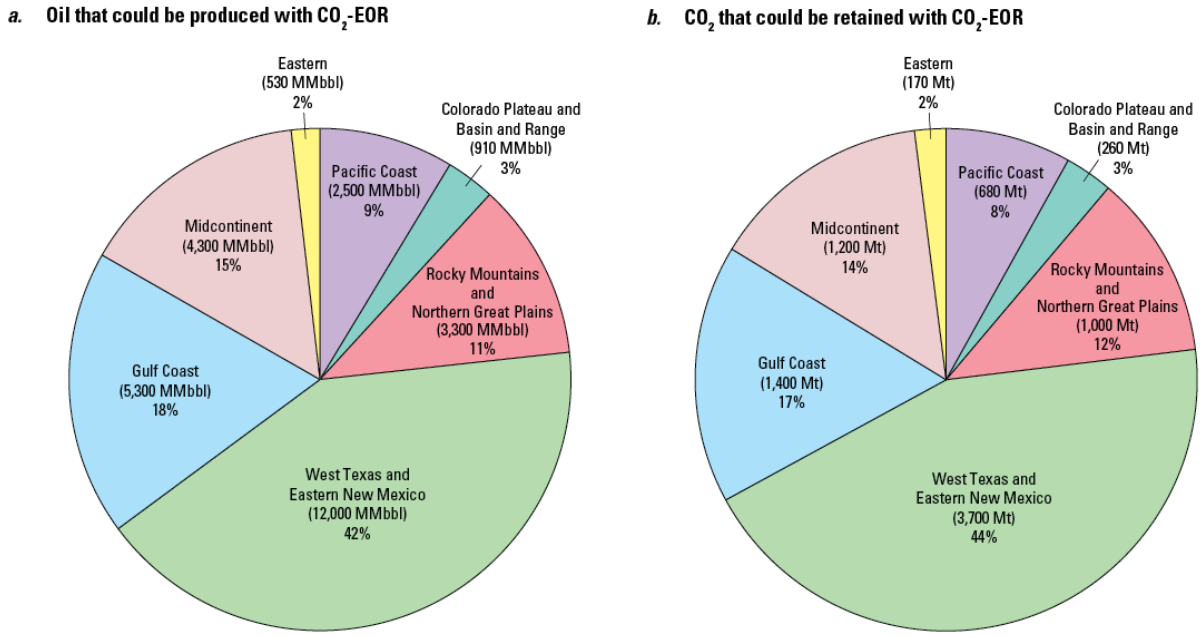

Figure 1-3 Regional mean estimates by the U.S. Geological Survey in 2020 of (a) volumes of oil that could be technically recoverable with CO_2 EOR and (b) amount of CO_2 that could be geologically sequestered with the application of miscible CO_2 EOR in conventional reservoirs (from *[3]*)

1.1 *In situ* CO_2 EOR

In situ CO_2 EOR (ICE) relates to the injection of a slug of fluid containing reactants capable of forming carbon dioxide inside the oil reservoir. Subsequently, the oil in the reservoir is displaced and recovered with the aid of a drive fluid such as waterflooding, if necessary. The use of ICE

overcomes some of the challenges associated with conventional CO_2 EOR including limited natural sources of CO_2, inadequate CO_2 transportation infrastructure such as pipelines, the requirement of special equipment both above and below ground in order to mix, blend and pump the CO_2 with carrier fluids (if required), viscous fingering and gravity segregation of CO_2 gas, asphaltene deposition near the wellbore and early gas breakthrough [6]. In this work, we used aqueous solutions of urea as the CO_2 generating agent in ICE due to its low cost, availability, ease of handling, high solubility in aqueous solutions, tolerance to high salinity conditions and high yield of CO_2.

1.2 Overview of Chapters

The goals of this dissertation are to experimentally investigate the application of in-situ CO_2 EOR in liquid-rich shale reservoirs and low-temperature reservoirs. The following are the main objectives of this dissertation:

1. Investigate the use of in-situ CO_2 EOR in liquid-rich shale reservoirs and establish proof of concept and fundamental oil recovery mechanisms (Chapters 2 and 3).

2. Investigate the use of in-situ CO_2 EOR in low-temperature reservoirs and expand the range of reservoir temperatures where the ICE system can be applied (Chapters 4 and 5).

Chapter 2 focuses on the development of effective ICE formulations for liquid-rich shale reservoirs. We used a simple alkane (dodecane) as the oil phase and urea as the gas-generating agent to investigate the applicability of ICE in liquid-rich shale reservoirs. Due to the extremely low permeability of shale, we combined the gas-generating agent with a thermally stable anionic surfactant to facilitate the imbibition of the ICE formulation into the shale matrix and enhance

the EOR performance of the formulation. We investigated the compatibility of the EOR formulations with dodecane and their stability at high temperature conditions. We also investigated the different mechanisms involved in the EOR process including wettability alteration and IFT reduction. The work from this chapter was presented at the 2020 Society of Petroleum Engineers (SPE) Improved Oil Recovery conference.

In Chapter 3 we further investigate the application of ICE in liquid-rich shale reservoirs. In this chapter, we used crude oil instead of dodecane as the oil phase to investigate the applicability of ICE in liquid-rich shale reservoirs. Combining site-specific crude oil samples and the shale cores, allows us to characterize and quantify the performance of the improved formulations for EOR under more realistic tight reservoir conditions and the various mechanisms involved in the EOR process. This chapter has been submitted to the journal, Fuel for peer review and publication.

In Chapter 4, we investigate the application of ICE in low-temperature oil reservoirs. The rate of spontaneous decomposition of aqueous solutions of urea to release CO_2 and ammonia at temperatures below 80 °C is not high enough for EOR applications. We used an enzyme, urease, to accelerate the hydrolysis of aqueous solutions of urea at low temperature conditions. We evaluated the kinetics of urease-catalyzed urea hydrolysis at different temperatures, urea concentrations and urease concentrations. Tertiary oil recovery sandpack flowthrough tests were also performed to evaluate the oil recovery potential of the urease-catalyzed ICE. We used highly purified commercially available urease and deionized water in these tests to establish proof of concept. This chapter has been published in the peer review journal, Fuel.

In Chapter 5, we further investigate the application of ICE in low-temperature oil reservoirs. We used crude urease extracts from jack bean, instead of the highly purified commercial urease used

in the last chapter. The goal of this approach was to develop a cheaper source of urease enzyme in order to improve the economic viability of urease catalyzed low-temperature ICE applications. The crude urease extracts were evaluated for urease activity, urea hydrolysis kinetics and urease adsorption on porous media. Tertiary oil recovery sandpack flowthrough tests were also carried out to evaluate the oil recovery potential of ICE with urease extracts. Moreover, the urease plus urea solutions used in the tests were prepared in artificial sea water (ASW), to replicate more realistic oil field conditions and evaluate the impact of high ionic strength and the presence of divalent ions on the low-temperature ICE system.

Chapter 6 summarizes the main findings of this research and suggests ideas for potential future research.

References

[1] International Energy Outlook Consumption - 2021 - U.S. Energy Information Administration (EIA) n.d. https://www.eia.gov/outlooks/ieo/narrative/consumption/sub-topic-01.php (accessed August 12, 2023).

[2] EOR production in the New Policies Scenario, 2000-2040 – Charts – Data & Statistics. IEA 2018. https://www.iea.org/data-and-statistics/charts/eor-production-in-the-new-policies-scenario-2000-2040 (accessed August 14, 2023).

[3] Warwick PD, Attanasi ED, Blondes MS, Brennan ST, Buursink ML, Cahan SM, et al. Assessment of carbon dioxide enhanced oil recovery and associated carbon dioxide retention resources of the United States 2022.

[4] U.S. crude oil production will increase to new records in 2023 and 2024 n.d. https://www.eia.gov/todayinenergy/detail.php?id=55299 (accessed August 17, 2023).

[5] US EPA O. Inventory of U.S. Greenhouse Gas Emissions and Sinks 2017. https://www.epa.gov/ghgemissions/inventory-us-greenhouse-gas-emissions-and-sinks (accessed August 17, 2023).

[6] Raifsnider PJ, Raifsnider DE. In-situ formed CO2 drive for oil recovery. United States patent US3532165A, 1970.

Chapter 2 Use of In Situ CO_2 Generation in Liquid-Rich Shale

Abstract

Modified *in situ* CO_2 generation was explored as an improved tool to deliver CO_2 indirectly to the target liquid-rich shale formations. Once injected, the special CO_2-generating compound, urea, decomposes deep in the fractures at elevated temperature conditions and releases significant amounts of CO_2. For field implementation, the minimum surface facility is required other than simple water injection equipment. Injection of urea solution may be easier and cheaper than most gas injection approaches.

In this work, *in situ* CO_2 treatment and designs were carried out on a group of Woodford shale core samples. The oil-saturated shale cores were soaked in different urea solutions kept in pressurized (1500 and 4000 psi) and heated extraction vessels at a temperature of 121 °C. The adopted treatment method closely simulates the huff-and-puff technique. A series of experiments were run with different formulations, including brine only, brine plus surfactant, brine plus urea and a ternary mixture of brine/surfactant/urea. In addition, the extraction experiments were tested at below and above MMP conditions to decipher the principal recovery mechanism.

Based on our preliminary observations, the sample cores did not lose their stability after an extended period of oil extraction with *in situ* CO_2 treatment. The urea-only case recovered up to 24% of the OOIP compared to about 6% for the brine-only case and 21% for the surfactant-only case. Also adding a pre-selected surfactant to the urea slug did not have any benefit. There was no significant difference in oil recovery when the test pressure was below or above MMP. The

main recovery mechanisms were oil swelling, viscosity reduction, low interfacial tension and wettability alteration in this effort.

Multiple researchers reported successful lab-scale CO_2 gas extraction EOR experiments for liquid-rich shale like the upper, middle and lower Bakken reservoir. The best scenario could recover 90% of the OOIP from the shale core samples. The results of this work offer a strong proof of concept of *in situ* CO_2 generation potential for liquid-rich shale reservoirs.

2.1 Introduction

The application of horizontal drilling and hydraulic fracturing has helped unlock the immense amount of oil and gas in shale and other tight formations. However, the production from these very low permeability formations declines sharply after the first couple of years. This necessitates the use of enhanced oil recovery (EOR) techniques to help boost the production and estimated ultimate recovery (EUR) from these wells. Some of the techniques that have been studied and trialed in the field include gas injection, water injection and surfactant injection [1]. Gas injection for EOR application in unconventional reservoirs can be in the form of gas flooding and huff-n-puff. The commonly used injection gases are nitrogen, CO_2, methane, ethane, and mixtures of methane/ethane. Several simulation, experimental and field studies have been performed to examine the oil recovery performance of gas injection [2–7]. Lashgari et al. [5] conducted a field scale numerical simulation of CO_2 and enriched natural gas injection in shale reservoirs and concluded that gas diffusion is crucial in oil production. Water injection for EOR application in shale reservoirs can be either in the form of water flooding or water huff-n-puff. The main concerns about water flooding in ultralow permeability shale reservoirs are water injectivity, low sweep efficiency and early water breakthrough. However, most of the field pilot tests conducted

so far do not appear to have injectivity issues [1]. The general mechanism for water huff-n-puff suggests that water preferentially invades the larger pores, imbibes into the smaller pores and displaces oil through a counter-current flow mechanism [1,8,9]. Another mechanism proposed by Sheng [1] is that the invaded and imbibed water increases the reservoir and local pressure, thereby boosting the drive energy. Generally, water-wet formations imbibe more water than oil-wet ones. Field applications of water flooding and water huff-n-puff for shale EOR are limited because they increase the oil recovery by about 2-3% above the primary depletion [1]. Surfactants can alter the wettability of shale from oil-wet to mixed wet or water-wet, thereby enhancing water imbibition. There has been numerous simulation and lab studies on surfactant imbibition EOR in shale . Another important mechanism of surfactant imbibition EOR is the reduction of aqueous phase trapping and formation damage in shale [12]. There have been few field trials of surfactant imbibition EOR in shale reservoirs. Kazempour et al. [13], carried out laboratory evaluation and a successful field trial of a surfactant blend designed to improve oil recovery by imbibition. Their results show that the EUR can be improved by up to 25% when a proper wettability-altering agent is injected into a shale reservoir. Bidhendi et al. [14] also developed a set of surfactant-based chemical formulations that were studied in the lab for their potential to alter the wettability of Wolfcamp cores and improve oil recovery. Their subsequent field trial showed a 39% increase in the 180-day cumulative oil recovery and increased oil cut.

CO_2 is widely used for EOR applications in conventional reservoirs and is increasingly being utilized in unconventional reservoirs. The US Department of Energy predicts that CO_2 EOR will help the US to tackle the dual challenges of energy independence and reduction of greenhouse emissions [15]. The three main ways this technology is currently applied in the field are CO_2 gas

flooding, carbonated water flooding and water alternating gas flooding (WAG). However, each of these methods has major drawbacks, that could hinder economical application in the field. For CO_2 gas flooding, the density and viscosity difference between CO_2 and oil leads to gravity segregation and viscous fingering, which reduces the sweep efficiency of the process. For WAG, the goal is to combine the benefits of gas injection and the mobility control provided by water injection [16]. The main drawbacks of WAG include early gas breakthroughs due to the channeling of gas through zones with high permeability and injectivity loss [16]. In CWI, sweep efficiency is enhanced when the dissolved CO_2 migrates to the oil phase leading to oil swelling, viscosity reduction and improved oil mobility [17]. Moreover, additional recovery drive energy can be obtained through the exsolution of CO_2 from the carbonated water. The solubility of CO_2 in water is a main determining factor in the efficiency of CWI EOR, since it determines the amount of CO_2 that can be delivered in the reservoir. Some researchers have used chemical promoters to increase the CO_2 / water ratio, however, this can substantially increase the cost of the project [18]. To overcome the challenges associated with CO_2 EOR, *in situ* CO_2 generation was proposed [19–26]. Most of these *in situ* CO_2 generating methods involve multiple streams of fluid injection including aluminium salt/carbamide/surfactant, sodium carbonate/acid/surfactant, ammonium carbamate/surfactant. The benefits of *in situ* CO_2 generation for EOR application include non-reliance on natural CO_2 sources and construction of CO_2 transportation pipeline, better sweep efficiency than CO_2 WAG, increased CO_2 GWR compared to CWI, simple and cost-effective, good tertiary recovery at both below and above minimum miscibility pressure conditions and excellent tolerance to salinity of reservoir brine [26]. Wang et al. [26], developed a method that uses urea as the *in situ* CO_2-generating agent. This system involves the injection of a single stream of urea

solution which hydrolyzes under reservoir temperature and pressure to produce CO_2 and ammonia according to the following two-step process:

$$NH_2CONH_2 + H_2O \rightarrow NH_2COONH_4 \quad (1)$$

$$NH_2COONH_4 \rightarrow 2NH_3 + CO_2 \quad (2)$$

CO_2 dissolves in oil resulting in a decrease in oil viscosity, oil swelling, reduction in the surface tension between oil and aqueous phases, re-pressurization of the formation and ultimately an increase in the oil production and sweep efficiency. The swelling factor (SF) is defined as the ratio of the volume of the CO_2 and oil mixture at reservoir temperature and pressure divided by the volume of the oil without CO_2 at the same temperature and atmospheric pressure [27].

$$SF = \frac{V_{CO_2+Oil}(P_R,T_R)}{V_{Oil}(P_{atm},T_R)} \quad (3)$$

where,

V_{CO_2+Oil} – volume of CO_2 + oil mixture

V_{Oil} – volume of oil

P_R – reservoir pressure

T_R – reservoir temperature

P_{atm} – atmospheric pressure

The swelling factor increases as the molecular weight of the crude oil decreases [28]. In their experiments, Simon and Graue [28] obtained crude oil swelling factors of up to 1.37 at 160°F and 2037 psia. Holm [29] stated that CO_2 can expand the crude oil volume by up to 60%. The oil swelling effect acts like an energy storage during the huff period and provides the driving force

in the puff period. The increase in oil volume due to the swelling leads to an increase in oil saturation and thus increase in oil relative permeability. The discontinuous oil droplets previously trapped in the pores gradually merge with the flowing oil phase as the oil swells [26].

The degree of viscosity reduction depends on the amount of dissolved CO_2, the initial viscosity of the oil and the reservoir temperature and pressure. Viscosity reduction will increase with the concentration of dissolved CO_2 in oil. Likewise, the higher the initial viscosity of the oil, the higher the degree of viscosity reduction. Moreover, viscosity reduction will be higher at lower temperatures, due to higher CO_2 solubility in oil [26]. Dissolved CO_2 can reduce the viscosity of the crude oil by 5 to 10-fold [29]. The degree of viscosity reduction and oil swelling is higher for the CW – hydrocarbon system compared to a similar system with pure CO_2 [30]. Emera and Sarma [27] developed correlations based on Genetic algorithm to predict the physical properties of the CO_2 – oil system including CO_2 solubility, oil swelling factor, CO_2 – oil density and viscosity, over a wide range of oil gravities, pressures up to 5000 psi, oil molecular weight > 490, oil viscosities up to 12,000 cP and temperatures up to 284 °F.

The ratio of the concentration of CO_2 in the oil phase ($C_{CO_2,O}$) to the concentration in the aqueous phase ($C_{CO_2,w}$) at equilibrium is referred to as the partition coefficient of CO_2 ($K_{CO_2,OW}$).

$$K_{CO_2,OW} = \frac{C_{CO_2,O}}{C_{CO_2,w}} \qquad (4)$$

It is a measure of the solubility of CO_2 in both immiscible phases, therefore it is dependent on both temperature and pressure. The partition coefficient of CO_2 decreases with pressure, implying that the solubility of CO_2 in water increases more than the solubility of CO_2 in oil, with increase in pressure. Conversely, the CO_2 partition coefficient increases with temperature.

Moreover, the change in partition coefficient with pressure is more significant at higher temperatures [17]. According to Altunina and Kuvshinov [31] the partition coefficient of CO_2 in the oil-water system in the temperature range of 35 – 100 °C and pressure range of 10 – 40 MPa is between 4 and 10, which implies that the concentration of CO_2 in the oil phase is 4 to 10 times the concentration of CO_2 in the aqueous phase.

The mass transfer of CO_2 from the aqueous phase to the oil phase is driven by the CO_2 concentration gradient in the hydrocarbon and the aqueous phases and also by the higher solubility of CO_2 in oil compared to the aqueous phase. Bagalkot and Hamouda [30] measured the diffusion coefficient of CO_2 in a CW – hydrocarbon system at different pressures ranging from 145 – 870 psi and temperature of 25 °C, using the axisymmetric pendant drop shape analysis (ADSA) method. The diffusion coefficient of CO_2 in the CW – decane system was determined to range from $0.0683 – 0.0169 \times 10^{-9}$ m^2 s^{-1}. The diffusion coefficient of CO_2 in brine is a function of temperature, pressure, salinity, salt composition and viscosity. The effective diffusivity will also depend on the porosity and tortuosity of the porous media [17,32]. The diffusion coefficient of CO_2 increases with temperature. The diffusion coefficient of CO_2 in water decreases with pressure, however this effect is quite small at temperatures below 120 °C [33].

Ammonia provides an added benefit to the system because it reacts with some of the components of crude oil to form *in situ* surfactants which can help to alter the wettability of the porous media from oil wet to intermediate wet or water wet [34]. Wang et al. [26] evaluated the tertiary oil recovery performance of urea using sandpack flooding at different conditions of flow rate, urea concentration, oil API, presence or absence of divalent ions and pressure ranging from below minimum miscibility pressure (MMP) to above MMP conditions.

All the applications of *in situ* CO_2 generation for EOR purposes in literature have been conducted with sandstone or carbonate reservoirs. In this study, we conduct a series of experiments designed to study the applicability of *in situ* CO_2 generation for EOR in liquid-rich shale formations. Tests were conducted with brine only, brine plus surfactant, brine plus urea and a ternary mixture of brine/surfactant/urea. Shale outcrops from the Woodford formation were used as the porous media and dodecane was used as the hydrocarbon fluid. First, we evaluated the compatibility of the surfactant with brine and urea solutions under the test conditions. Then we measured the interfacial tension (IFT) between the formulated fluids and dodecane at ambient and test temperature conditions, to quantify the change in IFT at different conditions and the relationship between the amount of recovered oil and IFT. We also quantified the wettability alteration potential for the different fluid formulations by contact angle measurements and related it to the amount of recovered oil. Lastly, soak tests designed to closely simulate the huff-n-puff technique were performed with oil-saturated shale core samples to determine the oil recovery potential of the different fluid formulations under reservoir temperature and pressure. The genetic algorithm-based correlations for predicting MMP, developed by Emera and Sarma [35] were used to calculate the MMP of dodecane and CO_2 at a reservoir temperature of 250°F. The calculated MMP value was 3200 psi, therefore tests were run at 1500 psi and 4000 psi to represent below MMP and above MMP reservoir conditions.

2.2 Materials

2.2.1 Porous media properties

We used cores from Woodford shale outcrop as the porous media for the experiments. The cores used were 1 inch in diameter and 2 inches long and were obtained from two blocks of outcrop shale to minimize rock property variations. Four cores were drilled from a 5-inch by 2-inch by 3-inch block (Outcrop A) and five cores were from a 15-inch by 15-inch by 5-inch (Outcrop B). The porosities of all the cores was measured using helium porosimeter and ranged from 5 to 7.5% for outcrop A and 5.5 to 7.6 for outcrop B. Further petrophysical properties analyses were carried out for outcrop B and are listed in Table *2-1*. FTIR analysis for outcrop B shows that the primary minerals are Dolomite (47.6 wt%), Quartz (15.6 wt%), Calcite (4.7 wt%) and clays including illite, kaolinite, chlorite and mixed clays (17.9 wt%). The total organic carbon content is 12.7 wt%, which is consistent with published data for the Woodford outcrop [36].

Table 2-1 Physical properties of Woodford core samples (Outcrop B) used in the experiments

Permeability, K_{N2} (micro darcy)		Porosity, Helium (%)	Average grain density (g/cm^3)	Total organic carbon (TOC), wt%
1500 psi effective pressure	4000 psi effective pressure			
0.057	0.043	5.5 to 7.6	2.5	12.7

2.2.2 Oil properties

Dodecane from Acros Organics was used as the oil for the experiments. At 68 °F and atmospheric pressure, the density and viscosity of dodecane are 0.749 g/mL and 1.468 cP respectively, while

at 121 °C, the values are 0.674 g/mL and 0.420 cP [37,38]. The interfacial tension for the dodecane water interface at atmospheric pressure and 68 °F is 52.87 mN/m [39].

2.2.3 Surfactant properties

The surfactant used for the experiments is a 12-carbon branched chain sodium diphenyl oxide disulfonate with an activity of 45.3 wt%. It is anionic and compatible with a broad range of high electrolyte solutions such as brine, acids and alkalis. The pH of the surfactant is 10.3 and the critical micelle concentration in 0.1M NaCl at 25 °C is 0.007 g/100g. The molecular structure of the surfactant is shown in Figure *2-1*

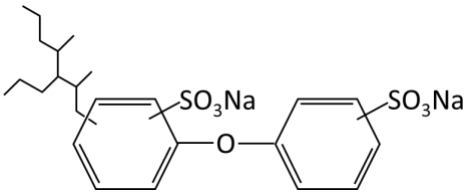

Figure 2-1 Molecular structure of surfactant used in the experiments

2.2.4 Other materials

High-purity urea (99 wt%) was purchased from Acros Organics. Urea is highly soluble in water, up to 50 wt% at 68 °F [40]. Potassium chloride (99 wt%) was purchased from Sigma-Aldrich.

2.3 Methodology

The workflow for the experiments can be categorized into the following steps:

1. Determination of the surfactant compatibility/stability at test conditions

2. IFT measurements between the oil phase and EOR chemical formulations
3. Contact angle measurements to quantify the wettability alteration potential of the formulations
4. Core soaking experiments to determine the oil recovery potential of the formulations

Below we discuss the experimental procedures in more detail.

2.3.1 Surfactant compatibility

Compatibility tests were performed to ensure that the surfactant remains stable under the test conditions. All the fluid formulations were prepared with 5 wt% KCl as the base brine. The stability of the surfactant was tested by preparing a 0.2 wt% surfactant solution in 5% brine and a 0.2% wt% surfactant/ 10 wt% urea in 5% brine. The solutions were placed in an oven at the test temperature of 121 °C and heated for 72 hours. It was assumed to be a stable solution if it remained clear and there was no visible precipitation.

2.3.2 IFT measurements

The IFT measurements between the oil phase and the EOR chemical formulations were performed with a spinning drop tensiometer (Grace Instrument M6500) and a pendant drop tensiometer (Biolin Scientific Attension Theta). The M6500 and Attension Theta can measure IFT in the range of 10^{-6} to 10^{2} mN/m and 0.01 to 1000 mN/m respectively. The spinning drop tensiometer was used for the formulations that contained surfactants, due to the ease of measuring lower IFT values, while the pendant drop was used for the formulations that did not have surfactants. IFT measurements were conducted at room temperature for all the fluids. About 30 mL of each fluid formulation was prepared separately and then divided into two bottles

with about 15 mL each. Then an equal volume of dodecane was added in each bottle and transferred to a slow-rotating mixer to equilibrate the oil and aqueous phases for 24 hours. One sample of each formulation was then used to measure the IFT at room temperature. The other sample was heated for 72 hours at 121 °C, transferred to the rotating mixer and cooled to room temperature while equilibrating. The IFT between the oil and aqueous phase was then measured. We repeat the IFT measurements at least three times for each sample and report the average values. A detailed description of the measurement procedure is given elsewhere [34].

2.3.3 Contact angle measurements

The contact angle measurements were carried out with the Biolin Scientific Attension Theta, using the captive bubble method. The shale core samples used for the wettability measurement were not aged in dodecane prior to measuring the contact angle since dodecane does not contain any polar components and consequently will not affect the rock surface wettability [41]. Similar to the IFT measurements, the EOR formulations were tested before and after heating for 72 hours at 121 °C. The surface of the shale core is carefully polished before immersing it in the EOR fluid formulation. It is then allowed to equilibrate with the fluid before attaching a drop of dodecane to the shale surface and measuring the contact angle. A detailed description of the test procedure is given elsewhere [34].

2.3.4 Core soaking/oil recovery experiments

The core soaking experiments were performed to evaluate the oil recovery potential of the EOR formulation fluids. The setup for the test is shown in Figure *2-2***.** The Woodford shale outcrop core samples were first prepared using the following procedure:

1. The cores were dried in an oven at 100 °C until their weight was constant
2. The porosity of the cores was then determined with a helium porosimeter
3. The dried cores were saturated with dodecane under a vacuum for 24 hours
4. The cores were then transferred to a high-pressure vessel and saturated with dodecane at 5000 psi for 24 hours
5. The amount of dodecane imbibed was determined by the weight difference between the dried sample and the saturated sample

The saturated cores were then transferred to the core holder and soaked in the EOR fluid at 121 °C and 1500 psi or 4000 psi for 72 hours. The EOR fluid is contained in the piston accumulator. The syringe pump is used to maintain the pressure in the system at 1500 psi throughout the test period. After the soaking period, the setup was allowed to cool to room temperature, while maintaining the test pressure. The recovered oil was collected in the graduated sample collector by slowly opening valve 3 as shown in Figure *2-2*. For the test at 4000 psi, we gradually reduced the pressure to 1500 psi using the syringe pump, before slowly opening valve 3 to collect the recovered oil. The system was then flushed with brine at a slow rate of 0.01 mL/min until all the produced oil was recovered.

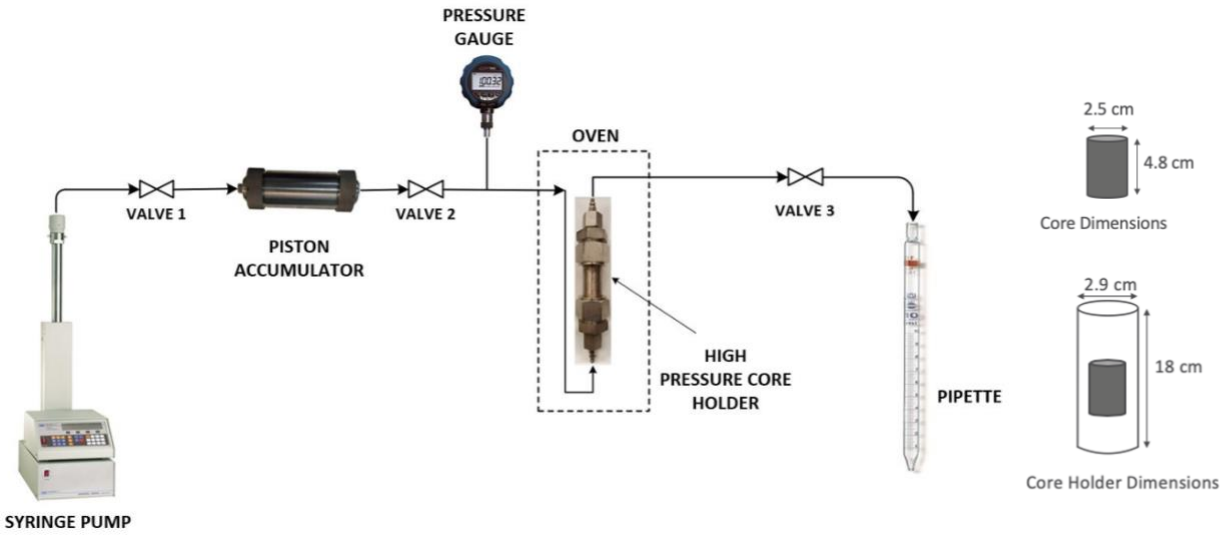

Figure 2-2 Setup for the oil recovery experiments

The characteristics of the core samples used in the oil recovery tests are shown in Table *2-2*.

Table 2-2 Characteristics of Woodford core samples used in the oil recovery tests

Sample	EOR Fluid	Dry weight, g	Diameter, cm	Length, cm	Grain density, g/ml	Porosity, %
1	5% KCl	60.99	2.54	5.01	2.53	5.05
2	10% urea	59.92	2.54	4.95	2.54	5.83
3	0.2% surfactant	58.57	2.54	4.96	2.52	7.49
4	10% urea + 0.2% surfactant	57.76	2.54	4.87	2.52	7.16
5	5% KCl	59.15	2.54	4.94	2.50	5.46
6	10% urea	58.62	2.54	4.93	2.50	6.30
7	10% urea	58.85	2.54	4.92	2.52	6.56
8	0.2% surfactant	57.68	2.54	4.94	2.49	7.56
9	10% urea + 0.2% surfactant	58.05	2.54	4.97	2.49	7.56

*All the tests were conducted at a pressure of 1500 psi except tests 5 and 7 which were conducted at 4000 psi.

2.4 Results and Discussions

This section presents and discusses the results of the compatibility tests conducted with the different EOR fluid formulations. We investigated the effect of salinity, temperature and the hydrolysis of urea on the stability of the fluid systems. Additionally, the IFT and contact angle measurement results are presented and discussed. Finally, we present the results of the core soaking experiments to determine the oil recovery potential of the EOR fluid formulations.

2.4.1 Compatibility tests

We used the transparency and absence of precipitates as an indication of the surfactant compatibility and stability. Figure 2-3 shows that the fluids remain transparent with no visible precipitates after they have been heated in the oven at 121 °C for 72 hours. This was expected since in general, sulfonates including those with alkoxy groups, are stable at high temperatures due to the presence of a sulfur-to-carbon bond which is not susceptible to hydrolysis [42].

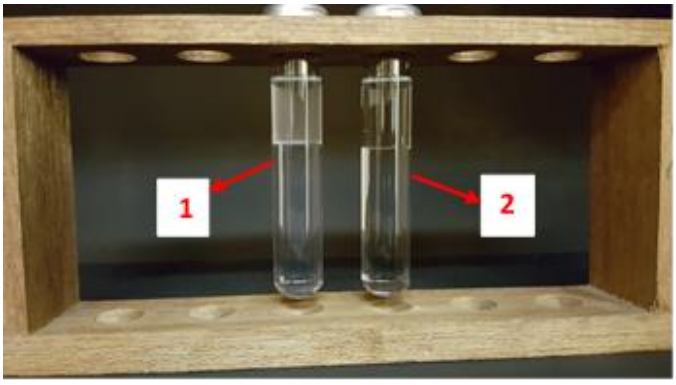

Figure 2-3 Compatibility test results. 1 - surfactant/dodecane and 2 - surfactant/urea/dodecane.

2.4.2 IFT measurement

The results of the IFT tests are shown in Table *2-3*. As mentioned earlier, all the EOR fluid formulations were prepared with 5 wt% KCl as the base brine and the IFT measurements were performed at room temperature. The samples that were heated to 121 °C for 72 hours were cooled down to room temperature before performing the IFT measurements. Adding urea or surfactant to the fluid formulation lowers the IFT between dodecane and the liquid phase. The IFT values are in good agreement with the values reported by Wang et al. [34]. However, the IFT values obtained in this work are slightly higher since we used 5% KCl as our base fluid, while deionized water (DI) was used as the base fluid in their work. It has been observed by various authors that the IFT between non-polar oils and brine generally increases with an increase in salinity though this trend can be affected by the aging time [43,44]. Urea is a nonionic hydrotrope that has properties similar to surfactants, but to a lesser degree, decreases the IFT as its concentration increases in aqueous solutions [34,45–47]. Jones [45] measured the IFT of aqueous urea – n-decane and aqueous urea + surfactant – n-decane interfaces and concluded that urea raises the CMC of the surfactant but does not affect the adsorption of the surfactant at the oil – aqueous interface. Since the surfactant concentration used in this study is significantly above the CMC, the increase in CMC should not affect the performance of the system. The IFT value for the 10% urea formulation was significantly lower after heating. This is due to the hydrolysis of the aqueous solution of urea to form ammonia and CO_2 both of which have IFT-reducing effects. For the formulations with surfactants, the IFT values after heating are slightly lower than before heating. This further confirms the stability of the sulfonate surfactant at high temperatures and salinity as shown in the previous section. It also shows that the IFT-reducing properties of the

surfactant are not affected by the ammonia and CO_2 in aqueous solution. Wang et al [48] reported that the pH in aqueous solutions of urea can increase up to 10 after hydrolysis due to the dissolved ammonia.

Table 2-3 Results of IFT measurements between dodecane and the EOR fluid formulations

	IFT, mN/m	
Fluid	Before	After heating
5% KCl*	46.7 ± 0.1	
10% Urea*	40.3 ± 0.4	26.3 ± 0.5
0.2% Surfactant**	0.9 ± 0.0	0.4 ± 0.0
10 % Urea/0.2% Surfactant**	1.1 ± 0.0	0.6 ± 0.0

* Measured with pendant drop tensiometer; ** Measured with spinning drop tensiometer

2.4.3 Contact angle measurement/ wettability alteration

The results of the contact angle measurements between dodecane and the shale surface are shown in Table *2-4* and Figure *2-4*.

Table 2-4 Results of the contact angle measurements

	Contact angle, °	
Fluid	Before heating	After heating
DI	29.0 ± 2.4	
5% KCl	33.8 ± 2.2	
10% Urea	18.3 ± 1.6	19.3 ± 2.9
0.2% Surfactant	30.3 ± 2.9	25.2 ± 3.3
10% Urea/0.2% Surfactant	26.6 ± 1.5	24.3 ± 3.0

Wettability is the readiness of an immiscible fluid to spread onto a solid surface in the presence of other immiscible fluids. Solid surfaces can demonstrate 3 different types of wettability behavior which can be quantified by measuring the contact angle between the wetting or non-wetting phase and the solid surface. Generally, a porous medium is considered to be water wet, intermediate wet or oil wet if the contact angle is 0° to 75°, 75° to 105° or 105° to 180°, respectively [41].

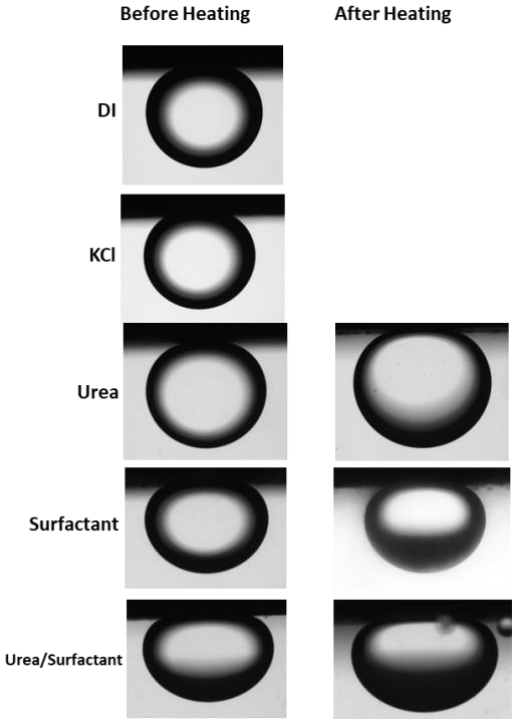

Figure 2-4 Results of the contact angle measurements showing images of the dodecane drop on the shale surface

From the result of the contact angle in DI, the shale sample is originally water-wet. This could be because we used shale outcrop cores for our tests. The contact angle increased with an increase in salinity from 0 to 5% KCl, indicating a decrease in the water wetness of the shale sample. This is in agreement with previously reported data by several authors [49,50]. Change in the electric

charge at the oil/brine and brine/rock interface is the primary reason for wettability alteration [49]. Introducing urea in the system resulted in a decrease in the contact angle compared to the DI case. Urea is a weak acceptor of protons [51]. The ionization caused by the urea in solution could lead to an increase in the negative charge at the interfaces of oil/brine and brine/rock and subsequently to an increase in the repulsion forces between rock and oil, making the rock more water wet. The hydrotropic properties of urea could also be a factor in the increase in water wetness. The fluid formulation with 0.2% surfactant showed a negligible change in contact angle compared to the DI case. However, combining urea and surfactant resulted in a decrease in the contact angle. Mixtures comprising of hydrotropic agents and surfactants exhibit different solution properties, which may be superior to those of the individual components, due to synergistic effects [46]. Additionally, hydrotropes influence the efficiency of surfactant solubilization in aqueous solutions. After heating and hydrolysis of the urea solution, the change in contact angle was negligible. Both fluid formulations with surfactant showed a decrease in contact angle. This further confirms the stability of the surfactant at the test conditions. In general, the wettability alteration effect of the various fluid formulations was not very significant, except the urea-only case. This could be due to the fact that the outcrop shale rock samples used in this study were originally water-wet. More wettability alteration effect will probably be observed if the rock sample was originally oil-wet. Also, the mechanism of wettability alteration due to the reaction of aqueous ammonia (alkali) with the acid components of crude oil to form *in situ* surfactants was not observed in this study since dodecane does not contain such acid components.

2.4.4 Core soaking/oil recovery tests

The results of the oil recovery tests are shown in Table *2-5*.

Table 2-5 Results of the oil recovery tests

Fluid	Oil recovery, %		
	Woodford A @ 1500 psi	Woodford B @ 1500 psi	Woodford B @ 4000 psi
5% KCl	5.9		5.9
10% Urea	14.9	23.0	24.3
0.2% Surfactant	19.9	21.1	
0.2% Surfactant/ 10% Urea	23.5	22.2	

The test results in Woodford A and B show good repeatability, except the 10% urea case in Woodford A. This could be due to trapping of recovered oil in the high-pressure core holder or along the flow lines. After each test, we made sure the flow lines were well flushed until no more oil was collected in the sample collector (pipette), but there is a possibility that some of the recovered oil was missed in this case. All the tests showed a substantial increase in oil recovery compared to the 5% KCl base fluid case. Therefore, adding urea or surfactant to the 5% KCl base fluid improves the oil recovery. The mechanisms that have been proposed for the improved oil recovery for the *in situ* CO_2 generating system using urea as the gas generating agent include oil swelling and viscosity reduction, wettability reversal and IFT reduction [34]. Using the correlations developed by Emera and Sarma [27], the mole fraction of CO_2 dissolved in dodecane at the experimental conditions of 250 °F and 1500 psi is estimated as 0.52. The dissolved CO_2 in the crude oil will lead to an estimated oil swelling factor of 1.16 at the test conditions. This implies that the dissolved CO_2 will increase the volume of the dodecane by about 16 %.

To investigate the effect of miscible versus immiscible CO_2/dodecane conditions, tests were run at 1500 psi and 4000 psi for the 10% urea fluid. As we mentioned earlier, the calculated MMP of the CO_2/dodecane system is 3200 psi at 250°F. The test results show a negligible increase in the oil recovery from 23% to 24.3%. A similar phenomenon was observed by Wang et al. [26] in their sand pack flooding tests. They observed better EOR performance in the sub-MMP test compared to the supra-MMP case, which was attributed to the absence of a separate CO_2 phase during the urea flooding. The generated CO_2 is dissolved in the aqueous phase and when it comes in contact with oil, it will migrate into the oil phase due to the high solubility of CO_2 in oil. Upon depletion of the CO_2 concentration in the aqueous phase, the reaction equilibrium will shift towards the generation of more CO_2 [26]. Therefore, there is no benefit to running the test at above MMP condition.

The results for Woodford B at 1500 psi show that synergism is not realized by combining urea and surfactant. This could be due to the original water wettability of the shale outcrop cores used in this test. In this case, the wettability and IFT altering effect of the surfactant and aqueous ammonia is minimal. Most shale reservoirs are oil wet therefore the potential of the surfactant and ammonia to reduce IFT and alter wettability to more water wet conditions will be greater. Hence, greater wettability reversal may be achieved by combining urea and surfactant. We intend to investigate this scenario in our future tests.

Figure *2-5* and Figure *2-6* show a plot of the oil recovery versus IFT and contact angle respectively, to establish any relationship between oil recovery, IFT reduction and wettability reversal. We used the oil recovery results from Woodford B at 1500 psi except for 5% KCl where we used the result at 4000 psi. We do not expect the oil recovery for 5% KCl to be dependent on the test

pressure as the result for Woodford A shows. From the plots, there is no clear relationship between the oil recovery and IFT values. However, with a decrease in the contact angle to more water-wet conditions, the oil recovery slightly increases.

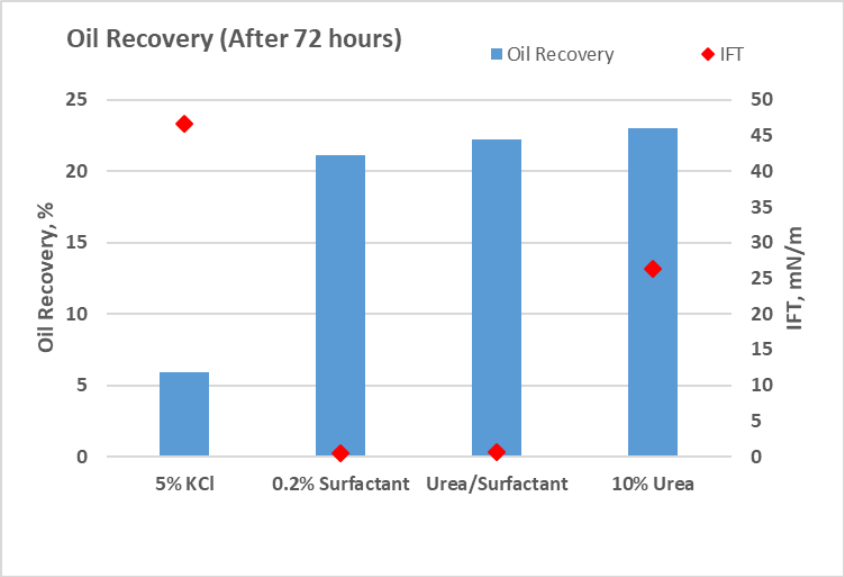

Figure 2-5 Oil recovery versus IFT

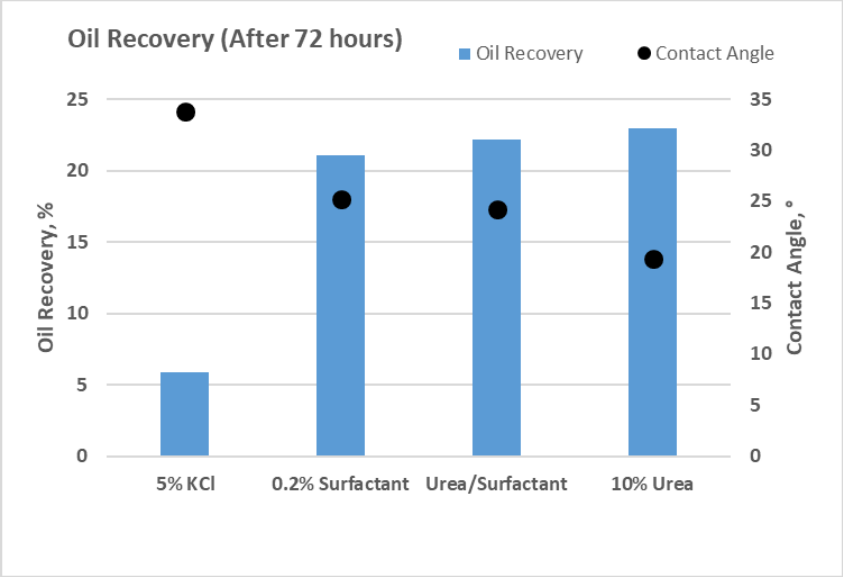

Figure 2-6 Oil recovery versus contact angle

2.5 Conclusions

1. The *in situ* CO_2 generation fluid system evaluated in this work shows a substantial increase in the oil recovery compared to the base case of only brine.
2. Adding urea or a compatible surfactant to brine substantially improves the oil recovery.
3. There is no benefit to running the *in situ* CO_2 generation EOR at above MMP conditions.
4. Both IFT reduction and wettability alteration play important roles in improving oil recovery. However, under the tested conditions, there is a stronger relationship between the oil recovery and wettability alteration.
5. Under the tested conditions, synergism was not realized by combining urea and surfactant.

6. Additional tests are required to determine whether synergism between urea and surfactant occurs in oil-wet cores.

References

[1] Sheng JJ. Critical review of field EOR projects in shale and tight reservoirs. Journal of Petroleum Science and Engineering 2017;159:654–65. https://doi.org/10.1016/j.petrol.2017.09.022.

[2] Wang X, Luo P, Er V, Huang S-SS. Assessment of CO2 Flooding Potential for Bakken Formation, Saskatchewan, Society of Petroleum Engineers; 2010. https://doi.org/10.2118/137728-MS.

[3] Sheng JJ, Chen K. Evaluation of the EOR potential of gas and water injection in shale oil reservoirs. Journal of Unconventional Oil and Gas Resources 2014;5:1–9. https://doi.org/10.1016/j.juogr.2013.12.001.

[4] Dong Y, Dindoruk B, Ishizawa C, Lewis EJ, Kubicek T. An Experimental Investigation of Carbonated Water Flooding, Society of Petroleum Engineers; 2011. https://doi.org/10.2118/145380-MS.

[5] Lashgari HR, Sun A, Zhang T, Pope GA, Lake LW. Evaluation of carbon dioxide storage and miscible gas EOR in shale oil reservoirs. Fuel 2019;241:1223–35. https://doi.org/10.1016/j.fuel.2018.11.076.

[6] Schmidt M, Sekar B. Innovative Unconventional2 EOR-A LightEOR an Unconventional Tertiary Recovery Approach to an Unconventional Bakken Reservoir in Southeast Saskatchewan 2014:12.

[7] Todd HB, Evans JG. Improved Oil Recovery IOR Pilot Projects in the Bakken Formation, Society of Petroleum Engineers; 2016. https://doi.org/10.2118/180270-MS.

[8] Foley AY, Nooruddin HA, Blunt MJ. The impact of capillary backpressure on spontaneous counter-current imbibition in porous media. Advances in Water Resources 2017;107:405–20. https://doi.org/10.1016/j.advwatres.2017.04.012.

[9] Dehghanpour H, Zubair HA, Chhabra A, Ullah A. Liquid Intake of Organic Shales. Energy Fuels 2012;26:5750–8. https://doi.org/10.1021/ef3009794.

[10] Alvarez JO, Schechter DS. Wettability Alteration and Spontaneous Imbibition in Unconventional Liquid Reservoirs by Surfactant Additives. SPE Reservoir Evaluation & Engineering 2017;20:107–17. https://doi.org/10.2118/177057-PA.

[11] Wang D, Butler R, Liu H, Ahmed S. Flow-Rate Behavior and Imbibition in Shale. SPE Reservoir Evaluation & Engineering 2011;14:485–92. https://doi.org/10.2118/138521-PA.

[12] Yarveicy H, Habibi A, Pegov S, Zolfaghari A, Dehghanpour H. Enhancing Oil Recovery by Adding Surfactants in Fracturing Water: A Montney Case Study, Society of Petroleum Engineers; 2018. https://doi.org/10.2118/189829-MS.

[13] Kazempour M, Kiani M, Nguyen D, Salehi M, Bidhendi MM, Lantz M. Boosting Oil Recovery in Unconventional Resources Utilizing Wettability Altering Agents: Successful Translation from Laboratory to Field, Society of Petroleum Engineers; 2018. https://doi.org/10.2118/190172-MS.

[14] Bidhendi MM, Kazempour M, Ibanga U, Nguyen D, Arruda J, Lantz M, et al. A Set of Successful Chemical EOR Trials in Permian Basin: Promising Field and Laboratory Results, Unconventional Resources Technology Conference; 2019. https://doi.org/10.15530/urtec-2019-881.

[15] National Energy Technology Laboratory (NETL). Storing CO2 and Producing Domestic Crude Oil with Next Generation CO2-EOR Technology: An Update 2010. http://large.stanford.edu/courses/2013/ph240/salehi2/docs/netl-2010-1417.pdf (accessed October 6, 2020).

[16] Afzali S, Rezaei N, Zendehboudi S. A comprehensive review on Enhanced Oil Recovery by Water Alternating Gas (WAG) injection. Fuel 2018;227:218–46. https://doi.org/10.1016/j.fuel.2018.04.015.

[17] Esene C, Rezaei N, Aborig A, Zendehboudi S. Comprehensive review of carbonated water injection for enhanced oil recovery. Fuel 2019;237:1086–107. https://doi.org/10.1016/j.fuel.2018.08.106.

[18] Shu WR. Carbonated waterflooding for viscous oil recovery. United States patent US4441555A, 1984.

[19] Altunina LK, Kuvshinov VA. Evolution Tendencies of Physico-Chemical EOR Methods, OnePetro; 2000. https://doi.org/10.2118/65173-MS.

[20] Gumersky KK, Dzhafarov IS, Shakhverdiev AK, Mamedov YG. In-Situ Generation of Carbon Dioxide: New Way To Increase Oil Recovery, OnePetro; 2000. https://doi.org/10.2118/65170-MS.

[21] Shiau BJ, Hsu T-P, Roberts BL, Harwell JH. Improved Chemical Flood Efficiency by In Situ CO2 Generation, OnePetro; 2010. https://doi.org/10.2118/129893-MS.

[22] Bakhtiyarov SI. Technology of In-Situ Gas Generation to Recover Residual Oil Reserves | netl.doe.gov 2008. https://netl.doe.gov/node/4028 (accessed December 29, 2019).

[23] Jia X, Ma K, Liu Y, Liu B, Zhang J, Li Y. Enhance Heavy Oil Recovery by In-Situ Carbon Dioxide Generation and Application in China Offshore Oilfield. SPE Enhanced Oil Recovery Conference, Kuala Lumpur, Malaysia: Society of Petroleum Engineers; 2013. https://doi.org/10.2118/165215-MS.

[24] Wang Y, Hou J, Tang Y. In-situ CO2 generation huff-n-puff for enhanced oil recovery: Laboratory experiments and numerical simulations. Journal of Petroleum Science and Engineering 2016;145:183–93. https://doi.org/10.1016/j.petrol.2016.04.002.

[25] Wang S, Kadhum MJ, Chen C, Shiau B, Harwell JH. Development of in Situ CO2 Generation Formulations for Enhanced Oil Recovery. Energy Fuels 2017;31:13475–86. https://doi.org/10.1021/acs.energyfuels.7b02810.

[26] Wang S, Chen C, Shiau B, Harwell JH. In-situ CO2 generation for EOR by using urea as a gas generation agent. Fuel 2018;217:499–507. https://doi.org/10.1016/j.fuel.2017.12.103.

[27] Emera MK, Sarma HK. Prediction of CO2 Solubility in Oil and the Effects on the Oil Physical Properties. Energy Sources, Part A: Recovery, Utilization, and Environmental Effects 2007;29:1233–42. https://doi.org/10.1080/00908310500434481.

[28] Simon R, Graue DJ. Generalized Correlations for Predicting Solubility, Swelling and Viscosity Behavior of CO2 -Crude Oil Systems. Journal of Petroleum Technology 1965;17:102–6. https://doi.org/10.2118/917-PA.

[29] Holm LW. CO2 Flooding: Its Time Has Come. Journal of Petroleum Technology 1982;34:2,739-2,745. https://doi.org/10.2118/11592-PA.

[30] Bagalkot N, Hamouda AA. Diffusion coefficient of CO2 into light hydrocarbons and interfacial tension of carbonated water–hydrocarbon system. Journal of Geophysics and Engineering 2018;15:2516–29. https://doi.org/10.1088/1742-2140/aad432.

[31] Altunina LK, Kuvshinov VA. Physicochemical methods for enhancing oil recovery from oil fields. Russ Chem Rev 2007;76:971–87. https://doi.org/10.1070/RC2007v076n10ABEH003723.

[32] Dang S, Sondergeld C, Rai C. Novel technique to measure mutual bulk fluid diffusion using NMR 1-D gradient. E3S Web Conf 2020;146:03007. https://doi.org/10.1051/e3sconf/202014603007.

[33] Lu W, Guo H, Chou IM, Burruss RC, Li L. Determination of diffusion coefficients of carbon dioxide in water between 268 and 473K in a high-pressure capillary optical cell with in situ Raman spectroscopic measurements. Geochimica et Cosmochimica Acta 2013;115:183–204. https://doi.org/10.1016/j.gca.2013.04.010.

[34] Wang S, Li K, Chen C, Onyekachi O, Shiau B, Harwell JH. Isolated mechanism study on in

situ CO2 EOR. Fuel 2019;254:115575. https://doi.org/10.1016/j.fuel.2019.05.158.

[35] Emera MK, Javadpour F, Sarma HK. Genetic Algorithm (GA)-Based Correlations Offer More Reliable Prediction of Minimum Miscibility Pressures (MMP) Between Reservoir Oil and CO or Flue Gas. Journal of Canadian Petroleum Technology 2007;46. https://doi.org/10.2118/07-08-01.

[36] Ekwunife IC. Assessing Mudrock Characteristics, High-resolution Chemostratigraphy, and Sequence Stratigraphy of the Woodford Shale in the McAlister Cemetery Quarry, Ardmore Basin, Oklahoma. University of Oklahoma; 2017.

[37] Knapstad B, Skjoelsvik PA, Oeye HA. Viscosity of pure hydrocarbons. J Chem Eng Data 1989;34:37–43. https://doi.org/10.1021/je00055a013.

[38] P.J Linstrom, W.G. Mallard. NIST Chemistry WebBook, NIST Standard Reference Database Number 69, National Institute of Standards and Technology, Gaithersburg MD, 20899. National Institute of Standards and Technology; n.d. https://doi.org/10.18434/T4D303.

[39] Zeppieri S, Rodríguez J, López de Ramos AL. Interfacial Tension of Alkane + Water Systems †. J Chem Eng Data 2001;46:1086–8. https://doi.org/10.1021/je000245r.

[40] Yalkowsky SH, He Y, Jain P, He Y, Jain P. Handbook of Aqueous Solubility Data. CRC Press; 2016. https://doi.org/10.1201/EBK1439802458.

[41] Anderson WG. Wettability Literature Survey- Part 1: Rock/Oil/Brine Interactions and the Effects of Core Handling on Wettability. Journal of Petroleum Technology 1986;38:1,125-1,144. https://doi.org/10.2118/13932-PA.

[42] Puerto M, Hirasaki GJ, Miller CA, Barnes JR. Surfactant Systems for EOR in High-Temperature, High-Salinity Environments. SPE Journal 2012;17:11–9. https://doi.org/10.2118/129675-PA.

[43] Aveyard R, Saleem SM. Interfacial tensions at alkane-aqueous electrolyte interfaces. J Chem Soc, Faraday Trans 1 1976;72:1609–17. https://doi.org/10.1039/F19767201609.

[44] Alotaibi MB, Nasr-El-Din HA. Salinity of Injection Water and Its Impact on Oil Recovery, Society of Petroleum Engineers; 2009. https://doi.org/10.2118/121569-MS.

[45] Jones MN. Interfacial tension studies at the aqueous urea-n-decane and aqueous urea + surfactant-n-decane interfaces. Journal of Colloid and Interface Science 1973;44:13–20. https://doi.org/10.1016/0021-9797(73)90187-2.

[46] Owuor ECA. Impact of hydrotropic agents on surfactant wetting of hydrophobic soils. Swinburne University of Technology, 2015.

[47] Balasubramanian D, Srinivas V, Gaikar VG, Sharma MM. Aggregation behavior of

hydrotropic compounds in aqueous solution. J Phys Chem 1989;93:3865–70. https://doi.org/10.1021/j100346a098.

[48] Wang S, Chen C, Li K, Yuan N, Shiau B, Harwell JH. In Situ CO2 Enhanced Oil Recovery: Parameters Affecting Reaction Kinetics and Recovery Performance. Energy Fuels 2019;33:3844–54. https://doi.org/10.1021/acs.energyfuels.8b03734.

[49] Nasralla RA, Bataweel MA, Nasr-El-Din HA. Investigation of Wettability Alteration by Low Salinity Water, Society of Petroleum Engineers; 2011. https://doi.org/10.2118/146322-MS.

[50] Alotaibi MB, Nasralla RA, Nasr-El-Din HA. Wettability Studies Using Low-Salinity Water in Sandstone Reservoirs. SPE Reservoir Evaluation & Engineering 2011;14:713–25. https://doi.org/10.2118/149942-PA.

[51] Raab RP. UREA FROM THE CHEMIST'S POINT OF VIEW. J Appl Cosmetol 1991:9–13.

Chapter 3 Enhanced Oil Recovery Formulations For Liquid-rich Shale Reservoirs

Abstract

The aim of this study is to evaluate in-situ CO_2 formulations and their oil recovery potential in liquid-rich shale reservoirs. The process involves injecting the CO_2-generating compound, aqueous solutions of urea, into the tight formation where it hydrolyzes to generate adequate amounts of CO_2 under reservoir conditions. Additionally, we study the synergistic effects of coupling urea with a thermally stable anionic surfactant to further improve oil recovery performance from low-permeability shale formations.

We designed the experimental procedures to simulate the huff-n-puff operation for oil recovery. Imbibition tests were carried out with oil-saturated Woodford outcrop shale cores for 3 and 14 days soaking periods. To assess recovery performance and mechanisms, tests were conducted with four different formulations: brine only, urea in brine, thermostable anionic surfactant in brine, and a blend of urea and surfactant in brine. Surfactant stability at test temperature was investigated. Furthermore, interfacial tension (IFT) and wettability alteration tests were conducted to understand their effect on total recovery.

Results revealed that the selected enhanced oil recovery (EOR) recipes are stable at reservoir conditions and compatible with the crude oil sample. There is a distinct difference in the oil recoveries for the 3-days and 14-days soaking periods in the case of the ternary brine/urea/surfactant mixture. This might indicate that the oil recovery processes in the shale cores are not only controlled by multiple mechanisms, such as wettability alteration, IFT reduction, fluid imbibition and CO_2 diffusion, but are also time-dependent. Oil recovery in the

case of the ternary mixture is 4% and 18% of the original oil in place (OOIP) after soaking periods of 3 days and 14 days, respectively. Combining urea with surfactant in the formulation showed a favorable synergistic effect in releasing oil from the shale core samples, leading to higher oil recovery after a 14-day soaking period. The oil recovered in the case of 14-days soaking time for the brine only, binary brine/urea, binary brine/surfactant, and ternary urea/surfactant/brine mixture was 7%, 9%, 5%, and 18% of the OOIP, respectively. Furthermore, we observed that both IFT reduction and wettability alteration play critical roles in improving oil recovery.

3.1 Introduction

The immense amount of oil and gas in shale and other tight formations has been unlocked with horizontal drilling and hydraulic fracturing. However, production from these very low permeability reservoirs declines sharply after the first couple of years, with very low primary oil recovery in the range of 5 – 10% [1,2]. Therefore, there is a great interest to evaluate and apply enhanced oil recovery techniques to improve the estimated ultimate recovery (EUR) of these oil-rich tight formations. CO_2 is widely used for EOR applications in conventional reservoirs and is increasingly being utilized in unconventional reservoirs, with the US Department of Energy reporting that proper CO_2 utilization in EOR could help the US to deal with the dual challenges of reduction of greenhouse emissions and energy independence [3]. It has a lower minimum miscibility pressure with shale oil compared to other commonly utilized EOR gases like nitrogen and methane. The injected CO_2 dissolves in crude oil resulting in several EOR favorable effects such as a decrease in oil viscosity, oil swelling, reduction in the surface tension between oil and aqueous phases, re-pressurization of the formation and ultimately leading to an increase in the oil production and sweep efficiency. In general, CO_2 injection for EOR application can be in the

form of gas flooding (continuous gas flooding or cyclic injection commonly referred to huff-n-puff), carbonated water injection (CWI), or water alternating gas flooding (WAG). During the huff-n-puff process, CO_2 is injected into the reservoir at a given pressure (the huff stage). The well is then shut-in for a predetermined period to allow the CO_2 to soak the reservoir and mobilize the hydrocarbon in place. Lastly, the well is put on production to recover the mobilized hydrocarbons during the puff stage. Hawthorne et al [4] proposed that in tight formations, the majority of the injected CO_2 gas will flow through the natural and induced fractures, and that the displacement mechanisms that occur in conventional reservoir rock matrix do not apply.

There are numerous operational and technical challenges that could hinder the economic application of CO_2 EOR in the field, including CO_2 availability, lack of infrastructure for CO_2 transportation, early gas breakthrough, gravity segregation, viscous fingering, low solubility of CO_2 in water, and asphaltene deposition, among others [5]. Over the years, numerous efforts have been made to address these challenges with limited success [6–9]. In-situ CO_2 generation is among the most promising improvements to address the inadequacies of CO_2 EOR [10–17]. The benefits of in-situ CO_2 generation for EOR applications include non-reliance on natural sources of CO_2 , no need for construction of a CO_2 transportation pipeline, better sweep efficiency than CO_2 WAG, higher CO_2 gas-water ratio (GWR) compared to CWI, simple and cost-effective operations, good tertiary recovery at both below and above minimum miscibility pressure (MMP), and excellent tolerance to high salinity reservoir brine [18]. During CO_2-EOR, a significant portion of the CO_2 injected remains trapped within the formation and cannot be produced back to the surface with the produced oil, gas or water [19]. Therefore, in-situ CO_2 EOR could contribute to the reduction of CO_2 in the atmosphere through carbon sequestration and storage, especially if

the CO_2 used to manufacture the CO_2-generating compound is captured from industrial waste streams or ambient air. An in-situ CO_2-generating method that uses the injection of a single stream of urea solution as the gas-generating agent was proposed by Wang et al. [18]. The aqueous urea solution hydrolyses at elevated reservoir temperature and pressure to produce CO_2 and ammonia according to the following equations:

$$NH_2CONH_2 + H_2O \rightarrow NH_2COONH_4 \quad (1)$$

$$NH_2COONH_4 \rightarrow 2NH_3 + CO_2 \quad (2)$$

Urea is highly soluble in water, up to 512 grams/L at 20 °C [20] and aqueous solutions can spontaneously hydrolyze at higher temperatures, with an increase in the rate of hydrolysis as the temperature rises. For example, the half-life of urea solution at 80 °C and 120 °C are 24.9 days and 1.0 days, respectively [21]. One metric ton of urea will generate about 0.73 metric tons (13.9 Mscf at standard conditions of 60 °F and 14.7 psi) of CO_2 gas upon complete hydrolysis. Urea in-situ CO_2 EOR (ICE) is a combination of carbonated water injection and alkaline (NH_4OH) flooding. In the temperature range of 35 – 100 °C and pressure range of 10 – 40 MPa, the partition coefficient of CO_2 in the oil-water system is between 4 and 10, whereas it does not exceed 6×10^{-4} for the more hydrophilic NH_3 molecules. This implies that most of the CO_2 is in the oil phase, while most of the NH_3 remains in the aqueous phase [22]. In the urea-ICE process, the generated NH_3 dissolves in the aqueous phase to form ammonium hydroxide and increases the pH of the aqueous phase to between 9 and 10 [23]. The ability of alkali to alter the wettability of reservoir rocks from oil-wet to water-wet and reduce the oil-water IFT has been extensively studied and is the basic principle for the use of alkaline flooding to improve oil recovery [24–26].

During IOR processes in conventional and unconventional reservoirs, the three main forces that control oil recovery are capillary, gravitational and viscous forces. In porous media, fluid capillary rise is controlled by the wettability of the rock surface, fluid interfacial interaction and the radius of curvature of the pore walls. If the porous medium is regarded as a bundle of capillaries with an average radius, r, then the Young-Laplace equation can be written as follows [27]:

$$P_O - P_W = P_c = \frac{2\sigma_{WO}cos\theta}{r} \quad (3)$$

where P_O is the pressure in the oil phase; P_W is the pressure in the water phase; P_c is the capillary pressure; σ_{WO} is the IFT between the water and oil phase; θ is the contact angle at the point of intersection between the two fluid phases and the solid surface.

Surfactants can reduce IFT and alter the wettability of shale from oil-wet to mixed-wet or water-wet, thereby enhancing oil recovery. There have been numerous simulation and lab studies on surfactant imbibition EOR in shale [28–33]. Another important mechanism of surfactant imbibition EOR is the reduction of aqueous phase trapping and formation damage in shale [34].

Based on the observations in the surfactant imbibition-dependent oil recovery experiments and simulations in shale rocks, it can be deduced that in unconventional reservoirs, typically with pores in the nano-size range, the initial imbibition of the aqueous phase is due to IFT reduction. Subsequently, the oil film on the rock surface is stripped through ion-pair formation and micellar-solubilization, thereby changing the wettability from oil-wet to water-wet [29,35]. The change in wettability changes the capillary pressure from a negative to a positive value, which in turn leads to more aqueous phase imbibition and expulsion of oil from the pores due to the countercurrent flow mechanism. Maintaining moderate positive capillary pressure values will enhance the

imbibition of the aqueous phase. Ultralow IFT, which will lead to very low capillary pressure values might be detrimental to the imbibition and oil recovery process. Therefore, surfactants that can change wettability from an initial oil-wet state to a water-wet state, while maintaining a moderately high IFT may be more efficient for imbibition EOR applications. There have been few field trials of surfactant imbibition EOR in shale reservoirs. Kazempour et al. [36] , carried out laboratory evaluation and successful field trial of a surfactant blend designed to improve oil recovery by imbibition. Their results show that the EUR can be improved by up to 25% when a proper wettability-altering agent is injected into a shale reservoir. Bidhendi et al. [37] also developed a set of surfactant-based chemical formulations that were studied in the lab for their potential to alter the wettability of Wolfcamp cores and improve oil recovery. Their subsequent field trial showed a 39% increase in the 180 days cumulative oil recovery and increased oil cut.

The literature on in-situ CO_2 generation for EOR (ICE) has focused exclusively on sandstone and carbonate reservoirs. In this study, we conduct a series of experiments to evaluate the applicability of urea ICE in liquid-rich shale reservoirs. Additionally, we study the synergistic effects of coupling urea with a thermally stable ionic surfactant to further improve oil recovery performance from low-permeability shale formations. We conducted tests with brine only, brine plus surfactant, brine plus urea and a ternary mixture of brine/surfactant/urea. Woodford shale outcrop samples were used as the porous media and Woodford stock tank crude oil was used as the hydrocarbon fluid. In our previous study, we used dodecane as the hydrocarbon fluid [5]. First, the compatibility of the surfactant with brine and urea solutions was evaluated under the test conditions. Next, the adsorption of the surfactant on porous media was quantified. IFT between the formulated fluids and crude oil was measured at ambient and test temperature

conditions to quantify the change in IFT at different conditions and the relationship between the amount of recovered oil and IFT. The wettability alteration potential for the different fluid formulations was quantified by contact angle measurements and related to the amount of recovered oil. Finally, soak tests were performed on oil-saturated shale core samples to determine the oil recovery potential of the different fluid formulations under reservoir temperature and pressure. The soak tests were designed to closely simulate the huff-n-puff technique.

3.2 Experimental

3.2.1 Porous media

Woodford shale outcrop cores were used as the porous media for the experiments. The cores were 1-in in diameter and 2-in long and were obtained from the same block of outcrop shale to minimize variation is rock properties. The petrophysical properties of the core samples are shown in Table *3-1* [5].

Table 3-1 Petrophysical properties of Woodford core samples used in the experiments

Permeability, K_{N2} (micro darcy)		Porosity, Helium (%)	Grain Density (g/cm^3)	Total organic carbon (TOC), wt%	Average pore size, nm
1500 psi effective pressure	4000 psi effective pressure				
0.057	0.043	5.9 to 7.2	2.50 to 2.54	12.7	27

The average pore size was measured with the low-pressure nitrogen adsorption technique and the LECO C844 carbon analyzer was used to measure the TOC. Fourier transform infrared (FTIR) spectroscopy analysis of the core samples show that the main mineral components are dolomite

(47.6 wt%), quartz (15.6 wt%), calcite (4.7 wt%), siderite (8.0 wt%) and clays including illite, kaolinite, chlorite and mixed clays (17.9 wt%). The characteristics of the core samples used for the

3.2.2 Oil properties

Woodford stock tank crude oil was used for the tests. The density and viscosity of the crude oil at room temperature were 0.83 g/cc and 10 cP respectively, while at 120 °C, the viscosity was 2.8 cP. The API gravity of the crude oil was 38.8 °, so it can be classified as light crude oil. The total acid number (TAN) of the crude oil was 0.13 mg KOH/g-sample. SARA (saturates, aromatics, resins and asphaltenes) analysis of the crude oil showed that it has 78.3 wt% saturates, 19.1 wt% aromatics, 2.6 wt% resins and no asphaltenes.

3.2.3 Surfactant properties

We selected a 12-carbon branched-chain sodium diphenyl oxide disulfonate surfactant with an activity of 45.3 wt% for our experiments. It is anionic and compatible with a broad range of strong electrolyte solutions such as acids, alkalis and brine, and has excellent thermal stability. The surfactant has a pH of 10.3 and the critical micelle concentration (CMC) in 0.1M NaCl at 25 °C is 0.007 g/ 100 g. The molecular structure is shown in *Figure 2-1*.

3.2.4 Other materials

High-purity urea (≥ 99 wt%) was purchased from Acros Organics. ACS grade Potassium chloride (≥ 99 wt%) was purchased from Sigma Aldrich.

3.3 Methodology

Experiments were carried out to quantify the oil recovery potential of different EOR chemical formulations and understand the different mechanisms and factors that play a role in the EOR process. The experimental workflow can be categorized as follows:

1. Determination of the compatibility/stability of the surfactant at test conditions

2. Determination of surfactant adsorption on the porous media

3. Measurement of the IFT between the oil phase and EOR chemical formulations in the aqueous phase

4. Measurement of contact angle to determine the effectiveness of the EOR chemical formulations to alter wettability

5. Core soaking experiments to determine the oil recovery potential of the formulations

Details of the experimental procedures are discussed below.

3.3.1 Surfactant compatibility

Compatibility tests were performed to determine the stability of the surfactant under the EOR test conditions. Tests were performed with two different formulations: a binary solution of 0.2 wt% surfactant in 5 wt% KCl brine and a ternary solution of 0.2 wt% surfactant, 10 wt% urea and 5 wt% KCl. Around 30 grams of the solutions were placed in a sealed glass vial and heated to the test temperature of 120 °C for 14 days. The solution was assumed to be stable if it remained clear with no visible precipitation at the end of the test period. A high-performance liquid chromatography (HPLC) analysis was also performed to measure the surfactant concentration

before and after the aging period. The HPLC is equipped with a UV-vis detector which was set at 230 nm wavelength. This wavelength was determined from a wavelength scan of the surfactant solution to determine the most adsorbed wavelength using a UV-vis spectrophotometer. A reverse phase C18 chromatography column separated the surfactant from the solution at 25 °C. The mobile phase was acetonitrile and water in a 75/25 volume ratio and the pumping rate was 1 mL/min. The samples were first filtered through a 0.2-micron syringe filter before measuring the surfactant concentration. Surfactant calibration curves were prepared using different concentrations of surfactant ranging from 0.05 to 0.2 wt% surfactant in a 5 wt.% KCl base brine solution. The calibration curve establishes the correlation between surfactant concentration and the area of the signal peak from the UV detector.

3.3.2 Static surfactant adsorption

The surfactant adsorption test was performed at reservoir temperature. Oil-saturated shale samples were first crushed and passed through an ASTM 50 sieve with openings no larger than 300 microns. The particles that passed through the sieve were used for the adsorption test. A 0.2 wt% surfactant solution was prepared in 5% KCl, and 20 grams of the solution was then loaded into a 30 cc glass vial containing 1 gram of the crushed porous media. Multiple replicate vials were prepared. The weight ratio of the surfactant solution to the porous media was 20: 1. After hand-mixing, the samples were transferred to an oven with the temperature maintained at 120 °C. After a predetermined time interval, one of the vials was removed from the oven. After a brief cooling period, a sample was taken from the vial and filtered through a 0.2 micron pore size syringe filter to remove any shale particles and stop the adsorption process. The cooling and sampling times were taken into account when determining the adsorption time. The

concentration of the surfactant in the sample was determined using the HPLC method described in the previous section. Surfactant concentration measurements were repeated at least 3 times to obtain an average value with a standard deviation. Surfactant adsorption was calculated at each time step using the following equation:

$$\theta_{ads} = \frac{\left(C_{surf}^{i} - C_{surf}^{f}\right) \times m_{surf} \times 10^{-3}}{m_{rock}} \qquad (4)$$

Where θ_{ads} is the amount of surfactant adsorbed on the rock surface (mg/gram-rock); C_{surf}^{i} is the initial concentration of surfactant in solution before equilibration with the rock (ppm); C_{surf}^{f} is the final concentration of surfactant in solution after equilibration with the rock (ppm); m_{surf} is the total quantity of the surfactant solution (gram); m_{rock} is the total quantity of rock (gram).

3.3.3 IFT measurements

To cover a broader range of IFT values, we used a spinning drop tensiometer (Grace Instrument M6500) and a pendant drop tensiometer (Kruss DSA 100) to measure the IFT between the oil and the aqueous phase. The spinning drop tensiometer was used for the surfactant solutions, due to the ease of measuring samples with low IFT values (< 1 mN/m). For the solutions that did not contain surfactants, we used the pendant drop tensiometer to measure the IFT. IFT measurements were conducted at ambient temperature and pressure conditions. A detailed description of the spinning drop tensiometer measurement procedure is given in our previous work [5,23]. Briefly, a predetermined volume of each EOR fluid formulation was mixed with an equal volume of crude oil in sealed glass vials and equilibrated for 24 hours in an end-over-end rotating mixer at 8 rpm. A portion of the equilibrated fluid was then used to measure the initial

IFT between the oil and aqueous phase, while the remainder was transferred to the oven and heated to 120 °C for 3 days or 2 weeks. After the heating period, the vials were transferred to the rotating mixer and cooled to room temperature. Then, the IFT between the oil and the aqueous phase was measured and recorded as IFT after heating. For the pendant drop measurements, we collected the aqueous phase from the vial and transferred it into a quartz glass cuvette. The oil phase was transferred into a syringe with a J-shaped needle. The tip of the needle was then submerged into the aqueous phase and an 8 μL oil bubble was created. Then a high-resolution camera recorded the shape of the oil bubble for the duration of the test. Due to the time dependence of crude oil IFT in brine [38], the oil bubble was allowed to equilibrate for 30 minutes while recording. The IFT was automatically calculated by the software using drop shape analysis which relies on the Young-Laplace equation. The IFT measurements are repeated at least 3 times to obtain an average value with a standard deviation.

3.3.4 Contact angle measurements

We used a drop shape analyzer (Kruss DSA 100) to carry out the contact angle measurements, using the captive bubble method at ambient temperature and pressure conditions. Prior to performing the contact angle measurements shale trims of 1-inch diameter and about 0.25-inch thick were prepared by polishing the surface using an aluminum oxide grinding wheel. The purpose of polishing the surface is to eliminate any errors in contact angle measurement due to surface irregularities. The shale trims were then aged in crude oil at 80 °C and 5000 psi for 2 weeks. Afterward, the initial contact angle of the trims was measured in freshly prepared 5% KCl solution as the aqueous phase. The trims were then soaked in the different EOR formulations at 120 ± 2 °C and 1500 psi for 3 days or 2 weeks in a high-pressure core holder, using the same setup

and procedure used in the oil recovery experiments, described in the next section. After the soaking period, the setup was allowed to cool to room temperature and the trims were removed. Any excess fluid on the surface of the trims was wiped with lint-free kimwipes before the contact angle measurement. The fluid in the high-pressure core holder was recovered and used as the aqueous phase in the contact angle measurement. A detailed description of the measurement procedure is given in our previous work [23].

3.3.5 Core soaking/oil recovery experiments

Oil recovery experiments were performed to evaluate the oil recovery potential of the different EOR fluid formulations. The set-up and procedure for the test are described in detail in our previous work [5]. Briefly, 1-inch diameter by 2-inch length Woodford shale outcrop core samples were dried and saturated with Woodford crude oil under a vacuum for 24 hours at room temperature. The cores were then transferred to a high-pressure/ high-temperature vessel and saturated with Woodford crude oil at 80 °C and 5000 psi for 2 weeks. The initial amount of oil in the samples was determined by the weight difference between the dried and oil-saturated samples. Afterwards, oil recovery tests were carried out with the oil-saturated cores for 3 days or 14 days at 120 $\pm$ 2 °C and 1500 or 4000 psi. After the test, the recovered oil was collected in a graduated sample collector. The experimental setup is shown in *Figure 2-2*.

The oil recovery is determined with the following equation:

$$Oil\ recovery\ (\%\ OOIP) = \frac{v_{or}}{\left(\frac{m_{oi}}{\rho_o}\right)} \times 100 \qquad (5)$$

Where v_{or} is the volume of oil recovered (ml); m_{oi} is the initial amount of oil in the core samples, determined by the weight difference between the clean and the oil-saturated cores (gram); ρ_o is

the oil density at room temperature (g/ml). The characteristics of the core samples used in the oil recovery tests are shown in Table *3-2*.

Table 3-2 Characteristics of the Woodford shale core samples used in the oil recovery tests

Sample	EOR Fluid	Test duration, days	Dry weight, g	Grain density, g/ml	Diameter, cm	Length, cm	Porosity, %
1	5% KCl	3	56.39	2.54	2.54	4.71	7.12
2	10% urea	3	58.10	2.51	2.54	4.85	5.89
3	0.2% surfactant	3	56.82	2.50	2.54	4.77	5.85
4	10% urea + 0.2% surfactant	3	58.78	2.51	2.54	4.93	6.45
5	5% KCl	14	58.96	2.51	2.54	4.94	6.30
6	10% urea	14	58.87	2.50	2.54	4.93	6.00
7	0.2% surfactant	14	58.45	2.53	2.54	4.91	7.22
8	10% urea + 0.2% surfactant	14	58.80	2.54	2.54	4.91	6.73

3.4 Results and Discussion

3.4.1 Surfactant compatibility tests

The long-term stability of the surfactant at reservoir conditions must be taken into consideration when designing the fluid system for EOR application. The EOR formulations that contained surfactants were tested to make sure that the surfactant remained stable under the test conditions of high temperature, salinity and pH. We tested the 0.2 wt% surfactant in 5 wt% KCl brine and the ternary solution of 0.2 wt% surfactant, 10 wt% urea and 5 wt% KCl brine. We used solution transparency and the absence of phase separation or precipitates as an indication of surfactant stability. Both surfactant-containing formulations remained transparent and there were no significant phase separations or precipitates after heating in the oven at 120 °C for 2 weeks. The stability of the surfactant solution was confirmed with HPLC analysis to determine the concentration of the surfactant before and after incubation. *Figure 3-1* shows the result of

the HPLC analysis of the 0.2 % surfactant sample before and after incubation at 120 °C for 2 weeks. The result shows that the concentration of the surfactant, which is calculated from the area of the curve under the chromatography signal peak, did not change after the 2 weeks incubation period. This result was anticipated since sulfonate and disulfonate surfactants contain sulfur-to-carbon bonds which are not susceptible to hydrolysis even at high temperatures [39,40].

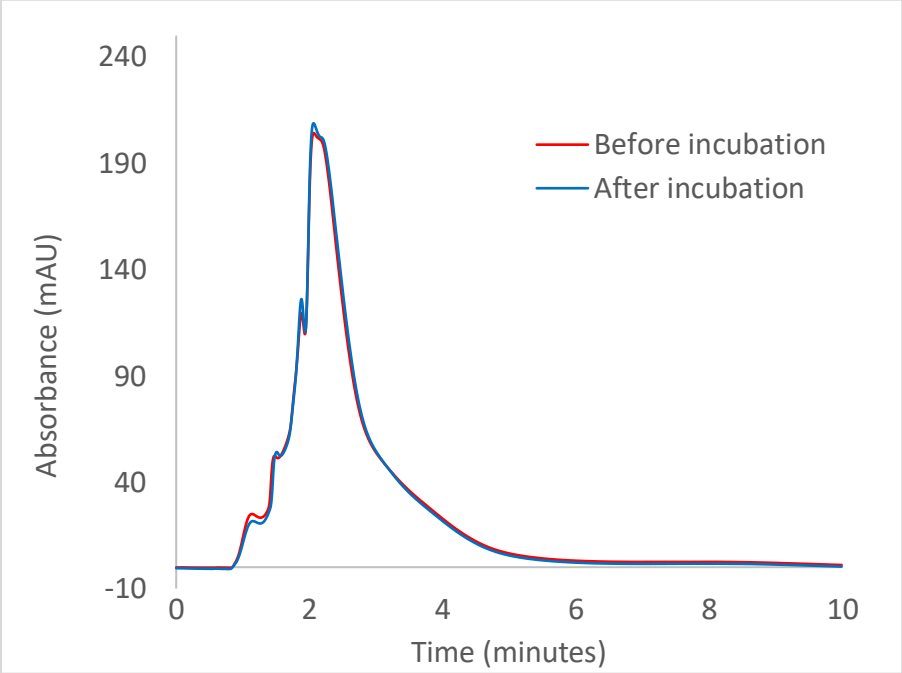

Figure 3-1 HPLC signals of surfactant before and after incubation at 120 °C for 14 days

3.4.2 Static surfactant adsorption

The result of the adsorption of surfactant on crushed shale samples is shown in Figure *3-2*. The total adsorption of the surfactant after equilibrium was 4.9 mg/gram of rock which is low. Other authors have reported adsorption values of 7.4 to 8 mg/gram of rock for anionic surfactants on shale substrates [41]. From the plot, it is evident that most of the surfactant adsorption occurs in

the first 2 hours. Some adsorption of the surfactant on the porous media is necessary to alter the wettability of the rock surface and reduce the IFT between the oil and aqueous phase. However, excessive surfactant adsorption will lead to loss of the surfactant in the areas of the reservoir near the wellbore and reduce the amount available to alter wettability or reduce IFT in the target producing zone. Many factors play a role in the amount of surfactants adsorbed by the porous media including the charge carried by the surfactant and rock particles and the content of clays in the porous media. The core used in our tests is composed of mainly dolomite (47.6 wt%), clays (17.9 wt%), and silica (15.6 wt%). The isoelectric point of dolomite has been reported as < 6 or 7 [42] so under the reservoir conditions we would expect the dolomite to be either positively or negatively charged.

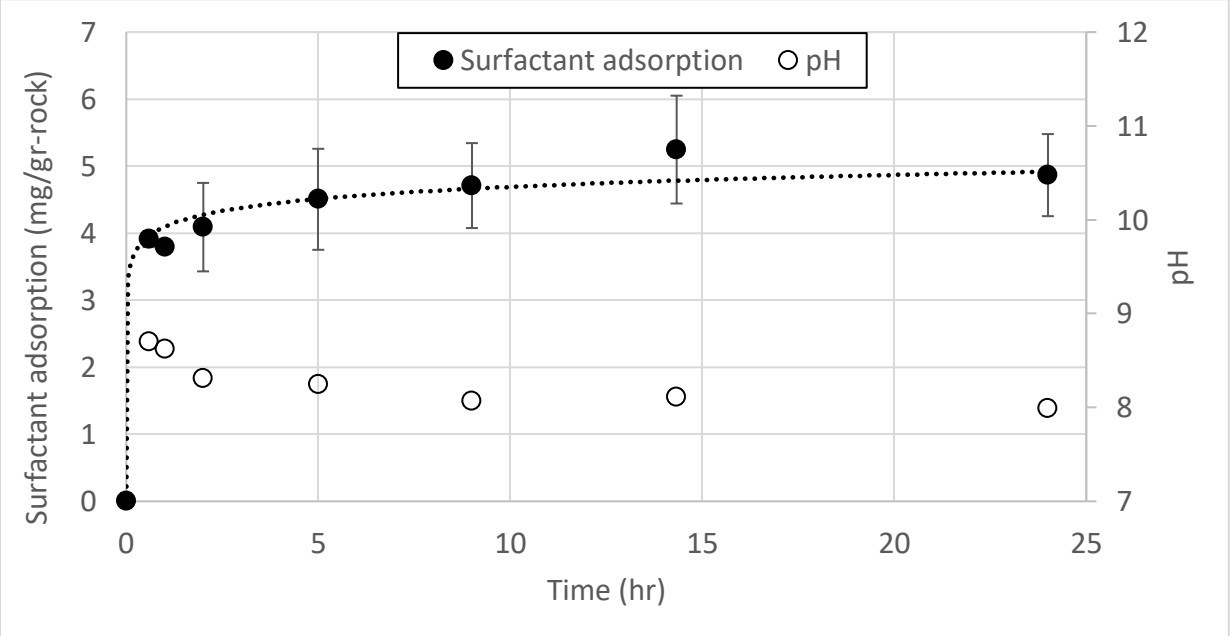

Figure 3-2 Surfactant adsorption on crushed shale

However, when the porous media encounters the alkaline treatment fluid containing the

surfactant, it may become negatively charged which will repel the negatively charged surfactant molecules and deter their adsorption on the porous media. Ammonia and other alkalis have been used to effectively reduce the adsorption of surfactants on porous media [39,43–45]. Clays and silica on the other hand are generally negatively charged at reservoir conditions [46] which should have a deterrent effect on anionic surfactant adsorption. However, clays also have a very high surface area which could boost surfactant adsorption. The loss of surfactant due to adsorption on the porous media will help inform the economic viability of using the surfactant to enhance oil recovery.

3.4.3 IFT measurements

The results of the IFT tests are shown in Table 3-3. The IFT measurements were performed at room temperature and the samples that were heated to 120 °C were cooled down to room temperature before measuring the IFT. The results of the IFT between urea and crude oil before heating were in agreement with the results obtained by Wang et al. [23]. Moreover, the IFT value between crude oil and 5% KCl before heating was significantly lower than the IFT value between dodecane and 5% KCl from our previous work [5]. The same trend was observed for crude oil and dodecane with urea solution prior to heating. This is also in good agreement with the results obtained by Wang et al. [23]. This is due to the presence of surface-active organic acids and bases dissolved in the crude oil. For the surfactant-containing solutions, we see a dramatic drop in IFT compared to the solutions without surfactants.

Table 3-3 Results of IFT measurements between crude oil and the EOR fluid formulations

Fluid	IFT, mN/m		
	Before heating	After heating	
		3 days	14 days
5% KCl*	14.7 ± 0.0	15.3 ± 0.2	15.3 ± 0.1
10% Urea*	12.1 ± 0.2	7.9 ± 0.1	9.7 ± 0.1
0.2% Surfactant**	0.5 ± 0.1	0.5 ± 0.0	0.8 ± 0.1
10 % Urea/0.2% Surfactant**	0.5 ± 0.0	0.2 ± 0.0	0.3 ± 0.0

* Measured with pendant drop tensiometer; ** Measured with spinning drop tensiometer

This indicates that the surfactant used in this test can reduce the IFT between the aqueous and oil phase to low values without dropping to the ultra-low IFT region. This is desirable since ultralow IFT values will decrease the capillary driving forces for imbibition according to the Young-Laplace equation (Equation 3). Ultralow IFT, which will lead to very low capillary pressure values, might be detrimental to the imbibition and oil recovery process in shale reservoirs [29,30]. However, we did not explore the validity of this hypothesis experimentally due to the scope of the work reported herein.

After heating the fluids we observed a drop in the IFT for the brine and urea solutions. A similar observation was reported in our previous work with dodecane for the brine and urea solutions [5]. The slight drop in the IFT for the urea solution is due to the NH_3 and CO_2 generated by the thermal hydrolysis of urea. The generated NH_3 dissolves in the aqueous phase to form ammonium hydroxide and increases the pH of the aqueous phase to between 9 and 10. The ability of alkali to reduce the oil-water IFT and alter the wettability of reservoir rocks from oil-wet to water-wet has been extensively studied and is the basic principle for the use of alkaline

flooding to improve oil recovery [24–26]. The chemical reaction between the alkali in the aqueous phase and the organic acids in the hydrocarbon phase generates in-situ surfactants. The surfactants can accumulate at the oil-water interface to lower the IFT and/or can adsorb onto the rock surface to alter the wettability of the reservoir rock. The alkali effect is not significant in this case due to the relatively low acid number of the Woodford crude oil used in our tests. For the surfactant-containing solutions, the IFT remains unchanged even after heating the fluids. This further confirms that the surfactant remains stable under the high temperature and pH conditions used in our study. It also shows that the presence of CO_2 and NH_3 in aqueous solution does not affect the stability of the surfactant. In our previous work with dodecane, we observed a slight drop in the IFT from 0.9 to 0.4 mN/m for the binary solution of surfactant in brine and 1.0 to 0.6 mN/m for the ternary solution of surfactant, urea and brine after heating [5]. In summary, combining urea with 0.2 wt. % of the thermally stable anionic surfactant results in more IFT reduction between the aqueous and oil phases compared to the fluids without the surfactant.

3.4.4 Contact angle measurements/wettability alteration

We used captive bubble contact angle measurements to evaluate the wettability alteration potential of the different EOR fluids. A sample measurement is shown in Figure 3-3.

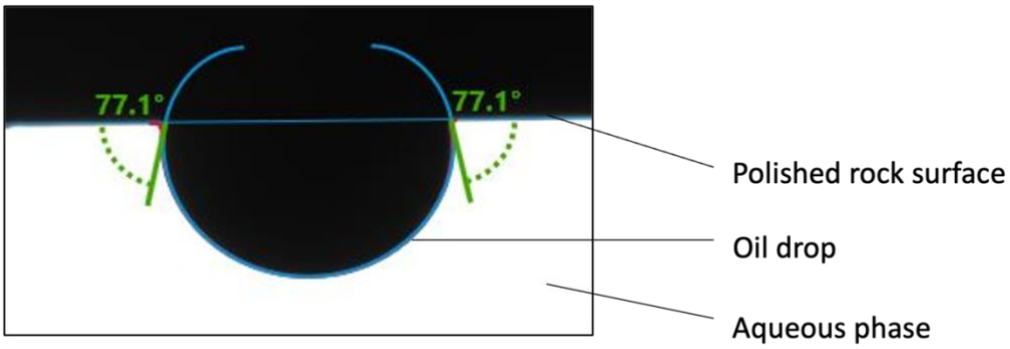

Figure 3-3 Sample captive bubble contact angle measurement

Generally, a porous medium is considered to be water wet, intermediate wet or oil wet if the contact angle is 0° to 75°, 75° to 105° or 105° to 180°, respectively [47]. The results of the contact angle measurements between Woodford crude oil and shale surface are shown in Figure *3-4* and *Figure 3-5*.

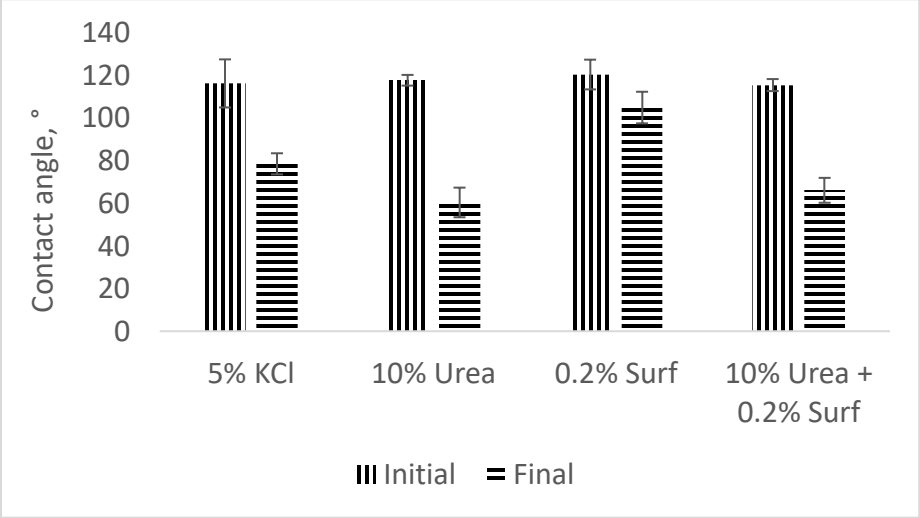

Figure 3-4 Results of contact angle measurements after 3 days soaking test

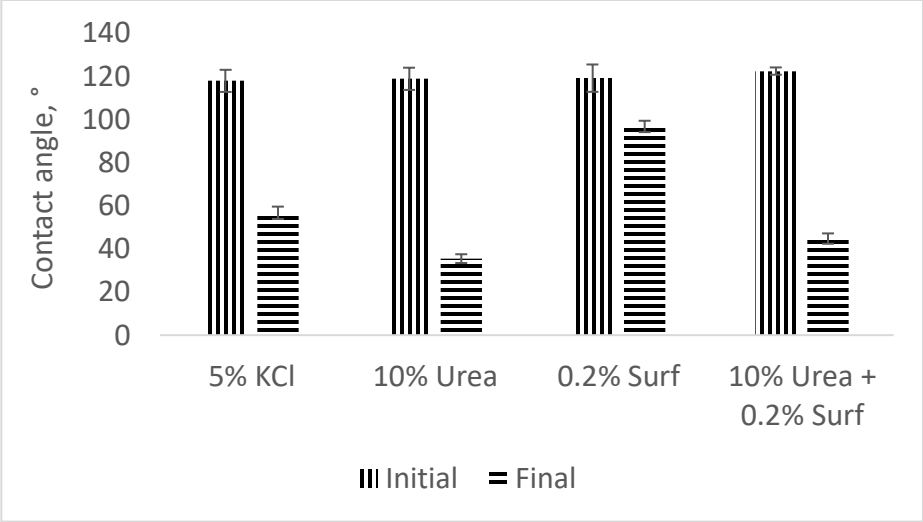

Figure 3-5 Results of contact angle measurements after 14 days soaking test

In our previous work, we established that the shale outcrop samples were originally water wet with contact angle of 33.8° in 5% KCl [5]. After aging the shale cores in Woodford crude oil at 80 °C and 5000 psi for 2 weeks, the wettability was altered from water wet to oil wet. This is due to the presence of surface active molecules such as aromatics and resins in the crude oil which interact with the rock minerals [48]. The SARA analysis of the crude oil shows that it has 19.1 wt% and 2.6 wt% aromatic and resin components, respectively. After soaking the oil-saturated shale cores in the EOR solutions for 3 days and 14 days, the wettability of the cores was altered to a more water-wet state. This is partly due to the release of some of the oil from the shale surface. The change in wettability also showed a time dependence, with an increase in the change in wettability after 14 days of soaking compared to the change after 3 days of soaking. The activation energy or energy barrier for the chemical reactions necessary to induce wettability alteration is critical. Several factors affect the activation energy for the wettability modification including the reservoir temperature, the strength of the bond between polar oil components and

the mineral surface, the solvency of the polar components, and the reactivity of the ions in the injected water [49]. If the reaction rate is slow, then the wettability of the surface will change over time until an equilibrium condition is attained. The change in contact angle for the different fluid systems is shown in *Table* 3-4. Here the change in contact angle is the difference between the initial contact angle of the oil-saturated core sample and the final contact angle after soaking the core in the EOR fluid.

Table 3-4 Change in shale contact angle after soaking in EOR fluid

Fluid	3 days	14 days
5% KCl	37.6 ± 12.3	61.1 ± 5.9
10% Urea	57.2 ± 7.4	83.3 ± 5.5
0.2% Surf	15.5 ±10.2	22.4 ± 6.9
10% Urea + 0.2% Surf	49.3 ± 6.5	77.6 ± 2.9

The 0.2% surfactant solution showed the least effect on the wettability of the shale samples. As mentioned earlier, the Woodford shale samples used in our study consist of mainly dolomite (47.6 wt%), clays (17.9 wt%) and quartz (15.6 wt%). Alvarez et al. [50] studied the wettability alteration of Wolfcamp shale cores made up of mainly calcite and dolomite rock minerals. They observed that anionic surfactants were less effective at altering the wettability of Wolfcamp shale cores compared to a blend of nonionic/cationic surfactants. During the aging process of the shale rock in oil, we would expect the negatively charged organic carboxylates from the crude oil to adsorb on the positively charged dolomite surface during aging. Hence, the inability of the anionic surfactant to substantially alter wettability could be due to the inability of the surfactant to irreversibly desorb the anionic organic carboxylates from the rock surface [51]. This is also in agreement with the proposed mechanisms for wettability alteration by surfactants namely: ion-

pair formation, hydrophobic interactions and micellar solubilization [35,52,53]. The highest degree of wettability alteration was obtained with the EOR fluid with 10% urea. This is also in agreement with our previous work with dodecane-saturated woodford shale samples [5]. The pH of the freshly prepared urea solution before hydrolysis was 7.97. The pH after 3 days of incubation at 120 °C was 10.24 and 9.78 after 14 days. The increase in pH is due to the NH_3 produced by the hydrolysis of urea, which dissolves in the brine to form ammonium hydroxide. There are several mechanisms involved in the alteration of wettability by NH_3 including, electrostatic interactions due to pH alteration, structural and solvation interactions due to the formation of in-situ surfactants and NH_3 adsorption [23].

Table 3-5 Change in EOR fluid pH after the incubation period

	pH		
EOR fluid	0 day	3 days	14 days
0.2% surfactant	8.54	6.97	6.42
10% urea	7.97	10.24	9.78
0.2% surfactant/10% urea	8.33	9.69	9.8

* Note: All fluids were prepared with 5% KCl as the base fluid. The incubation temperature was 120 °C.

Crude oil normally contains acidic components such as carboxylate, fatty and stearate acid groups and basic components such as amine groups. The surface charge of crude oil droplets in water is the net charge of the acid-base interactions. The carboxylic acid group undergoes significant deprotonation at a pH range of 3 – 4, while the basic amine component starts to become protonated below the pH range of 4 – 5 [54]. Buckley et al [55] reported the point of zero charge

of crude oil samples at between pH values of 3 to 5. This indicates that the oil droplets will be negatively charged at the pH values of the hydrolyzed urea solutions, after incubation at 120 °C, as shown in *Table* 3-5. As mentioned earlier in the surfactant adsorption section, the shale rock surface composed mainly of dolomite, clay and quartz will also be negatively charged at this high pH condition. Therefore, we will expect a repulsive electrostatic interaction between the crude oil and the rock surface, which could induce wettability reversal to a more water-wet condition. The acid number of the Woodford crude oil was 0.13 mg KOH/g, which indicates the presence of some acid components in the oil that can generate in-situ surfactants. The generated in-situ surfactant will contribute to the wettability reversal. Hsieh [56] and Clark et al. [57] reported the modification of the surface free energy of silica substrates due to the heat of adsorption of NH_3 on their surface. The modification of the surface energy is directly related to the wettability characteristics of the surface [58]. Lastly, the removal of the polar components of the oil from the rock surface due to the aforementioned mechanisms will also lead to a reversal in wettability.

The 5 wt% KCl showed better wettability alteration potential than the anionic surfactant solution. This could be due to the same mechanisms involved in low salinity water (LSW) injection for EOR purposes. Low salinity water is an aqueous solution of dissolved salts at a concentration significantly less than the formation produced water. In conventional reservoirs, oil recovery using LSW can be more than that obtained using produced water. Wettability alteration and improved oil recovery in carbonate reservoirs are believed to occur when the surface charge at the oil-brine and rock-brine interfaces are similar [54]. Laboratory experiments using LSW in unconventional reservoirs indicate there are several mechanisms that could be responsible for the oil recovery. These mechanisms include wettability alteration, detachment of clays,

multicomponent ion exchange, desorption of polar components from rock surfaces, formation of cracks in shale due to LSW imbibition and osmosis [33]. The pH of the 5 wt% KCl was 7.84. As in the case of the urea solution, we would expect the main mineral components of the shale and the oil droplets to be negatively charged at this pH, leading to a repulsive electrostatic interaction between the crude oil and rock surface. This could induce wettability reversal to a more water-wet condition.

The combination of urea and surfactant altered the wettability to a slightly lesser degree than the urea-only solution. The same trend was also observed in our previous work with dodecane-saturated shale samples [5] and could be due to the inability of the surfactant to irreversibly desorb the anionic organic carboxylates from the rock surface which may also interfere with the efficiency of the ammonia-induced wettability alteration. More work is needed to understand the interaction between the ammonia and anionic surfactant and the effect of this interaction on the wettability alteration of the shale.

3.4.5 Core soaking/oil recovery tests

The results of the oil recovery tests are shown in Figure *3-6*.

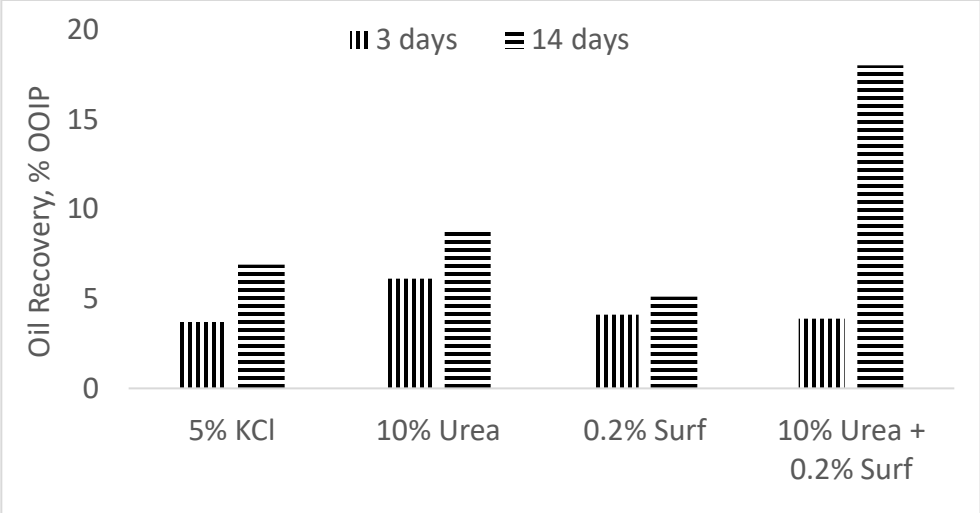

Figure 3-6 Oil recovery results for the different EOR fluids and soaking times

Results are shown for both the 3 days and 14 days soaking tests for the 3 tested EOR fluids plus the base fluid. The oil recovery increased with an increase in the soaking time for all the tested fluids. This is not surprising since the shale rock samples used in our test have extremely low permeability. Additionally, the core samples were aged in crude oil which altered the wettability of the cores to an oil-wet state. To increase oil recovery in shale oil reservoirs through water imbibition, it is necessary to modify the wettability of the shale matrix to a more water-wet state and overcome capillary forces in the shale nanopores. Maximizing water imbibition into the matrix/microfractures can lead to increased counter-current flow and increased oil recovery. Moreover, the generated CO_2 needs to migrate from the aqueous phase into the oil phase. This process is mainly governed by molecular diffusion which could be a very slow process, especially in unconventional reservoirs, and therefore requires a longer soaking period [59]. For the 14 days test, the recovery from the 10% urea case was lower than the recovery from the combination of urea and surfactant, despite the generation of CO_2 and ammonia in both cases. This could be due

to the higher IFT (9.7 mN/m) in the urea case compared to the combination of urea and surfactant case (0.3 mN/m). While most of the laboratory evaluation of surfactant EOR in shale has highlighted wettability alteration as the more important oil recovery mechanism, a few have attributed higher oil recovery to IFT reduction [33,60,61]. This could suggest that there is an optimum combination of wettability reversal and IFT reduction that results in higher oil recovery.

The oil recovery for the surfactant-only case was limited by the inability of the surfactant to substantially alter the wettability of the shale from oil-wet to a water-wet state and the absence of in-situ generated CO_2. The surfactant altered the wettability from oil-wet (119 °) to intermediate wet (96.7 °) state for the 14 days test. For the 5% KCl case, the oil recovery was low despite the relatively high wettability alteration. This could be due to the higher IFT values in addition to the absence of in-situ generated CO_2. The results for the 14 days soaking test show that synergism is realized by combining urea and surfactant. We hypothesize that the reduction in IFT by the anionic surfactant and the alteration in wettability by the generated ammonia allows the EOR fluid to penetrate further into the shale core sample. Thus, the generated CO_2 has more contact with the crude oil thereby facilitating improved oil recovery. In general, the more surface area of the rock matrix that can be contacted by the in-situ generated CO_2, the more the quantity and rate of hydrocarbon recovery [62].

The molecular weight of the Woodford crude oil can be estimated using the Cragoe correlation [63] :

$$MW_o = \frac{6084}{^\circ API - 5.9} \qquad (6)$$

Where MW_o is the molecular weight of the crude oil (g/mole) and °API is the API gravity (degrees

API). Using the above correlation, the molecular weight of the Woodford crude oil is estimated as 185 g/mole. Using the correlations developed by Emera and Sarma [64], the mole fraction of CO_2 dissolved in the Woodford crude oil at the experimental conditions of 250 °F and 1500 psi is estimated as 0.49. The dissolved CO_2 in the crude oil will lead to an estimated oil swelling factor of 1.047 at the test conditions. This implies that the dissolved CO_2 increases the volume of the crude oil by about 5 %. The solubility of CO_2 in the crude oil and the swelling of the oil due to the dissolved CO_2 is less for the crude oil compared to dodecane, due to the higher specific gravity and molecular weight of the crude oil.

Figure *3-7* and *Figure 3-8* show the plots of the oil recovery versus IFT for the 3 and 14 days tests, respectively. From these plots, there is no clear relationship between the oil recovery and IFT values. A similar observation was made in our previous study with dodecane-saturated Woodford shale samples [5]. Other researchers studying shale EOR using aqueous surfactant solutions have also observed the non-relationship between IFT values and oil recovery [65,66].

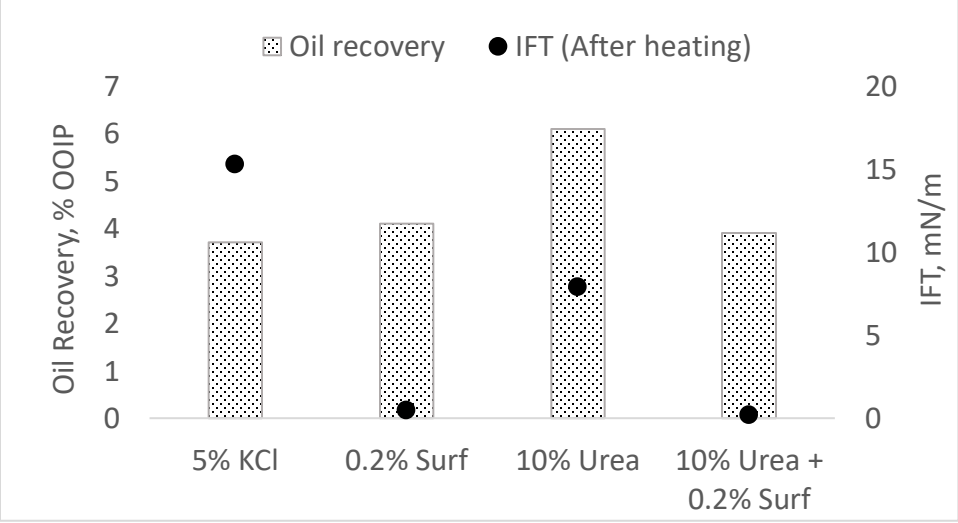

Figure 3-7 Oil recovery versus IFT for the 3 days EOR test

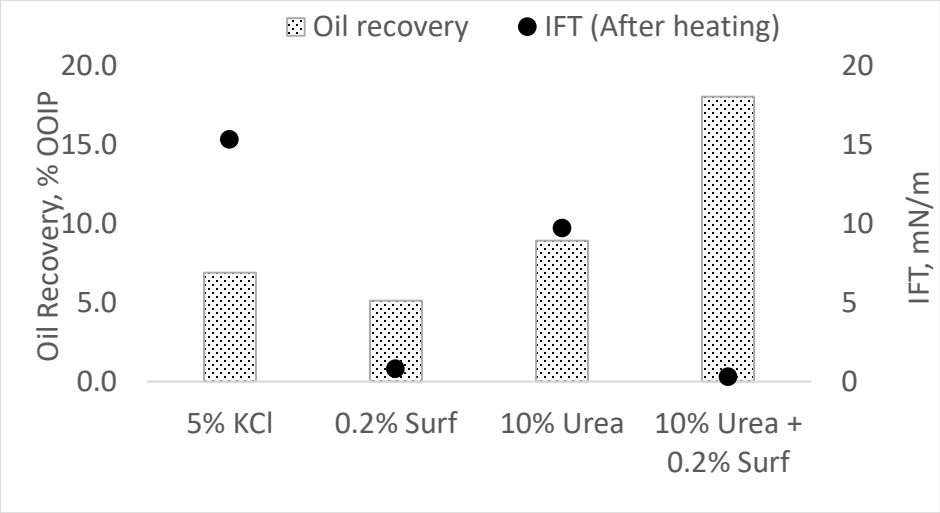

Figure 3-8 Oil recovery versus IFT for the 14 days test

Figure 3-9 and *Figure 3-10* show the plots of the oil recovery versus the change in contact angle for the 3 and 14 days tests, respectively. Since the initial contact angles for the oil-saturated cores were similar, as shown in Figure *3-4* and *Figure 3-5*, we used the change in contact angle to compare the performance of the different EOR fluids. There appears to be no clear relationship between the oil recovery and the change in contact angle for the 3 and 14 days tests. The lack of a clear relationship between the oil recovery, IFT and wettability alteration could be due to the complex mechanisms involved in the oil recovery process besides wettability alteration and IFT reduction, such as CO_2 diffusion. This is in contrast to our observation in the tests with dodecane-saturated shale core samples where we observed a slight increase in oil recovery with a decrease in the contact angle [5]. In that work, we obtained oil recoveries of 5.9 %, 21.1 %, 22.2 % and 23.0 % OOIP for the 5% KCl, surfactant-only, urea plus surfactant and urea-only fluids, respectively. However, the difference between the oil recoveries for the different EOR fluid systems was quite small and could be within experimental error. Moreover, the dodecane-saturated shale cores

used in our previous work were water-wet since dodecane does not contain surface active components that will alter the wettability of the shale cores.

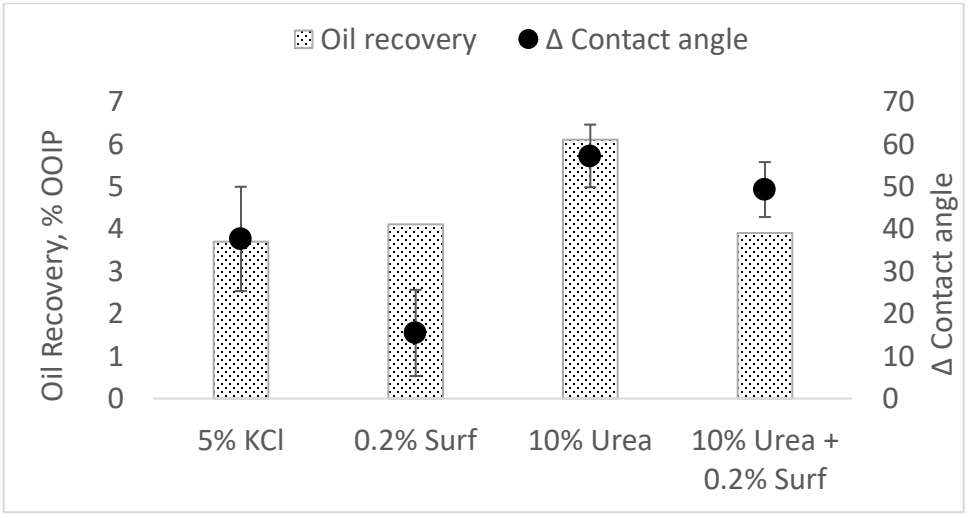

Figure 3-9 Oil recovery versus the change in contact angle for the 3 days test

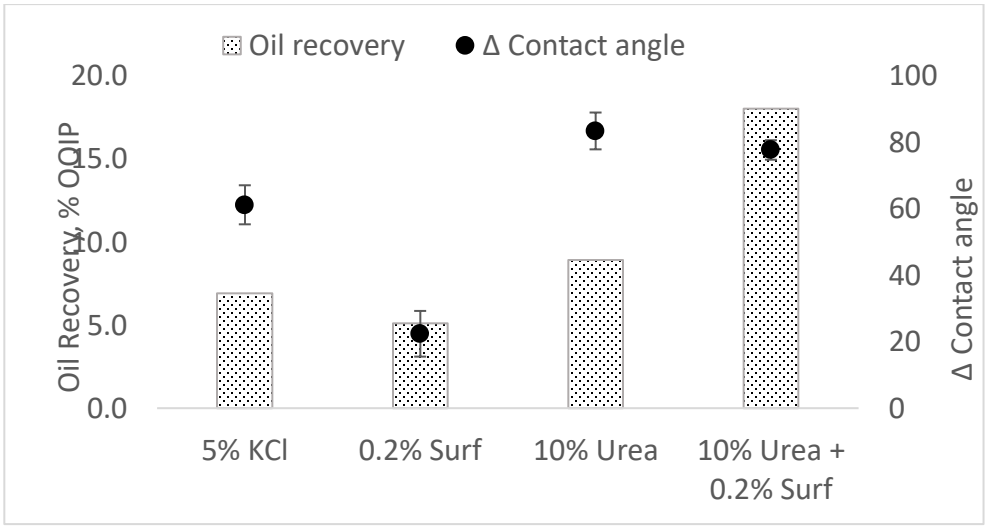

Figure 3-10 Oil recovery versus the change in contact angle for the 14 days test

The results also show that with the combination of urea and surfactant, the surfactant only needs to be capable of reducing the IFT between the oil and aqueous phase since the generated ammonia can alter the wettability of the shale cores from oil-wet to water-wet, especially for oil

samples with higher acid numbers. This implies that a broader range of surfactants can be used in the in-situ CO_2 generation fluid system.

To investigate the effect of miscible versus immiscible CO_2/crude oil conditions, the 2 weeks EOR tests were run at 1500 psi and 4000 psi for the 10% urea fluid. The minimum miscibility pressure (MMP) for pure CO_2 with Bakken light crude oil samples at 110 °C was determined to be 2528 psi [67], therefore we expect our crude oil sample to have an MMP value within the same range. The test results show a negligible increase in the oil recovery from 8.9 % to 10.4 % OOIP. We observed a similar phenomenon in previous tests conducted by our research group with dodecane-saturated shale core samples and sand pack flooding tests [5,18]. This is attributed to the absence of a separate CO_2 gas phase during urea flooding. The proposed mechanism is that the generated CO_2 is dissolved in the aqueous phase and when it encounters oil, it will migrate into the oil phase due to the higher solubility of CO_2 in the oil. The urea hydrolysis reaction equilibrium will shift towards the generation of more CO_2, upon depletion of the CO_2 concentration in the aqueous phase [18]. This implies that there is no apparent benefit to running the test at pressures above the MMP.

3.5 Conclusions

Laboratory tests with crude oil-saturated shale cores show that the use of in-situ generated CO_2 in liquid-rich shale is a viable EOR option. Both IFT reduction and wettability alteration play important roles in improving oil recovery from shale. The best oil recovery was achieved with the hybrid EOR formulation that combines urea and surfactant. The generated ammonia alters the wettability of the shale from an oil-wet state to a more water-wet state while the surfactant

reduces the IFT, thereby facilitating the imbibition of the EOR fluid into the shale matrix. The imbibition of the EOR fluid into the shale matrix allows the generated CO_2 to contact more oil and promotes oil recovery through a counter-current flow mechanism. Under the tested conditions, synergism was realized by combining urea and surfactant, especially for the longer duration (14 days) oil recovery test. Test results also show that there is no benefit to running the in-situ CO_2 generation EOR at above MMP conditions.

References

[1] Clark AJ. Determination of Recovery Factor in the Bakken Formation, Mountrail County, ND, OnePetro; 2009. https://doi.org/10.2118/133719-STU.

[2] Shoaib S, Hoffman BT. CO2 Flooding the Elm Coulee Field, Society of Petroleum Engineers; 2009. https://doi.org/10.2118/123176-MS.

[3] National Energy Technology Laboratory (NETL), https://netl.doe.gov/sites/default/files/2023-04/Program-157.pdf. Enhanced Oil Recovery Programme 157 2022.

[4] Hawthorne SB, Gorecki CD, Sorensen JA, Steadman EN, Harju JA, Melzer S. Hydrocarbon Mobilization Mechanisms from Upper, Middle, and Lower Bakken Reservoir Rocks Exposed to CO. SPE Unconventional Resources Conference Canada, Calgary, Alberta, Canada: Society of Petroleum Engineers; 2013. https://doi.org/10.2118/167200-MS.

[5] Ogbonnaya O, Wang S, Shiau B, Harwell J. Use of In-Situ CO2 Generation in Liquid-Rich Shale, Society of Petroleum Engineers; 2020. https://doi.org/10.2118/200383-MS.

[6] Shu WR. Carbonated waterflooding for viscous oil recovery. United States patent US4441555A, 1984.

[7] Teklu TW, Alameri W, Graves RM, Kazemi H, AlSumaiti AM. Low-salinity water-alternating-CO2 EOR. Journal of Petroleum Science and Engineering 2016;142:101–18. https://doi.org/10.1016/j.petrol.2016.01.031.

[8] Afzali S, Rezaei N, Zendehboudi S. A comprehensive review on Enhanced Oil Recovery by Water Alternating Gas (WAG) injection. Fuel 2018;227:218–46. https://doi.org/10.1016/j.fuel.2018.04.015.

[9] Esene C, Rezaei N, Aborig A, Zendehboudi S. Comprehensive review of carbonated water

injection for enhanced oil recovery. Fuel 2019;237:1086–107. https://doi.org/10.1016/j.fuel.2018.08.106.

[10] Bakhtiyarov SI. Technology of In-Situ Gas Generation to Recover Residual Oil Reserves | netl.doe.gov 2008. https://netl.doe.gov/node/4028 (accessed December 29, 2019).

[11] Jia X, Ma K, Liu Y, Liu B, Zhang J, Li Y. Enhance Heavy Oil Recovery by In-Situ Carbon Dioxide Generation and Application in China Offshore Oilfield. SPE Enhanced Oil Recovery Conference, Kuala Lumpur, Malaysia: Society of Petroleum Engineers; 2013. https://doi.org/10.2118/165215-MS.

[12] Wang Y, Hou J, Tang Y. In-situ CO2 generation huff-n-puff for enhanced oil recovery: Laboratory experiments and numerical simulations. Journal of Petroleum Science and Engineering 2016;145:183–93. https://doi.org/10.1016/j.petrol.2016.04.002.

[13] Wang S, Kadhum M, Yuan Q, Shiau B-J, Harwell JH. Carbon Dioxide in Situ Generation for Enhanced Oil Recovery. Carbon Management Technology Conference, Houston, Texas, USA: Carbon Management Technology Conference; 2017. https://doi.org/10.7122/486365-MS.

[14] Wang S, Kadhum MJ, Chen C, Shiau B, Harwell JH. Development of in Situ CO2 Generation Formulations for Enhanced Oil Recovery. Energy Fuels 2017;31:13475–86. https://doi.org/10.1021/acs.energyfuels.7b02810.

[15] Altunina LK, Kuvshinov VA. Evolution Tendencies of Physico-Chemical EOR Methods, OnePetro; 2000. https://doi.org/10.2118/65173-MS.

[16] Gumersky KK, Dzhafarov IS, Shakhverdiev AK, Mamedov YG. In-Situ Generation of Carbon Dioxide: New Way To Increase Oil Recovery, OnePetro; 2000. https://doi.org/10.2118/65170-MS.

[17] Shiau BJ, Hsu T-P, Roberts BL, Harwell JH. Improved Chemical Flood Efficiency by In Situ CO2 Generation, OnePetro; 2010. https://doi.org/10.2118/129893-MS.

[18] Wang S, Chen C, Shiau B, Harwell JH. In-situ CO2 generation for EOR by using urea as a gas generation agent. Fuel 2018;217:499–507. https://doi.org/10.1016/j.fuel.2017.12.103.

[19] Núñez-López V, Moskal E. Potential of CO2-EOR for Near-Term Decarbonization. Frontiers in Climate 2019;1. https://doi.org/10.3389/fclim.2019.00005.

[20] Yalkowsky SH, He Y, Jain P, He Y, Jain P. Handbook of Aqueous Solubility Data. CRC Press; 2016. https://doi.org/10.1201/EBK1439802458.

[21] Wang S, Chen C, Li K, Yuan N, Shiau B, Harwell JH. In Situ CO2 Enhanced Oil Recovery: Parameters Affecting Reaction Kinetics and Recovery Performance. Energy Fuels

2019;33:3844–54. https://doi.org/10.1021/acs.energyfuels.8b03734.

[22] Altunina LK, Kuvshinov VA. Physicochemical methods for enhancing oil recovery from oil fields. Russ Chem Rev 2007;76:971–87. https://doi.org/10.1070/RC2007v076n10ABEH003723.

[23] Wang S, Li K, Chen C, Onyekachi O, Shiau B, Harwell JH. Isolated mechanism study on in situ CO2 EOR. Fuel 2019;254:115575. https://doi.org/10.1016/j.fuel.2019.05.158.

[24] Mungan N. Certain Wettability Effects In Laboratory Waterfloods. Journal of Petroleum Technology 1966;18:247–52. https://doi.org/10.2118/1203-PA.

[25] Ehrlich R, Hasiba HH, Raimondi P. Alkaline Waterflooding for Wettability Alteration-Evaluating a Potential Field Application. Journal of Petroleum Technology 1974;26:1335–43. https://doi.org/10.2118/4905-PA.

[26] Johnson CEJ. Status of Caustic and Emulsion Methods. Journal of Petroleum Technology 1976;28:85–92. https://doi.org/10.2118/5561-PA.

[27] Spinler EA, Baldwin BA. Surfactant Induced Wettability Alteration in Porous Media. In: Schramm LL, editor. Surfactants: Fundamentals and Applications in the Petroleum Industry, Cambridge: Cambridge University Press; 2000, p. 159–202. https://doi.org/10.1017/CBO9780511524844.006.

[28] Wang D, Butler R, Liu H, Ahmed S. Flow-Rate Behavior and Imbibition in Shale. SPE Reservoir Evaluation & Engineering 2011;14:485–92. https://doi.org/10.2118/138521-PA.

[29] Alvarez JO, Schechter DS. Wettability Alteration and Spontaneous Imbibition in Unconventional Liquid Reservoirs by Surfactant Additives. SPE Reservoir Evaluation & Engineering 2017;20:107–17. https://doi.org/10.2118/177057-PA.

[30] Sheng JJ. What type of surfactants should be used to enhance spontaneous imbibition in shale and tight reservoirs? Journal of Petroleum Science and Engineering 2017;159:635–43. https://doi.org/10.1016/j.petrol.2017.09.071.

[31] Alharthy N, Teklu TW, Kazemi H, Graves RM, Hawthorne SB, Braunberger J, et al. Enhanced Oil Recovery in Liquid-Rich Shale Reservoirs: Laboratory to Field. SPE Reservoir Evaluation & Engineering 2018;21:137–59. https://doi.org/10.2118/175034-PA.

[32] Teklu TW, Li X, Zhou Z, Alharthy N, Wang L, Abass H. Low-salinity water and surfactants for hydraulic fracturing and EOR of shales. Journal of Petroleum Science and Engineering 2018;162:367–77. https://doi.org/10.1016/j.petrol.2017.12.057.

[33] Burrows LC, Haeri F, Cvetic P, Sanguinito S, Shi F, Tapriyal D, et al. A Literature Review of CO2, Natural Gas, and Water-Based Fluids for Enhanced Oil Recovery in Unconventional

Reservoirs. Energy Fuels 2020;34:5331–80. https://doi.org/10.1021/acs.energyfuels.9b03658.

[34] Yarveicy H, Habibi A, Pegov S, Zolfaghari A, Dehghanpour H. Enhancing Oil Recovery by Adding Surfactants in Fracturing Water: A Montney Case Study, Society of Petroleum Engineers; 2018. https://doi.org/10.2118/189829-MS.

[35] Kumar K, Dao EK, Mohanty KK. Atomic Force Microscopy Study of Wettability Alteration by Surfactants. SPE Journal 2008;13:137–45. https://doi.org/10.2118/93009-PA.

[36] Kazempour M, Kiani M, Nguyen D, Salehi M, Bidhendi MM, Lantz M. Boosting Oil Recovery in Unconventional Resources Utilizing Wettability Altering Agents: Successful Translation from Laboratory to Field, Society of Petroleum Engineers; 2018. https://doi.org/10.2118/190172-MS.

[37] Bidhendi MM, Kazempour M, Ibanga U, Nguyen D, Arruda J, Lantz M, et al. A Set of Successful Chemical EOR Trials in Permian Basin: Promising Field and Laboratory Results, Unconventional Resources Technology Conference; 2019. https://doi.org/10.15530/urtec-2019-881.

[38] Buckley JS, Fan T. Crude Oil/Brine Interfacial Tensions1. Petrophysics - The SPWLA Journal of Formation Evaluation and Reservoir Description 2007;48.

[39] Hirasaki G, Miller CA, Puerto M. Recent Advances in Surfactant EOR. SPE Journal 2011;16:889–907. https://doi.org/10.2118/115386-PA.

[40] Puerto M, Hirasaki GJ, Miller CA, Barnes JR. Surfactant Systems for EOR in High-Temperature, High-Salinity Environments. SPE Journal 2012;17:11–9. https://doi.org/10.2118/129675-PA.

[41] Alvarez JO, Saputra IWR, Schechter DS. Potential of Improving Oil Recovery with Surfactant Additives to Completion Fluids for the Bakken. Energy Fuels 2017;31:5982–94. https://doi.org/10.1021/acs.energyfuels.7b00573.

[42] Maini B, Wassmuth F, Schramm LL. Fines Migration in Petroleum Reservoirs. Suspensions: Fundamentals and Applications in the Petroleum Industry, vol. 251, American Chemical Society; 1996, p. 321–75. https://doi.org/10.1021/ba-1996-0251.ch007.

[43] van den Pol E, T. van Rijn CH, van Batenburg DW, Southwick JG, Mastan AA, Abdul Manap AA, et al. Alkali Surfactant Polymer Flooding Using Ammonia for Offshore use, International Petroleum Technology Conference; 2014. https://doi.org/10.2523/IPTC-18077-MS.

[44] Sharma H, Lu J, Weerasooriya UP, Pope GA, Mohanty KK. Adsorption in Chemical Floods with Ammonia as the Alkali, Society of Petroleum Engineers; 2016. https://doi.org/10.2118/179682-MS.

[45] Southwick JG, van den Pol E, van Rijn CHT, van Batenburg DW, Boersma D, Svec Y, et al. Ammonia as Alkali for Alkaline/Surfactant/Polymer Floods. SPE Journal 2016;21:10–21. https://doi.org/10.2118/169057-PA.

[46] Zeng T, Kim KT, Werth CJ, Katz LE, Mohanty KK. Surfactant Adsorption on Shale Samples: Experiments and an Additive Model. Energy Fuels 2020;34:5436–43. https://doi.org/10.1021/acs.energyfuels.9b04016.

[47] Anderson WG. Wettability Literature Survey- Part 1: Rock/Oil/Brine Interactions and the Effects of Core Handling on Wettability. Journal of Petroleum Technology 1986;38:1,125-1,144. https://doi.org/10.2118/13932-PA.

[48] Saputra IWR, Adebisi O, Ladan EB, Bagareddy A, Sarmah A, Schechter DS. The Influence of Oil Composition, Rock Mineralogy, Aging Time, and Brine Pre-soak on Shale Wettability. ACS Omega 2021;7:85–100. https://doi.org/10.1021/acsomega.1c03940.

[49] RezaeiDoust A, Puntervold T, Strand S, Austad T. Smart Water as Wettability Modifier in Carbonate and Sandstone: A Discussion of Similarities/Differences in the Chemical Mechanisms. Energy Fuels 2009;23:4479–85. https://doi.org/10.1021/ef900185q.

[50] Alvarez JO, Tovar FD, Schechter DS. Improving Oil Recovery in the Wolfcamp Reservoir by Soaking/Flowback Production Schedule With Surfactant Additives. SPE Reservoir Evaluation & Engineering 2018;21:1,083-1,096. https://doi.org/10.2118/187483-PA.

[51] Sheng JJ. Review of Surfactant Enhanced Oil Recovery in Carbonate Reservoirs. Advances in Petroleum Exploration and Development 2013;6:1–10. https://doi.org/10.3968/j.aped.1925543820130601.1582.

[52] Austad T, Milter J. Spontaneous Imbibition of Water Into Low Permeable Chalk at Different Wettabilities Using Surfactants, Society of Petroleum Engineers; 1997. https://doi.org/10.2118/37236-MS.

[53] Standnes DC, Austad T. Wettability alteration in chalk: 2. Mechanism for wettability alteration from oil-wet to water-wet using surfactants. Journal of Petroleum Science and Engineering 2000;28:123–43. https://doi.org/10.1016/S0920-4105(00)00084-X.

[54] Tetteh JT, Brady PV, Barati Ghahfarokhi R. Review of low salinity waterflooding in carbonate rocks: mechanisms, investigation techniques, and future directions. Advances in Colloid and Interface Science 2020;284:102253. https://doi.org/10.1016/j.cis.2020.102253.

[55] Buckley JS, Takamura K, Morrow NR. Influence of Electrical Surface Charges on the Wetting Properties of Crude Oils. SPE Reservoir Engineering 1989;4:332–40. https://doi.org/10.2118/16964-PA.

[56] Hsieh PY. Heats of adsorption of ammonia on silica-alumina catalysts and their surface

energy distributions. Journal of Catalysis 1963;2:211–22. https://doi.org/10.1016/0021-9517(63)90046-0.

[57] Clark A, Holm VCF, Blackburn DM. The nature of silica-alumina surfaces: I. Thermodynamics of adsorption of ammonia. Journal of Catalysis 1962;1:244–54. https://doi.org/10.1016/0021-9517(62)90053-2.

[58] Fowkes FM. ATTRACTIVE FORCES AT INTERFACES. Ind Eng Chem 1964;56:40–52. https://doi.org/10.1021/ie50660a008.

[59] Kanfar MS, Ghaderi SM, Clarkson CR, Reynolds MM, Hetherington C. A Modeling Study of EOR Potential for CO2 Huff-n-Puff in Tight Oil Reservoirs - Example from the Bakken Formation. SPE Unconventional Resources Conference, Calgary, Alberta, Canada: Society of Petroleum Engineers; 2017. https://doi.org/10.2118/185026-MS.

[60] B. Alamdari B, Hsu T-P, Nguyen D, Kiani M, Salehi M. Understanding the Oil Recovery Mechanism in Mixed-Wet Unconventional Reservoirs: Uniqueness and Challenges of Developing Chemical Formulations, OnePetro; 2018. https://doi.org/10.2118/190201-MS.

[61] Chevalier T, Labaume J, Gautier S, Chevallier E, Chabert M. A Novel Experimental Approach for Accurate Evaluation of Chemical EOR Processes in Tight Reservoir Rocks, OnePetro; 2018. https://doi.org/10.2118/190171-MS.

[62] Alfarge D, Wei M, Bai B. Factors Affecting CO2-EOR in Shale-Oil Reservoirs: Numerical Simulation Study and Pilot Tests. Energy Fuels 2017;31:8462–80. https://doi.org/10.1021/acs.energyfuels.7b01623.

[63] Cragoe CS. Thermal Properties of Petroleum Products 1929: November 9, 1929. U.S. Government Printing Office; 1929.

[64] Emera MK, Sarma HK. Prediction of CO2 Solubility in Oil and the Effects on the Oil Physical Properties. Energy Sources, Part A: Recovery, Utilization, and Environmental Effects 2007;29:1233–42. https://doi.org/10.1080/00908310500434481.

[65] Nguyen D, Wang D, Oladapo A, Zhang J, Sickorez J, Butler R, et al. Evaluation of Surfactants for Oil Recovery Potential in Shale Reservoirs. All Days, Tulsa, Oklahoma, USA: SPE; 2014, p. SPE-169085-MS. https://doi.org/10.2118/169085-MS.

[66] Zhang F, Saputra IWR, Adel IA, Schechter DS. Scaling for Wettability Alteration Induced by the Addition of Surfactants in Completion Fluids: Surfactant Selection for Optimum Performance, Unconventional Resources Technology Conference; 2018. https://doi.org/10.15530/URTEC-2018-2889308.

[67] Jin L, Hawthorne S, Sorensen J, Pekot L, Bosshart N, Gorecki C, et al. Utilization of Produced Gas for Improved Oil Recovery and Reduced Emissions from the Bakken

Formation, OnePetro; 2017. https://doi.org/10.2118/184414-MS.

Chapter 4 Low-temperature *In Situ* CO_2 Enhanced Oil Recovery

Abstract

The new generation *in situ* CO_2 enhanced oil recovery (ICE), which delivers CO_2 by injection of a CO_2 generating agent solution, was proven to offer robust recovery performances and potential cost and workflow benefits. However, the developed ICE systems are either formulated with a complex fluid recipe or a simplified version of a fluid system limited by high-temperature requirements. This work focused on removing the requirement of high reservoir temperature in our previous work while maintaining the simplicity of the single fluid injection system. Urease is studied as the catalyst for urea hydrolysis and evaluated experimentally. The denaturation behavior of urease and the reaction kinetics of the catalyzed urea hydrolysis process are tested at different urea concentrations, urease concentrations, and temperatures. Four sets of one-dimensional sand pack flowthrough experiments are conducted to verify the tertiary recovery potential of the newly developed low-temperature ICE system with different lithology. The extent of wettability alteration and the recovery mechanism for different lithologies was determined through core sample imbibition experiments and direct contact angle measurements. From the experimental results, urease-catalyzed urea hydrolysis is proven to be effective in tertiary oil recovery applications below the 50 °C reservoir temperature range with urea conversion ratio up to 68.7%. The selected low-temperature ICE system (10 wt% urea solution with 31 U/g urease) had superior tertiary recoveries(E_{tr}) in the flowthrough test for sandstone (E_{tr}=31.3%) and limestone (E_{tr}=27.5%) than the corresponding high-temperature cases. Imbibition tests of this improved formulation with various porous media show distinct wettability reversal trends

towards a more water-wet state post-imbibition. This trend is associated with the produced NH_3 and CO_2 due to urea hydrolysis. Both oil-aged sandstone and limestone imbibition tests show noticeable water wetness improvement. The observations of this work significantly expand the operational envelopes of the current ICE system.

4.1 Introduction

CO_2-enhanced oil recovery is well-proven in field applications [1] and is the most commonly used enhanced oil recovery(EOR) technique in the US [2]. The diversity of CO_2-related EOR applications has expanded tremendously over the years. Foam-assisted CO_2 EOR, carbonated water injection, and CO_2 water alternating gas [3-8] have been extensively studied to improve EOR performance by providing better mobility control during flooding. However, CO_2 availability limits its application to some CO_2-suitable reservoir candidates [9]. The *in situ* CO_2 EOR(ICE) developed by our research group was initially designed to overcome the challenges associated with offshore reservoir applications, including the dependence of the CO_2 EOR process on the availability of a CO_2 source, CO_2 transportation and injection infrastructure, by delivering CO_2 indirectly to the reservoir through the injection of a single gas generating agent solution. The introduced chemical decomposes at reservoir conditions and releases significant amounts of CO_2. Under the offshore reservoir context, the reservoir temperature could range from 158 °C [10] to over 176 °C [11]. With high enough temperatures, the previous studies did not consider CO_2 generation reaction rate kinetics-related issues. However, for onshore reservoir applications, low reservoir temperatures are commonly reported. To expand the operational envelope of the ICE to onshore, shallow brown reservoirs, the operating temperature needs to be lowered to around the 50 °C range [12]. Aqueous phase injection for shale reservoirs has also proven effective [13, 14]. There

is also a lot of potential for CO_2 shale EOR [15]. Urea injection application showed good tertiary recovery in a pilot test in Liaohe oil field[16]. After the urea-assisted steam treatment [17], the water cut of the production well decreased from 94.8% to 85.1%. Based on the laboratory study, the chemical cost of the urea application is estimated to be $6 per additional barrel of oil [18]. Moreover, a urea-related EOR study showed good prospects for bitumen reservoirs [19] and liquid-rich shale [20]. Hence, the application of the ICE as an aqueous phase injection with CO_2-related EOR mechanisms also needs to be explored for shale applications. For example, some Eagle Ford wells have reservoir temperatures of around 101 °C [21], which is lower than the operating temperature of the previously published ICE system. Therefore, a study on the low-temperature compatible ICE system is necessary.

The currently available low-temperature CO_2 generating systems are based on acid and base reactions with dual fluid systems and multiple slug injections. Some examples in the literature include low pH HEDTA-EDTA-carbonate reservoir [22, 23], citric acid-carbonate reservoir [24], bicarbonate-citric acid [25], sodium carbonate-acid [26-28] and carbonate salt-acid-surfactant [29, 30]. To maintain the single-fluid ICE system's simplicity, we targeted the one slug injection single-fluid system in this work.

Our previous high-temperature ICE system used urea as the gas-generating agent because of its accessibility, large manufacturing scale, minimum human/environmental concerns, and superior water solubility for EOR field operations. Therefore, the ideal solution would be to keep the currently available system by adding a catalyst to reduce the required reservoir temperature. Multiple potential urea hydrolysis catalysts are available for this purpose. Sodium Ortho Vanadate and Vanadium Pentoxide are reported to be effective in catalyzing the urea hydrolysis

by Schell [31]. However, we did not see catalyzed urea hydrolysis using Sodium Ortho Vanadate and Vanadium Pentoxide at our target temperature range (around 50 °C).

Urea is hydrolytically stable under ambient conditions. Some researchers claimed that the half-life of urea at 38°C and pH 7 is 3.6 years, and the urease-catalyzed hydrolysis of urea is at least 10^{14} as fast as spontaneous urea hydrolysis [33]. Sumner [34] first crystallized urease as a pure protein and reported that it might act as an enzyme. Urease catalyzes the hydrolysis of urea to form carbamate, which spontaneously decomposes to CO_2 and NH_3. In nature, bacteria, fungi, yeast, and plants produce urease, which catalyzes urea degradation to nitrogen for their growth [35]. Therefore, for decades, urea has been one of the most used nitrogen fertilizers worldwide. However, the active urease on the soil surface catalyzes the urea hydrolysis resulting in 70% nitrogen loss to the environment before the target plant utilization. To meet the future challenge of food security, urease inhibitor studies have attracted a lot of research interests [36]. In contrast, urea application in the petroleum industry requires low-temperature urease catalyzed hydrolysis of urea. The overwhelmingly studied urease inhibitors could be used to guide the study of catalyzed urea hydrolysis.

Ureases are nickel-dependent enzymes that catalyze urea hydrolysis as shown in the following equation [37]:

$$NH_2CONH_2 + H_2O \xrightarrow{urease} NH_2COOH + NH_3 + H_2O \xrightarrow{spontaneous} 2NH3_3 + H_2CO_3 \qquad (6)$$

$$H_2CO_3 \leftrightarrow H_2O + CO_2 \qquad (7)$$

$$H_2O + NH_3(aq.) \leftrightarrow OH^- + NH_4^+ \qquad (8)$$

Since the available urease inhibitor studies are performed under normal biological conditions, i.e., low urea/urease concentration, atmospheric pressure, and pH control, EOR-related urease study needs to be performed to gain more insights into this application. Type III urease is found in jack beans and is extensively studied. Therefore, type III urease is selected in this work. The application costs can be lower if jack bean powder rather than purified urease is used. There are currently no studies of urease application in petroleum extraction. Hence, urease catalyzed ICE systems are studied to understand chemical concentration requirements and design as well as reaction environment control. After the chemical slug formulation design, the newly developed low-temperature ICE is tested in sand pack flooding to determine and compare its tertiary recovery ability. Finally, imbibition tests and direct contact angle measurements are performed to further explore the individual contributions of NH_3 and CO_2 in different porous media. Besides the temperature, all the experiments are performed at the same condition as our previously published high-temperature work [38]. Dead crude oil is used in this research. Because of the solution gas, the viscosity of live oil is notably lower than that of dead oil. Besides the viscosity, the gas diffusion coefficient, the interfacial tension between phases, and the gas expansion energy-induced oil production depend on the dissolved gas [39, 40]. Therefore, dead oil does not account for some mechanisms of enhanced oil recovery process. This initial study focuses on the basic mechanism of the chemical system. Additionally, this paper provides proof of concept for applying urease catalyzed urea hydrolysis in enhanced oil recovery. With the result of this work, the operational envelope is expanded to a much wider temperature range.

4.2 Experimental

4.2.1 Material

Type III urease (jack bean), 500-800 units/mL in glycerol solution, was purchased from Sigma-Aldrich. One unit of activity corresponds to the amount of the enzyme that liberates 1.0 μmol NH_3 from urea per minute at pH 7.0 and 25°C[41]. Urea (99 wt.%) was purchased from Acros Organics. Abu Dhabi National Oil Company (ME oil) donated the crude oil. The Ottawa sand F-75(99.7% Silica) was purchased from U.S. Silica for sand pack preparation. Berea sandstone core (93% Silica, 16.2% porosity, 115 mD permeability) and Indiana limestone cores (98% Calcite 19.4% porosity, 64 mD permeability) were purchased from Kocurek Industries for the wettability study.

4.2.2 Urease-catalyzed urea hydrolysis

Urease-catalyzed urea hydrolysis was performed at different temperatures. The tested temperature range covered the common low-temperature mature oil field formation condition. The urea concentration change during hydrolysis was determined and recorded to study the hydrolysis kinetics. 2.5 wt.% or 10 wt.% urea solution with different urease concentrations was prepared with deionized water (DI water). 20 ml of the mixture solution was loaded into a sealed vial. In each hydrolysis test, multiple replicate vials of the individual targeted solution system were prepared depending on the hydrolysis duration. The group of sample vials was then loaded into the incubator at the targeted temperature. At each designated time interval, one of the vials was taken from the incubator. No special treatment was applied to terminate the reaction at the specified sampling time. The sample analysis was applied right after sample collection. pH of each

collected sample was determined before any other analysis. The time for sampling and analysis was taken into account to offset any timing errors caused by not terminating the reaction. Each case was repeated three times to quantify the experimental uncertainty. Since the urease activity is highly dependent on the pH, the urea concentration of the hydrolysis test is a crucial parameter.

The urea solution was analyzed using a high-performance liquid chromatography (HPLC) equipped with a UV-vis detector [42]. The wavelength of the UV detector was set at 200 nm. A reverse-phase C18 column separated urea from the reaction mixture at 30 °C. A methanol and water (5/95) solution was used as the mobile phase and the HPLC pumping rate was 0.7 mL/min.

4.2.3 Sand pack flooding

The sand pack flooding test was adopted from this group's previous work [18]. The setup for the sand pack flooding tests is shown in Figure *4-1*. This is the first study on a low-temperature urease-catalyzed enhanced oil recovery system. Therefore, no electrolyte was introduced to the system to prevent any possible complex phenomenon besides the reaction kinetics of the enzyme-catalyzed reaction. The flowthrough test was performed at 1500 psi and 50 °C. Ottawa sand and crushed Indiana limestone were used to prepare the sand pack which was then saturated with crude oil and aged for 24 hours at 80 °C [18]. The sand pack was about 6.0 inches long and 0.8 inches in diameter. Afterward, water flooding was initiated by injecting 6-8 pore volume (PV) of water until the oil cut dropped to zero. Once the residual oil saturation was established, 1 PV of treatment fluid was injected, followed by a 72-hour shut-in period. The shut-in time was designed to allow enough urea hydrolysis and overcome the mass transfer resistance

of CO_2 between the aqueous phase and the oil phase at the experimental condition. During the urea hydrolysis reaction, water is consumed, leading to a decrease in the aqueous phase volume

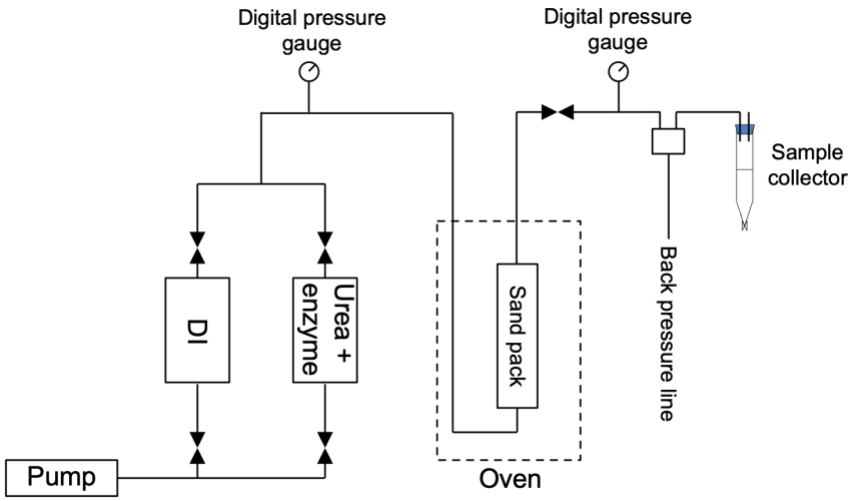

Figure 4-1 Setup for the sand pack flooding

and subsequent drop in pressure. To mimic a reservoir with a constant pressure boundary, we used an ISCO 500D syringe pump to maintain a constant pressure in the system throughout the test. The reaction-induced volume change is documented in our previous work [43]. After the shut-in period, the water flooding was resumed to collect all the mobilized oil until no additional oil was produced.

4.2.4 Rock surface wettability alteration

The contact angle of the crude oil/brine/rock system was measured to study the wettability alteration caused by the ICE treatment. A Berea sandstone and Indiana limestone core were used for the contact angle measurement. Each core sample was polished with a 60-grit aluminum oxide wheel. The dimensions of the polished core sample were 1-inch diameter and around 1 cm thickness. For the base case test, the core was saturated with DI only. For the tested case, the

cores were saturated and aged with crude oil for 24 hours at 80 °C. After the core aging, the tested cores were treated by a low-temperature ICE imbibition at 1500 psi and 50 °C. A DI imbibition at the same conditions benchmarked the ICE imbibition test.

The ICE solution or DI was loaded into the high-pressure cell. A syringe pump controlled the pressure at a fixed 1500 psi to compensate for the pressure drop caused by water consumption during the hydrolysis. Then the system was pressurized at 50 °C for 72 hours. Based on the reaction kinetics of the low-temperature catalyzed system, the reaction stopped within 72 hours. At the end of the imbibition test, the system was depressurized, cooled to room temperature and the core sample and solution were recovered for contact angle measurement.

Before contact angle measurements, the excess fluid on the polished surface was cleaned with lint-free Kimwipes. After the core sample preparation, the recovered solution was loaded into the quartz cell and the core sample was submerged in the solution for 5 minutes before oil contact. Each contact angle measurement was repeated at least three times to quantify the experimental uncertainty.

The captive bubble method [38] was used to measure the contact angle when the rock surface was submerged in the liquid. The oil bubble was generated by a "J" shaped 0.74 mm diameter needle and carefully attached to the core surface. Then the bubble was allowed to equilibrate with the solution and rock surface before contact angle measurement. The Biolin ATTENSION Theta ADSA system recorded the video for 10 seconds at 12 frames per second when a stable contact angle reading was obtained. At least three bubbles were generated for each solution to estimate the standard deviation of the measurement. The core disc could be water wet($\theta<75$), oil-wet($\theta>115$), or intermediate-wet($75<\theta<115$).

4.3 Results and Discussion

4.3.1 Urea hydrolysis

In the previously published urease study, the urea concentration used in the experiments was relatively low since the research interest was enzyme inhibition. The tested urea concentration was at a few millimolar to 2.5 molar range [37, 44]. The optimal pH for urease activity was reported as 9.0 and 7.0. Therefore, the pH of urease-related studies was controlled with a buffer at pH=9.0 [44, 45] or pH=7.0 [46, 47]. For jack bean urease, pH=7.0 was commonly used as the optimal in the activity studies [41, 48-51]. Urea concentration and reaction temperature can also affect urease activity. The optimal temperatures for urease activity were reported at different pH values [52].

The reaction rate of the urease-catalyzed ICE system is characterized in this section. For the ICE application, one primary target is to achieve enough chemical conversion ratio and reaction rate with minimum cost and fluid complexity. The other target is to generate enough CO_2 and NH_3 to mobilize the residual oil. Therefore, in this study, the only modification was the introduction of urease to the currently available ICE system. No buffer was introduced to control the solution pH. The buffered system always showed better urease activity than the non-buffered system [45, 51, 53]. Also, heavy metal ions in the solution affect urease activity [48]. Therefore, this section is designed to study the urease activity without buffer and salt at high urea concentrations. The hydrolysis of urea in a possible ICE application is explored in this section since no urease-related enhanced oil recovery application exists in the literature.

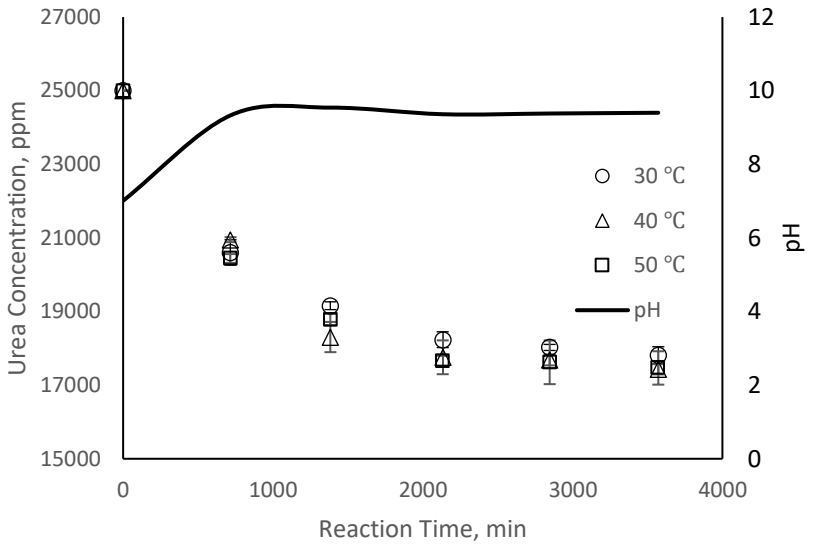

Figure 4-2 Urea concentration change of the jack bean urease catalyzed hydrolysis system at different temperatures. 2.5 wt.% urea and 0.31 unit/g urease

Figure *4-2* shows the urea concentration change of the jack bean urease-catalyzed hydrolysis system. Based on the literature review, the first target of this work is to test the effect of jack bean urease on catalyzing possible ICE systems at low reservoir temperature conditions. Since the study for the activity of jack bean urease [50] and soil urease [45] showed a temperature dependence, the possible optimal temperature in the urease-catalyzed ICE system was also studied. The highest temperature was selected to be the same as the well-studied low-temperature CO_2 EOR candidate (50 °C) [54]. The urea hydrolysis reaction rate for high-temperature reservoirs was shown to be high enough for the ICE treatment purpose [18]. 2.5 wt.% urea with 0.31 units/g urease systems were tested as the initial system at different temperatures without buffers to prove the concept.

From Figure *4-2*, the 0.31 units/g urease can hydrolyze urea at low-temperature conditions without buffer. The pH displayed in the plot is the average pH of three samples at different hydrolysis temperatures because the pH of different samples at the same hydrolysis time are

very similar. The pH of the solution increased quickly within the first 1000 minutes and plateaued at pH=9.55. Overall, the concentration trend at different temperatures showed no significant difference and the final urea concentration after hydrolysis were similar. The conversion ratio of 30, 40, 50 °C samples was 27.2%, 28.5% and 27.9% respectively. The measured conversion ratio agrees with the literature reported jack bean urease optimal temperature [37]. After 2133 minutes, the urea concentration of the three cases stabilizes at around 18000 ppm, indicating full denaturation of urease at this condition. Pettit et al. [51] studied the stability of different urease, including the jack bean urease. In their buffered system, the urease solution showed a similar effect as the observation in Figure *4-2*. For example, the half-life of the jack bean urease at 37 °C was measured to be 1.3 days. Overall, the half-life of all their tested urease samples decreased with an increase in temperature. For some low-temperature cases, the urease activity plateaued at a certain value. Comparing the documented literature data to the measured data in this work, the half-life of jack bean urease in our tested condition was much shorter than their buffered case, which could be attributed to the high urea concentration [52] and elevated pH in our tests.

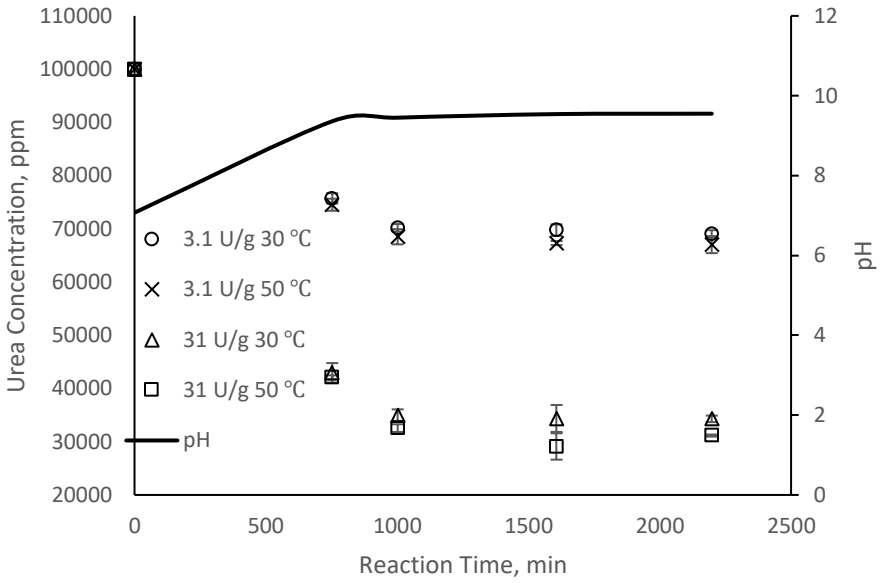

Figure 4-3 Urea concentration change of the jack bean urease catalyzed hydrolysis at different temperatures with different urease dosages and 10 wt.% urea

Based on the observations from the initial urease-catalyzed tests, it could be concluded that the non-buffered high urea concentration system could be hydrolyzed at low temperatures by simply adding urease. However, the low conversion ratio in a 2.5 wt.% urea system is not enough to be used as an ICE system to mobilize the residual oil [18]. Therefore, the potential of the urease-catalyzed system needs to be further expanded. A faster reaction rate, higher conversion ratio, and more generated CO_2 and NH_3 quantity would be the ideal candidate for ICE. Figure *4-3* shows the urea concentration change of the jack bean urease-catalyzed hydrolysis system with higher urea and urease concentrations. The pH displayed in the plot is also the average pH since no significant pH difference is observed among the samples analyzed at the same time interval. The final pH and the overall urea concentration trend of the high urea concentration test are similar to the low urea concentration test. The urea concentrations drop in the first 1000 minutes, then plateau at a certain concentration. The urease denaturation time shown in Figure *4-3* is shorter

than the low urea concentration test. Therefore, the urease denaturation time is dependent on the urea concentration but not the temperature at the tested conditions. This observation is inconsistent with the observation reported by Pettit et al. [51], which could be mainly attributed to the buffer usage and urea concentration difference between these tests.

The 3.1 unit/g and 31 unit/g tests had the same urease denaturation time, which indicates that the urease denaturation time is not dependent on the urease concentration in the high urea concentration non-buffered system. The final urea conversion ratios for the 3.1 units/g system are 27.9% and 33.0% at 30 °C and 50 °C, respectively. For the 31 units/g system, the final urea conversion ratios are 63.3% and 68.7% at 30 °C and 50 °C , respectively. The 50 °C test showed better conversion ratios. Compared to the previous test, two more observations could be deduced. Firstly, the urea hydrolysis product concentration is different in 3.1 units/g and 31 units/g cases. However, the urease denaturation time is the same. Therefore, the urease denaturation time is not dependent on the urea hydrolysis product concentration. Secondly, with a shorter urease denaturation time in the high urea concentration test, a higher urease dosage could achieve a better conversion ratio and reaction rate. Urease activity is also dependent on the urea concentration [52]. Therefore, the conversion ratio increases nonlinearly with the increase of the urease units and urea ratio in this section. The proof of concept of the urease-catalyzed high-concentration urea hydrolysis is provided in this section. The achieved urea conversion ratio of the proposed system falls within the known ICE operation envelope [18], which makes the low-temperature ICE possible. A more detailed study of the urease catalyzed ICE system needs to be carried out in the future.

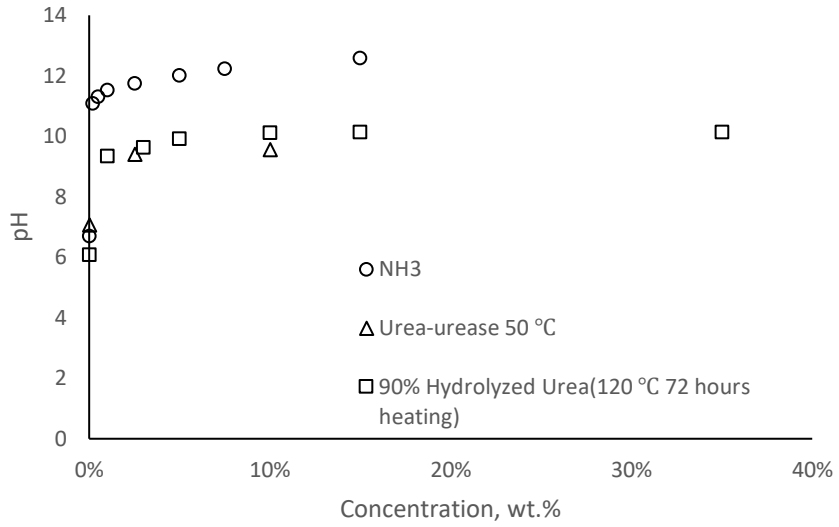

Figure 4-4 pH of the ICE system

Figure *4-4* compares the pH of the current ICE systems and NH_3(aq) solution. The NH_3(aq) concentration was selected to have the same NH_3 concentration as 90% hydrolyzed urea solution (e.g., 35 wt.% urea corresponds to 15% NH_3). The NH_3(aq) solution had the highest pH. The resulting solution after urea hydrolysis reaction at 120 °C had a much lower pH than aqueous NH_3 solution with a similar concentration of NH_3. This is due to the CO_2 generated during the hydrolysis of urea, which will reduce the solution pH. The urease catalyzed urea solution showed a lower pH than the 120 °C hydrolyzed urea solution. The pH of the urease-catalyzed system was mainly affected by the carbamic acid formed in eq 1 and the buffer in the original urease solution, which was used to preserve the urease activity. The low pH could reduce the scaling possibility in the reservoir application.

4.3.2 Low-temperature ICE sand pack flooding

In the previous section, we showed that the non-buffered low-temperature urease-urea hydrolysis system could generate enough NH_3 and CO_2 for tertiary recovery applications.

Therefore, the goal of this section is to provide evidence of the tertiary recovery in porous media under reservoir conditions. The pressure dependence of the proposed urease-urea system is not studied. All the urease inhibitor-related studies in the literature were conducted at ambient conditions with relatively low temperatures. Data at high-pressure reservoir conditions do not exist. Also, the previous low-temperature urea hydrolysis tests did not involve any porous media.

Urease is a large organic molecule and could be adsorbed onto the porous media grain surface. The urease catalyzed low-temperature urea hydrolysis reaction rate could improve or deteriorate due to the urease adsorption. Therefore, these potential effects were explored by different experimental designs.

Sandstone (Ottawa sand) and limestone (crushed Indiana limestone) were selected for the study to show the effect of porous media surface property and mineralogy. Both grains had sieve sizes between 105 to 250 microns. Besides the predetermined temperature, the rest of the experimental conditions were set to be the same as the previously published work [38] to reveal more information from the comparison. The NH_3(aq) flooding was used as the baseline to benchmark the effect of the proposed low-temperature ICE system. The concentration of the NH_3(aq) solution was prepared to match the urea conversion ratio of the hydrolyzed system for each case. The water consumption during the urea hydrolysis was not considered for the corresponding NH_3(aq) concentration calculated from the urea conversion ratio. The consumed water was compensated with DI water by using the syringe pump to control the pressure at a constant value. The parameters of the sand pack studies are summarized in Table *4-1*.

Table 4-1 Summary of the Sand Pack flooding experiments conditions

Test #	Oil type	Chemical Slug Type	Porous Media Type	Residual Oil Saturation, %	Permeability, mD	Porosity,%
1	Middle-East oil	Low T ICE	Ottawa Sand	31.32	3879	33.88
2	Middle-East oil	4.12 % NH_3	Ottawa Sand	32.40	4080	34.90
3	Middle-East oil	Low T ICE	Crushed Indiana Limestone	41.43	4687	37.87
4	Middle-East oil	4.12 % NH_3	Crushed Indiana Limestone	41.55	4465	36.80

*Note: In all tests, sand pack aging time was 24 hours (80 °C), the injection rate was 0.3 mL/min, DI was used in water flooding, back pressure was 1500 psi, and the test temperature was 50 °C.

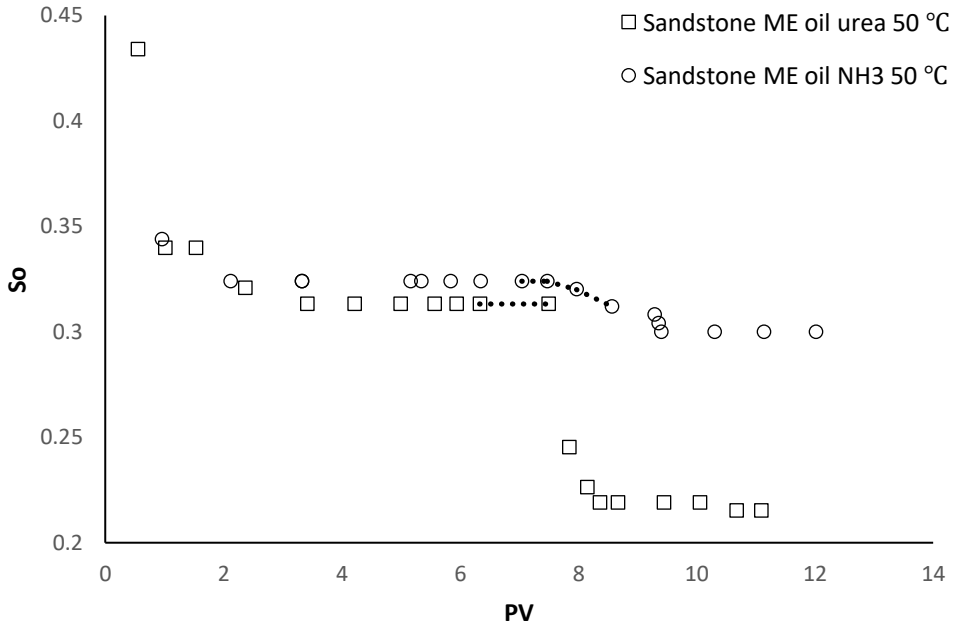

Figure 4-5 The effect of the CO_2 in the low-temperature ICE system for sandstone

Figure 4-5 The effect of the CO2 in the low-temperature ICE system for sandstone shows the tertiary recovery of the proposed low-temperature ICE system for sandstone. Based on the previous hydrolysis test, 10% urea with 31 U/g urease solution was selected for the test. The NH_3(aq) solution flooding was also performed for comparison. In this test, the conversion ratio

of the urea was 72.75%, which corresponded to 4.12 wt% NH_3(aq) solution at the experimental condition. Therefore, 4.12 wt% NH_3(aq) flooding was performed as the base case against the ICE test. The pressure dependence was explored in this test. 1500 psi was selected to be the backpressure, which could be compared with the previous work of our group.

The dashed line shown in Figure *4-5* indicates the injection of the chemical slug. The water flooding stages of both ICE and NH_3 tests reached residual oil saturation at about 6 PVs injection. The residual oil saturation of the ICE and NH_3 are 31.3% and 32.4%, respectively. The similar residual oil saturation showed good porous media structure repeatability of the sand packs. For the NH_3(aq) flooding case, the oil saturation started to drop during the injection of the NH_3(aq) slug, which indicates that the oil mobilization started at the time the NH_3(aq) solution contacted the sand grain surface and residual oil. The acid number of the ME oil used in this test is 0.19 mg KOH/g [38]. The aging process could make the sand grain of the sand pack more oil wet [55]. Therefore, the elevated alkalinity of the aqueous phase and the water wetness improvement of the sand grain caused by the ammonium hydroxide could account for the tertiary recovery. The tertiary recovery was 7.4%. Compared to the previous study from our group [38] in Figure *4-7*, the tertiary recovery in this test is lower than the previous similar high-temperature test(13.16%). The previous test had a higher NH_3 concentration (15%). In the 15 % NH_3(aq) test, the wettability reversal-related mechanism recovered extra oil when the IFT reduction-related mechanism in both cases were similar. Therefore, receiving a lower tertiary recovery in the low-temperature test is reasonable.

The low-temperature ICE system in Figure *4-5* shows a better tertiary recovery (31.3%) than the corresponding NH_3(aq) flooding. The oil breakthrough behavior of the low-temperature ICE is

different from the NH_3(aq) solution flooding. Because only a minimal amount of the chemicals responsible for the tertiary oil recovery are generated during the chemical injection and the unreacted urea-urease mixture cannot induce tertiary recovery, the oil production starts after the shut-in reaction in the ICE system. While the oil breakthrough behavior matches our previous high-temperature ICE system, the test in this work shows higher tertiary recovery with less chemical dosage at a lower temperature than the tertiary recovery of the high-temperature system (26.09%) [38]. The reason for the lower tertiary recovery of the high-temperature system, despite having 3.5 times more chemical dosage, is that the lower CO_2 solubility at 120 °C reduced the tertiary recovery potential of the CO_2. Experimental and modeling works [56, 57] suggest that CO_2 oil solubility decreases with an increase in temperature. From the CO_2 solubility estimation based on the model proposed by Emera and Sarma [58, 59], the CO_2 solubility increased by 34.5% when the temperature dropped from 120 °C to 50 °C, while keeping other parameters constant. Therefore, receiving a higher tertiary recovery in the low-temperature ICE system with less chemical dosage is reasonable. It also suggests that the 35% chemical dosage was not optimized in the high-temperature system. Less than 10% chemical could achieve a similar recovery since the CO_2 solubility at high temperatures is lower. Also, comparing the corresponding NH_3(aq) cases in the low and high-temperature tests, the sandstone wettability was responsive to NH_3 with no significant temperature dependence. Hence, the extra oil production in the low-temperature ICE test could be attributed to the CO_2 oil solubility effect.

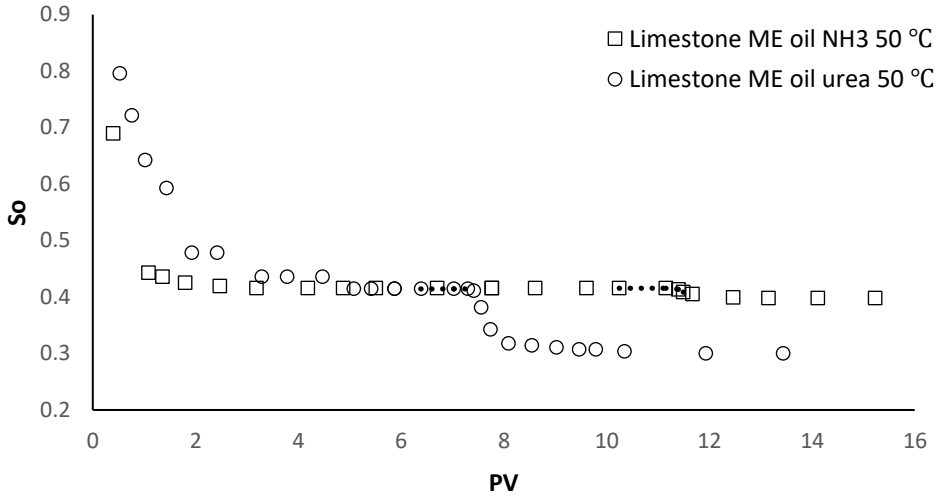

Figure 4-6 The effect of the CO_2 in low-temperature ICE system for carbonate

Figure *4-6* shows the performance of the low-temperature ICE system in carbonate porous media. The crushed limestone was also sieved to 105 to 250-micron diameter range for better consistency. 10% urea solution with 31 U/g urease was tested at 1500 psi and 50 °C to be compared with the corresponding NH_3(aq) solution treatment. The urea conversion ratio in this carbonate test was 84.18%, with a generated NH_3 concentration equivalent to 4.77% NH_3(aq) solution.

Around 8 and 10 PVs water flooding were applied to reach residual oil saturation for low-temperature ICE and NH_3(aq) systems, respectively. The DI flooding in the NH_3(aq) test established a residual oil saturation of 41.55%, and the residual oil saturation of the ICE test was 41.43%. The residual oil saturation in these tests showed high consistency in the porous media structures. The NH_3(aq) test served as a reference to separate the NH_3 and CO_2-related tertiary recovery mechanism. Wang et al. [38] studied the wettability alteration of NH_3 on carbonate and concluded that the wettability alteration caused by NH_3 was insignificant. Therefore, the tertiary recovery mechanism is primarily dominated by IFT reduction caused by the introduced NH_3. The

tertiary recovery in the low-temperature test was 4.1%, within the experimental error of the 2.8% recovery for the high-temperature system in our previous study [38]. The high-temperature test had three times as much NH_3 dosage as the low-temperature test. This observation was reasonable because the wettability of the carbonate system is not very responsive to NH_3.

Figure *4-6* also shows the performance of the low-temperature ICE system. The CO_2 and NH_3 combined system generated 27.5% tertiary recovery, which was higher than the NH_3-only flooding. The oil breakthrough happened after the chemical reaction for the ICE system while the NH_3 system produced extra oil during the chemical injection stage. The same reasons as the sandstone tests shown in Figure *4-5* explain these oil breakthrough behaviors. The low-temperature ICE for carbonate yields significantly higher tertiary recovery than the 120 °C ICE system (12.37%). This observation is different from the sandstone tests, where the low-temperature ICE for sandstone only generated slightly higher tertiary recovery than the 120 °C ICE. Since the high-temperature ICE used a high chemical dosage, the NH3-induced tertiary recovery could account for 50% of the total tertiary recovery in sandstone. The increased CO_2 solubility in the low-temperature ICE test compensated for the tertiary recovery loss caused by low NH_3 concentration.

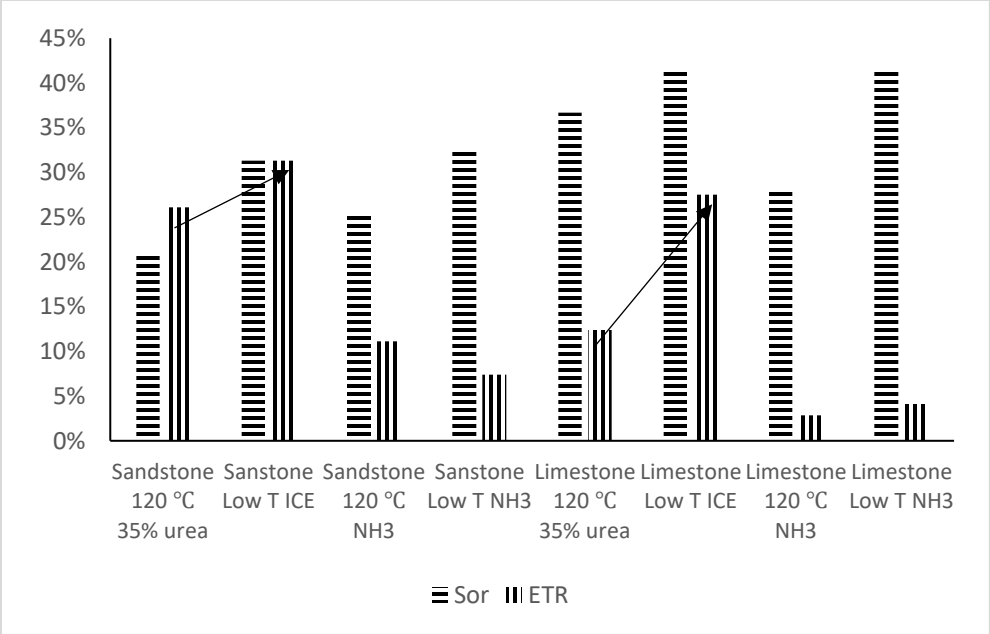

Figure 4-7 Tertiary recovery comparison between low-temperature and high-temperature [38] ICE

In contrast, the wettability of carbonate is not responsive to NH_3. Only the *in situ* formed surfactant could generate a small portion of the tertiary recovery. Therefore, the increased CO_2 solubility improved the tertiary recovery for the low-temperature carbonate test since the high NH_3 dosage in the previous high-temperature test was ineffective, and no tertiary recovery was compensated. It could be observed that if the NH_3 contributions are deducted from the total tertiary recovery in both low and high-temperature ICE tests, the CO_2-induced recovery in both sandstone and carbonate is similar. This observation indicates that the amount of generated CO_2 could saturate the residual oil in both cases. The CO_2 part of the ICE system could be simplified to a carbonated water injection system [60].

From the collected urea conversion ratio in Figure *4-5* and Figure *4-6*, the urease-catalyzed urea hydrolysis does not show pressure dependence at 1500 psi. The conversion ratio is similar to the low-pressure test tube tests. However, the presence of the porous media shows a positive effect

on urea conversion. The conversion ratio for the batch test in Figure 3 is 68.74% which is lower than the sandstone (72.75%) and carbonate (84.18%) tests. There is evidence that urease adsorption on the porous media could help protect the enzyme activity [61]. The related mechanism still needs to be explored in the future.

4.3.3 Low-temperature ICE imbibition and wettability study

The wettability of the porous media controls the residual oil saturation and its distribution [62, 63]. The preferred pristine reservoir wettability condition for ICE system is oil-wet because the ICE system alters the wettability of the mineral surface from oil-wet to water-wet [38]. Therefore, it is necessary to quantify the wettability alteration ability of the low-temperature ICE. Both sandstone and carbonate cores were aged and tested for this study. The low-temperature ICE was benchmarked by the DI soaking test at the same condition. The measured contact angles are summarized in Table *4-2*.

Table 4-2 The contact angle with different fluid treatments and mineralogy

	Sandstone	Carbonate
Clean, °	27.1 ± 1.7	39.9 ± 0.4
Aged, °	121.8 ± 1.3	145.4 ± 2.1
DI Soaking, °	94.8 ± 0.5	137.9 ± 1.0
Low-temperature ICE, °	27.3 ± 0.6	58.5 ± 0.4

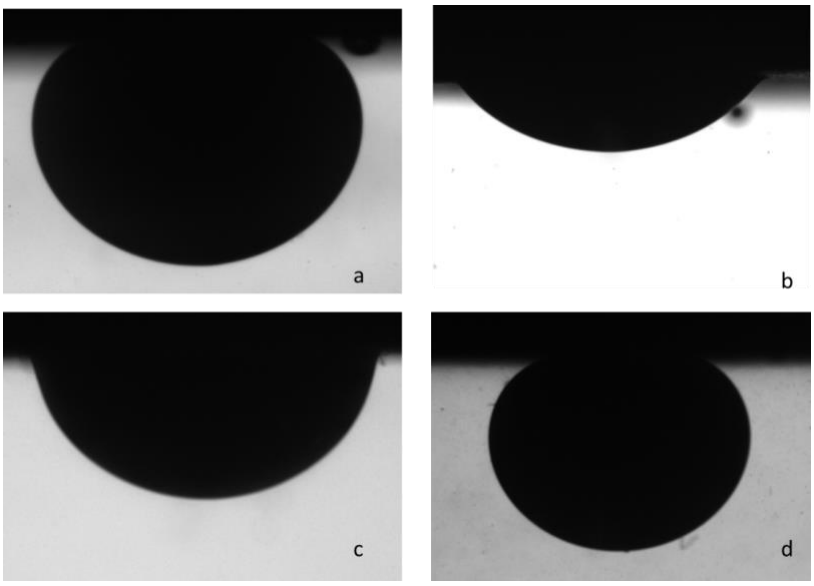

Figure 4-8 Sandstone contact angle change with different treatments; a: Clean, b: Oil Aged, c: DI Soaking, d: ICE Soaking

Figure *4-8* shows sample images from the sandstone test. The clean Berea core is water-wet in DI/ME oil system. The same conclusion was documented by Teklu et al. and Al-Rossies et al. [64, 65]. After aging with ME oil at 80 °C for 24 hours, the sandstone wettability was altered to oil-wet [66]. DI and low-temperature ICE tests were performed on different cores. After the DI and low-temperature ICE soaking for 72 hours at 1500 psi and 50 °C, the DI case turned from oil-wet to intermediate-wet, corresponding to a 27° reduction in the contact angle. The contact angle change could be attributed to hydrocarbon production during the DI imbibition process. The oil-wet behavior of the sandstone after the aging process was caused by the adsorption of the polar components in the crude oil on the sandstone surface [67]. Since the original silica surface was water-wet, DI water imbibition released some of the adsorbed oil during the soaking. Therefore, a small contact angle change was observed. On the contrary, the low-temperature ICE significantly improved water wetness, restoring the clean sandstone wettability. This is similar to the observation for the ICE system treatment at 120 °C, and is a combination of NH3-induced

wettability alteration(electrostatic interaction and structural interaction related) and CO_2-induced hydrocarbon release [38].

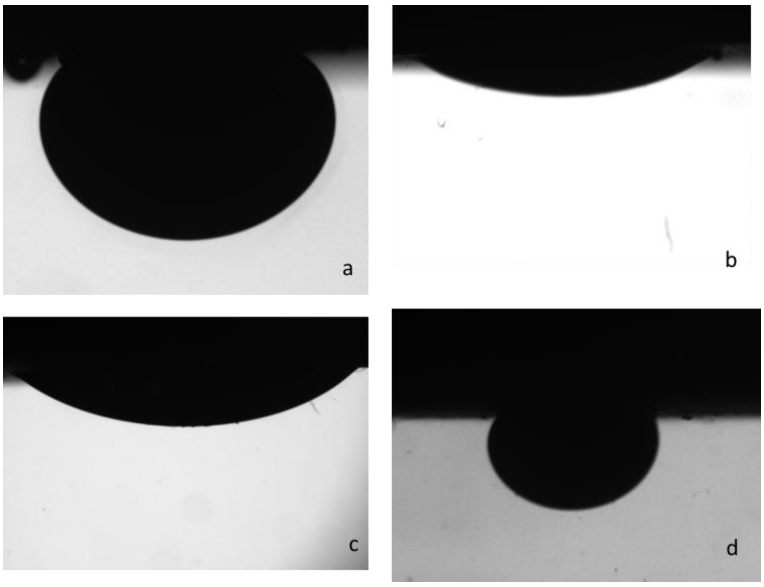

Figure 4-9 Carbonate contact angle change with different treatments; a: Clean, b: Oil Aged, c: DI Soaking, d: ICE Soaking

Figure *4-9* shows the results for the carbonate test. The clean and oil-aged samples showed similar wettability alteration behavior to sandstone. The oil wetness improvement of the carbonate by oil aging was also documented by Teklu et al. [64]. The only difference between sandstone and carbonate was that the clean carbonate is less water-wet than sandstone and the aged carbonate is more oil-wet than sandstone. The point of zero charge (PZC) of sandstone is between 2.2 and 2.8, and the PZC for carbonate is between 9.4 and 9.6 [68-70]. The crude oil PZC was reported at 3 [71]. Because the DI system has a pH of around 6 the carbonate can have a stronger attraction to oil drops than sandstone does at this condition. After the DI soaking, the contact angle change was within experimental error. It can be concluded that DI could not release the pre-saturated oil during aging. The adsorbed oil was not released during the DI imbibition.

After the low-temperature ICE treatment, the wettability of the carbonate core was altered to water-wet. This alteration was caused by the oil removal by the generated CO_2. It can be deduced that the low-temperature ICE system showed the same effect on the aged sandstone and carbonate wettability as the high-temperature tests [38].

4.4 Conclusions

Laboratory and pilot tests proved that urea is effective in high-temperature EOR processes. We explored the enzyme-catalyzed system to expand the operating temperature range of urea-related EOR processes. This paper successfully demonstrates that the urea ICE system could be applied to low-temperature reservoirs. The proposed low-temperature ICE system showed tertiary recovery as high as 31.3% at 1500 psi and 50 °C. The urease-catalyzed urea hydrolysis is studied under non-buffered and high urea concentration conditions, which are applicable in the petroleum industry. From the urea concentration analysis during the low-temperature hydrolysis, the reaction rate of urease-catalyzed urea hydrolysis is not significantly dependent on the temperature (ranging from 30 to 50 °C). The urease was denatured in the non-buffered system within 2000 minutes. Low-temperature ICE yields higher oil recovery than the high-temperature case since the CO_2 solubility in oil at low temperatures is higher than that at high temperatures. At low-temperature conditions, the CO_2-related mechanism contributes more than the NH_3-related mechanism toward tertiary oil recovery. Contact angle measurements conducted after the imbibition tests showed that the urease-catalyzed ICE system improved water wetness for both carbonate and sandstone cores.

References

[1] Jablonowski CJ, Singh A. A Survey of CO_2-EOR and CO_2 Storage Project Costs. *SPE International Conference on* CO_2 *Capture, Storage, and Utilization.* New Orleans, Louisiana, USA: Society of Petroleum Engineers; 2010:4.

[2] Hill B, Hovorka S, Melzer S. Geologic carbon storage through enhanced oil recovery. Energy Procedia 2013;37:6808-30.

[3] Talebian SH, Masoudi R, Tan IM, Zitha PLJ. Foam assisted CO_2-EOR: A review of concept, challenges, and future prospects. Journal of Petroleum Science and Engineering 2014;120:202-15.

[4] Christensen JR, Stenby EH, Skauge A. Review of WAG Field Experience. SPE Reservoir Evaluation & Engineering 2001;4(02):97-106.

[5] Esene C, Rezaei N, Aborig A, Zendehboudi S. Comprehensive review of carbonated water injection for enhanced oil recovery. Fuel 2019;237:1086-107.

[6] Spivak A, Garrison WH, Nguyen JP. Review of an Immiscible CO_2 Project, Tar Zone, Fault Block V, Wilmington Field, California. SPE Reservoir Engineering 1990;5(02):155-62.

[7] Ferguson RC, Kuuskraa VA, Van Leeuwen TS, Remson D. Storing CO_2 With Next-Generation CO_2-EOR Technology. *SPE International Conference on* CO_2 *Capture, Storage, and Utilization.* New Orleans, Louisiana, USA: Society of Petroleum Engineers; 2010:7.

[8] Ghedan S. Global laboratory experience of CO_2-EOR flooding. *SPE/EAGE Reservoir Characterization & Simulation Conference.* 2009.

[9] NETL N. Carbon dioxide enhanced oil recovery-untapped domestic energy supply and long term carbon storage solution. The Energy Lab 2010.

[10] van Domelen MS, Reddingius AA, Faber MJ, Buijse MA. High-Temperature Acid Stimulation Offshore The Netherlands. *SPE European Formation Damage Conference.* The Hague, Netherlands: Society of Petroleum Engineers; 1997:14.

[11] Close F, McCavitt RD, Smith B. Deepwater Gulf of Mexico Development Challenges Overview. *SPE North Africa Technical Conference & Exhibition.* Marrakech, Morocco: Society of Petroleum Engineers; 2008:15.

[12] Wang S, Chen C, Yuan N, Ma Y, Ogbonnaya OI, Shiau B, et al. Design of extended surfactant-only EOR formulations for an ultrahigh salinity oil field by using hydrophilic lipophilic deviation (HLD) approach: From laboratory screening to simulation. Fuel 2019;254:115698.

[13] Dehghanpour H, Zubair HA, Chhabra A, Ullah A. Liquid Intake of Organic Shales. Energy & Fuels 2012;26(9):5750-8.

[14] Dehghanpour H, Lan Q, Saeed Y, Fei H, Qi Z. Spontaneous Imbibition of Brine and Oil in Gas Shales: Effect of Water Adsorption and Resulting Microfractures. Energy & Fuels 2013;27(6):3039-49.

[15] Carpenter C. Viability of Gas-Injection EOR in Eagle Ford Shale Reservoirs. Journal of Petroleum Technology 2019;71(01):50-2.

[16] Liu P, Li W, Shen D. Experimental study and pilot test of urea-and urea-and-foam-assisted steam flooding in heavy oil reservoirs. Journal of Petroleum Science and Engineering 2015;135:291-8.

[17] Li Y-B, Zhang Y-Q, Luo C, Gao H, Li K, Xiao Z-R, et al. The experimental and numerical investigation of *in situ* re-energization mechanism of urea-assisted steam drive in superficial heavy oil reservoir. Fuel 2019;249:188-97.

[18] Wang S, Chen C, Li K, Yuan N, Shiau B, Harwell JH. In Situ CO_2 Enhanced Oil Recovery: Parameters Affecting Reaction Kinetics and Recovery Performance. Energy & Fuels 2019;33(5):3844-54.

[19] Dahbag MB, Al-Gawfi A, Hassanzadeh H. Suitability of hot urea solutions for wettability alteration of bitumen reservoirs–Simulation of laboratory flooding experiments. Fuel 2020;272:117713.

[20] Ogbonnaya O, Wang S, Shiau B, Harwell J. Use of In-Situ CO_2 Generation in Liquid-Rich Shale. *SPE Improved Oil Recovery Conference.* OnePetro; 2020.

[21] Ganjdanesh R, Yu W, Fiallos MX, Kerr E, Sepehrnoori K, Ambrose R. Gas Injection EOR in Eagle Ford Shale Gas Condensate Reservoirs. *SPE/AAPG/SEG Unconventional Resources Technology Conference.* Denver, Colorado, USA: Unconventional Resources Technology Conference; 2019:16.

[22] Abdelgawad K, Mahmoud M. In-Situ Generation of CO 2 to Eliminate the Problem of Gravity Override in EOR of Carbonate Reservoirs. *SPE Middle East Oil & Gas Show and Conference.* Society of Petroleum Engineers; 2015.

[23] Mahmoud MANED, Sultan AS, Abdelgawad KZ. Method for enhanced oil recovery by *in situ* carbon dioxide generation. Google Patents; 2014.

[24] Alam M, Mahmoud M, Sibaweihi N. A Slow Release CO 2 for Enhanced Oil Recovery in Carbonate Reservoirs. *SPE Middle East Oil & Gas Show and Conference.* Society of Petroleum Engineers; 2015.

[25] Venkatesan VN. Oil recovery process employing CO_2 produced *in situ*. Google Patents; 1985.

[26] Zhu D, Hou J, Wang J, Wu X, Wang P, Bai B. Acid-alternating-base (AAB) technology for blockage removal and enhanced oil recovery in sandstone reservoirs. Fuel 2018;215:619-30.

[27] Gumersky K, Dzhafarov I, Shakhverdiev AK, Mamedov YG. *In situ* generation of carbon dioxide: New way to increase oil recovery. *SPE European Petroleum Conference.* Society of Petroleum Engineers; 2000.

[28] Li Y, Ma K, Liu Y, Zhang J, Jia X, Liu B. Enhance Heavy Oil Recovery by In-Situ Carbon Dioxide Generation and Application in China Offshore Oilfield. Society of Petroleum Engineers; 2013.

[29] Bakhtiyarov S. Technology on *in situ* gas generation to recover residual oil reserves. New Mexico Institute Of Mining And Technology; 2008.

[30] Bakhtiyarov SI, Shakhverdiev AK, Panakhov GM, Abbasov EM. Effect of Surfactant on Volume and Pressure of Generated CO_2 Gas. *Production and Operations Symposium.* Society of Petroleum Engineers; 2007.

[31] Schell LP. Catalytic method for hydrolyzing urea. Google Patents; 1979.

[32] Estiu G, Merz KM. The Hydrolysis of Urea and the Proficiency of Urease. Journal of the American Chemical Society 2004;126(22):6932-44.

[33] Blakeley RL, Treston A, Andrews RK, Zerner B. Nickel(II)-promoted ethanolysis and hydrolysis of N-(2-pyridylmethyl)urea. A model for urease. Journal of the American Chemical Society 1982;104(2):612-4.

[34] Sumner JB. The isolation and crystallization of the enzyme urease preliminary paper. Journal of Biological Chemistry 1926;69(2):435-41.

[35] Kafarski P, Talma M. Recent advances in design of new urease inhibitors: A review. Journal of Advanced Research 2018;13:101-12.

[36] Modolo LV, da-Silva CJ, Brandão DS, Chaves IS. A minireview on what we have learned about urease inhibitors of agricultural interest since mid-2000s. Journal of advanced research 2018;13:29-37.

[37] Krajewska B. A combined temperature-pH study of urease kinetics. Assigning pKa values to ionizable groups of the active site involved in the catalytic reaction. Journal of Molecular Catalysis B: Enzymatic 2016;124:70-6.

[38] Wang S, Li K, Chen C, Onyekachi O, Shiau B, Harwell JH. Isolated mechanism study on *in situ* CO_2 EOR. Fuel 2019;254:115575.

[39] Mahzari P, Mitchell TM, Jones AP, Oelkers EH, Striolo A, Iacoviello F, et al. Novel laboratory investigation of huff-n-puff gas injection for shale oils under realistic reservoir conditions. Fuel 2021;284:118950.

[40] Mahzari P, Oelkers E, Mitchell T, Jones A. An improved understanding about CO_2 EOR and CO_2 storage in liquid-rich shale reservoirs. *SPE Europec featured at 81st EAGE Conference and Exhibition.* OnePetro; 2019.

[41] Krajewska B, Zaborska W. The effect of phosphate buffer in the range of pH 5.80–8.07 on jack bean urease activity. Journal of Molecular Catalysis B: Enzymatic 1999;6(1):75-81.

[42] Sahu JN, Mahalik K, Patwardhan AV, Meikap BC. Equilibrium and Kinetic Studies on the Hydrolysis of Urea for Ammonia Generation in a Semibatch Reactor. Industrial & Engineering Chemistry Research 2008;47(14):4689-96.

[43] Wang S, Yuan Q, Kadhum M, Chen C, Yuan N, Shiau B-J, et al. In Situ Carbon Dioxide Generation for Improved Recovery: Part II. Concentrated Urea Solutions. *SPE Improved Oil Recovery Conference.* Tulsa, Oklahoma, USA: Society of Petroleum Engineers; 2018:12.

[44] Tabatabai MA, Bremner JM. Assay of urease activity in soils. Soil Biology and Biochemistry 1972;4(4):479-87.

[45] Sahrawat K. Effects of temperature and moisture on urease activity in semi-arid tropical soils. Plant and Soil 1984;78(3):401-8.

[46] Klose S, Tabatabai MA. Urease activity of microbial biomass in soils. Soil Biology and Biochemistry 1999;31(2):205-11.

[47] Dai X, Karring H. A determination and comparison of urease activity in feces and fresh manure from pig and cattle in relation to ammonia production and pH changes. PLoS One 2014;9(11):e110402.

[48] Zaborska W, Krajewska B, Olech Z. Heavy metal ions inhibition of jack bean urease: potential for rapid contaminant probing. Journal of Enzyme Inhibition and Medicinal Chemistry 2004;19(1):65-9.

[49] Blakeley RL, Zerner B. Jack bean urease: the first nickel enzyme. Journal of Molecular Catalysis 1984;23(2):263-92.

[50] Krajewska B, Ciurli S. Jack bean (Canavalia ensiformis) urease. Probing acid–base groups of the active site by pH variation. Plant Physiology and Biochemistry 2005;43(7):651-8.

[51] Pettit NM, Smith ARJ, Freedman RB, Burns RG. Soil urease: Activity, stability and kinetic properties. Soil Biology and Biochemistry 1976;8(6):479-84.

[52] Howell SF, Sumner JB. The specific effects of buffers upon urease activity. Journal of Biological Chemistry 1934;104(3):619-26.

[53] Zantua MI, Bremner JM. Comparison of methods of assaying urease activity in soils. Soil Biology and Biochemistry 1975;7(4):291-5.

[54] Ghahfarokhi RB, Pennell S, Matson M, Linroth M. Overview of CO_2 Injection and WAG Sensitivity in SACROC. *SPE Improved Oil Recovery Conference.* Tulsa, Oklahoma, USA: Society of Petroleum Engineers; 2016:22.

[55] Wang S, Kadhum MJ, Chen C, Shiau B, Harwell JH. Development of in Situ CO_2 Generation Formulations for Enhanced Oil Recovery. Energy & Fuels 2017.

[56] Rostami A, Arabloo M, Kamari A, Mohammadi AH. Modeling of CO_2 solubility in crude oil during carbon dioxide enhanced oil recovery using gene expression programming. Fuel 2017;210:768-82.

[57] Barclay TH, Mishra S. New correlations for CO_2-Oil solubility and viscosity reduction for light oils. Journal of Petroleum Exploration and Production Technology 2016;6(4):815-23.

[58] Emera M, Sarma H. A genetic algorithm-based model to predict co-oil physical properties for dead and live oil. *Canadian International Petroleum Conference.* Petroleum Society of Canada; 2006.

[59] Emera MK, Sarma HK. Prediction of CO_2 Solubility in Oil and the Effects on the Oil Physical Properties. Energy Sources, Part A: Recovery, Utilization, and Environmental Effects 2007;29(13):1233-42.

[60] Mosavat N. Utilization of Carbonated Water Injection (CWI) as a Means of Improved Oil Recovery in Light Oil Systems: Pore-Scale Mechanisms and Recovery Evaluation. Faculty of Graduate Studies and Research, University of Regina; 2014.

[61] Kato K, Kawachi Y, Nakamura H. Silica–enzyme–ionic liquid composites for improved enzymatic activity. Journal of Asian Ceramic Societies 2014;2(1):33-40.

[62] Maini BB, Ionescu E, Batycky JP. Miscible Displacement Of Residual Oil - Effect Of Wettability On Dispersion In Porous Media. Journal of Canadian Petroleum Technology 1986;25(03):7.

[63] Wood AR, Wilcox TC, MacDonald DG, Flynn JJ, Angert PF. Determining Effective Residual Oil Saturation for Mixed Wettability Reservoirs: Endicott Field, Alaska. *SPE Annual Technical Conference and Exhibition.* Dallas, Texas: Society of Petroleum Engineers; 1991:8.

[64] Teklu TW, Alameri W, Kazemi H, Graves RM. Contact Angle Measurements on Conventional and Unconventional Reservoir Cores. *Unconventional Resources Technology Conference.* San Antonio, Texas, USA: Unconventional Resources Technology Conference; 2015:17.

[65] Al-Rossies AAS, Al-Anazi BD, Paiaman AM. Effect of pH-values on the contact angle and interfacial tension. Nafta 2010;61(4):181-6.

[66] Buckley J, Liu Y, Monsterleet S. Mechanisms of wetting alteration by crude oils. SPE journal 1998;3(01):54-61.

[67] Hirasaki GJ. Wettability: Fundamentals and Surface Forces. SPE-17367-PA 1991;6(02):217-26.

[68] Jaafar M, Nasir AM, Hamid M. Measurement of isoelectric point of sandstone and carbonate rock for monitoring water encroachment. Journal of Applied Sciences 2014;14(23):3349-53.

[69] Pokrovsky O, Schott J, Mielczarski J. Surface speciation of dolomite and calcite in aqueous solutions. Encyclopedia of surface and colloid science 2002;4:5081-95.

[70] Gupta R, Mohanty KK. Wettability Alteration Mechanism for Oil Recovery from Fractured Carbonate Rocks. Transport in Porous Media 2011;87(2):635-52.

[71] Takamura K, Chow RS. The electric properties of the bitumen/water interface Part II. Application of the ionizable surface-group model. Colloids and Surfaces 1985;15:35-48.

Chapter 5 Modified Enzyme Catalyzed Low-temperature In Situ CO_2-enhanced Oil Recovery

Abstract

In situ CO_2-enhanced oil recovery (ICE) delivers CO_2 to the target reservoir through the injection of an aqueous solution of a CO_2-generating compound, urea. This method offers potential improvements in oil recovery, operational efficiency, and superior economic performance compared to conventional gas injection techniques for enhanced oil recovery (EOR). At temperatures below 80 °C, the rate of spontaneous decomposition of urea in aqueous solutions to release CO_2 and ammonia is not high enough for EOR applications. The utilization of urease, an enzyme that catalyzes urea hydrolysis, has shown effectiveness in EOR applications in low-temperature reservoirs. In this work, we investigated the use of crude extracts from jack beans as a source of urease enzyme for low-temperature ICE. We also conducted batch tests to study the kinetics of the urease-catalyzed hydrolysis of urea at different temperatures and to examine the adsorption of the crude enzyme extract on porous media. One-dimensional sand pack flowthrough experiments were conducted with different lithologies at 50 °C and 70 °C to evaluate the tertiary oil recovery potential of low-temperature ICE using the modified formulations. The results show that urease was effectively extracted from jack beans using a simple and cost-efficient extraction procedure. Urease-catalyzed hydrolysis of urea in the batch tests show that the crude urease extract was effective in generating CO_2 at the test temperatures with urea conversion rate of over 95 % at 50 °C. The urea hydrolysis rate and urea conversion ratio were lower at 70 °C compared to 50 °C. The adsorption tests show that urease was significantly

adsorbed on limestone surfaces while the adsorption on sandstone was insignificant. The flowthrough tests show that the tertiary recovery for the limestone and sandstone tests were lower at 70 °C compared to 50 °C. The tertiary recoveries at 50 °C were 28.0 % and 10.6 % for the limestone and sandstone tests, respectively. At 70 °C, the tertiary recoveries were 22.5 % and 8.6 % for the limestone and sandstone tests, respectively. Overall, the simplicity of the technique used to produce the crude urease extract from jack beans will significantly reduce the cost of enzyme-catalyzed low-temperature ICE, thus overcoming a major economic barrier and enabling practical applications in the oilfield.

5.1 Introduction

CO_2 is used extensively in the US for enhanced oil recovery (EOR) applications in both conventional and unconventional reservoirs. It has gained significant attention in recent years due to its potential for mitigating carbon emissions and increasing oil production rates [1–3]. When CO_2 dissolves in oil, it leads to a series of EOR favorable phenomena, including decrease in oil viscosity, oil swelling, reduced interfacial tension between oil and water phases, re-pressurization of the formation, and ultimately, increased oil production and sweep efficiency. Generally, CO_2 injection for EOR applications can take the form of gas flooding (continuous injection or cyclic injection – commonly known as huff-n-puff), carbonated water injection (CWI), or water-alternating- gas (WAG) flooding. The implementation of CO_2 EOR continues, however, to be hindered by operational and technical challenges such as CO_2 availability, CO_2 transportation availability, pipeline corrosion, gravity segregation, viscous fingering, early gas breakthrough, asphaltene deposition, and the low solubility of CO_2 in water, among others [4]. Numerous endeavors have been undertaken to enhance the effectiveness of CO_2 EOR [5–9]. One

of the most promising approaches to mitigate some of the limitations associated with CO_2 EOR is the concept of *in situ* CO_2 EOR [10–17] . It involves the injection of a solution or multiple solutions which interact at reservoir conditions to generate CO_2 inside the reservoir. *In situ* generation of CO_2 for EOR applications offers several potential advantages over alternative methods, including non-reliance on natural sources of CO_2, elimination of need for a dedicated CO_2 transportation pipeline, improved sweep efficiency compared to WAG process, higher CO_2 gas-water ratio (GWR) than CWI method, simplicity and cost-effectiveness, good tertiary recovery performance at both below and above the minimum miscibility pressure (MMP) and tolerance to high salinity reservoir brine [18].

Altunina and Kuvshinov [19,20] proposed the use of an ammonium nitrate/carbamide (urea)/surfactant system to generate an *in situ* alkaline buffer system and CO_2 for EOR purposes. The hydrolysis of the urea at reservoir temperature generated CO_2 which dissolved in the oil phase and ammonia which combined with the ammonium nitrate to form an alkaline buffer system in the aqueous phase. The adsorption of the surfactant on reservoir rock in the alkaline buffer system was less than the adsorption of surfactant in a surfactant/water system without the alkali. Their EOR fluid system was used in combination with steam flooding in a pilot test for a high-viscosity oil formation in Siberia, with an average 40 % increase in oil production. The same authors also proposed another multi-component fluid system that combined an aqueous solution of an aluminium salt, urea and surfactant with a gel-forming system to generate an inorganic gel and CO_2 in the reservoir. The gel improved the sweep efficiency during reservoir flooding. These fluid systems were complex which could result in operational difficulties in the field and could also impact their economic viability. Gumersky et al. [12] proposed the use of

successive injection of aqueous solutions of hydrochloric acid and sodium carbonate , which reacted *in situ* to generate CO_2. A surfactant and polymer could also be added to the fluid system to create stable foams which help displace the oil during the flooding process. Oil recovery was improved by an additional 16 % compared to displacement by water, in lab tests. This system involves the injection of multiple streams of fluid, which, again, might complicate field application. Bakhtiyarov [21] proposed the sequential injection of aqueous solutions of an acid and base (carbonate salt) which react in the reservoir to yield CO_2. Water soluble foam generating surfactants can also be added to improve sweep efficiency, according to the author. The proposed fluid system was successfully applied in a pilot test and resulted in increased oil and reduced water production. For field application, however, the process might be complicated due to the use of multiple fluid injection streams similar to the system proposed by Gumersky et al. [12] . In 2010, Shiau et al. [14] investigated the use of aqueous solutions of ammonium carbamate and 2-Amino-2-methyl-1-propanol (AMP) as *in situ* gas generation agents for EOR purposes. Ammonium carbamate solutions generated significant amounts of CO_2 at elevated temperatures above 85 °C, while the AMP solutions required much higher temperatures above 100 °C to generate significant amounts of CO_2. In a subsequent sand pack column test, the carbamate solution recovered an additional 9.7% OOIP when paired with a polymer and surfactant compared to a polymer surfactant system without carbamate. The oil recovery was negligible when the carbamate solution was used without added surfactant, especially for light crude oil. The ultralow IFT achievable with the added surfactant enhanced oil mobility due to increased capillary number.

Multiple streams of fluid injection are used in most of these proposed *in situ* CO_2 generating methods including surfactants, polymer, alkali and acid systems, to enhance the CO_2 generating capacity, harness synergistic effects and dissolve reservoir rocks (for example by the interaction of acid and carbonate rock). Wang et al. [18] proposed a simplified system involving the injection of a single stream of urea solution as the CO_2 generating agent. Urea is non-toxic, easy to handle and highly soluble in water up to 512 grams/L at 68 °F [22]. It is widely used in fertilizers as a nitrogen source and is readily available in bulk quantities at a reasonable price. The primary raw material used to manufacture urea is natural gas, therefore most new urea manufacturing plants are located in areas with large natural gas reserves, which will likely be close to the oilfields where urea can be used for EOR.

Aqueous solutions of urea ranging in pH from 2 to 12 are stable to hydrolysis at ambient conditions with a long half-life of 40 years at 25 °C and 3.6 years at 38 °C [23,24]. The rate of urea hydrolysis increases, however, with temperature, with a half-life of 24.9 days and 1.0 days at temperatures of 80 °C and 120 °C, respectively, according to the urea hydrolysis study conducted by our research group [25]. Urease-catalyzed hydrolysis of urea is at least 10^{14} times as fast as the uncatalyzed reaction at pH 7.0 and 38 °C [26,27]. Urease can be found in bacteria, plants and some invertebrates, with jack bean as the most common commercial source. The activity of urease is dependent on multiple parameters such as pH, temperature, salt concentration, urea concentration, and pressure. For jack bean urease, the optimum pH for enzyme activity is at pH 7 to 7.5 [27,28]. Under buffered conditions, at temperatures between 10 °C and 50 °C, the urease-catalyzed urea hydrolysis rate is nearly doubled for every 10 °C rise in temperature [29]. However, when the temperature rises further, above 60 °C, the activity of the enzyme decreases until it

completely halts at 100 °C [30]. Urease activity will not be adversely affected within the range of typical pressures encountered in oil and gas operations [28]. The urease-catalyzed hydrolysis of aqueous urea solution is shown in Equations 1 – 3 [31,32].

$$NH_2CONH_2 + H_2O \xrightarrow{urease} NH_2COOH + NH_3 \xrightarrow{+ H_2O\ (spontaneous)} H_2CO_3 + 2NH_3 \quad (1)$$

$$H_2CO_3 \leftrightarrow H_2O + CO_2 \quad (2)$$

$$H_2O + NH_3 \leftrightarrow OH^- + NH_4^+ \quad (3)$$

Commercially available urease enzyme is expensive mainly due to its limited production in a refined state, intended for specialized uses such as research, the food industry, and medical applications [33]. When implementing low-temperature urease catalyzed ICE in the field, bulk quantities (in the range of tonnes) of urease will be required. Consequently, it is crucial to decrease the expense associated with urease enzyme to render low-temperature ICE applications economically viable. Previous studies have demonstrated that urease can be extracted from various plant and bacterial sources with the use of relatively simple techniques requiring only basic laboratory equipment [30,33–35]. In our previous work we demonstrated the application of highly purified commercially available urease in low-temperature urease-catalyzed ICE. In that work, urease was used to catalyze the hydrolysis of urea at a relatively low reservoir temperature of 50 °C. Flowthrough tertiary oil recovery tests showed that the low-temperature ICE system effectively recovered oil from sandstone and limestone sand packs. The urease plus urea solutions were prepared with deionized (DI) water and all the waterflooding stages were performed with DI water, to reduce the complexity of the fluid system [36]. The work reported herein evaluated the use of crude urease extracts from jack bean, instead of highly purified commercial urease, for low temperature ICE applications. Crude urease extracts were evaluated

for urease activity, urea hydrolysis kinetics and urease adsorption on porous media. Tertiary oil recovery flowthrough tests were also carried out to evaluate the oil recovery potential of ICE with urease extracts. Furthermore, the urease plus urea solutions used in the tests were prepared in artificial sea water (ASW), to replicate more realistic oil field conditions and evaluate the impact of high ionic strength and the presence of divalent ions on the low-temperature ICE system. The hydrolysis kinetics and flowthrough tests were performed at 50 °C and 70 °C to expand the range of reservoir temperatures where the ICE system can be applied.

5.2 Experimental

5.2.1 Material

Whole Jack beans (*Canavalia ensiformis*) was purchased from Sigma-Aldrich. Urea (99 wt.%) was purchased from Acros Organics. Crude oil was donated by Abu Dhabi National Oil Company (ME oil). Ottawa sand F-75 (99.7% Silica) was purchased from U.S. Silica for sand pack preparation. Indiana limestone cores (98% Calcite) were purchased from Kocurek Industries. Ammonium hydroxide solution as 28% NH_3 in water was purchased from Sigma-Aldrich. Sodium chloride (99.5 wt%), calcium chloride dihydrate (99%), potassium chloride (99%), magnesium chloride (98%) and magnesium sulfate (99%) were purchased from Sigma-Aldrich. For high-performance liquid chromatography (HPLC) purposes, acetonitrile (ACN) (HPLC grade, ≥99.93%) and water (HPLC Plus) were purchased from Sigma-Aldrich. For Berthelot test, Phenol (≥99.0 %), sodium nitroprusside dihydrate (≥99.0 %) and sodium hypochlorite solution (4.0 – 5.0 % available chlorine) were purchased from Sigma-Aldrich.

5.2.2 Urease extraction and characterization

Much work has been done to purify and crystalize jack bean urease [35,37,38], however, the purification process is expensive and would make the use of urease in petroleum applications uneconomical. Therefore, we decided to use urease extracted directly from jack beans, without the expensive purification process. The extraction process was a modification of the method used by Mateer and Marshall [34]. To extract urease from jack beans, the beans were finely ground to a powder in a nut grinder. During the grinding process, it's important to avoid heat buildup, which could denature the enzyme. The powder was then passed through an ASTM 80 sieve with openings no larger than 180 microns and the particles that passed through the sieve were collected and used for enzyme extraction. One part of the powder was treated with five parts of DI water and allowed to stand for one hour with occasional agitation. Whereas Mateer and Marshall [34] used a ratio of one part of the powder to 10 parts of distilled water to extract urease from the beans, our urease activity tests showed that using one part of powder to 5 parts of DI resulted in less than 5% loss of urease activity due to a reduction in extraction efficiency with less water. The suspension was then centrifuged for 10 mins at 335 RPM (17.5 x g) and filtered through a 2.7 micron Whatman GF/D glass microfiber filter.

The enzymatic activity of urease solutions was determined using the Berthelot method [39]. One unit of activity corresponds to the amount of the enzyme that liberates 1.0 μmol NH_3 from urea per minute at pH 7.0 and 25°C [40]. The method determines the amount of ammonium ions produced by the hydrolysis of urea in aqueous solutions and has a detection limit as low as 7 μM (0.12 μg/mL) NH_3 [41]. The urease solutions were diluted with DI water in order to adjust the concentration of urease to within the limits of the method. For the crude jack bean urease

extracts we used a dilution factor of about 1601 consisting of 0.1 g crude jack bean extract plus 160 g DI water. 200 μL of the diluted urease solution was added to 800 μL of a 0.5 M urea solution (pH adjusted to 6.9 to 7.0 using 0.05 M phosphate buffer or 0.25 M HEPES buffer) and the reaction solution was transferred to an oven that was preset at 25 °C. The reaction was terminated after 3 to 5 minutes by the addition of 5 mL of a phenol solution. Afterwards, 5 mL of a hypochlorite solution was added and the reaction solution was allowed to stand for at least 30 minutes at 25 °C before measuring the absorbance of the solution at 635 nm wavelength using UV-Vis. The absorbance value was then compared to a calibration curve to determine the amount of ammonia nitrogen (NH_3-N) in the sample. The calibration curve was prepared with ammonium chloride solutions containing known amounts of NH_3-N. The UV-Vis principle is based on Beer's law which states that the absorbance, A, is proportional to the path length, b, through the sample and the concentration of the absorbing species, c as shown in Equation 4.

$$A = \varepsilon . b . c \qquad (4)$$

Where, ε is the proportionality constant called the extinction coefficient.

On the Thermoo Scientific Genesys 10S UV-Vis instrument Beer's law was followed in the concentration range of 0 to 2.27 μg/ml which corresponds to 0 to 25 μg of NH_3-N since the total solution volume was 11 ml.

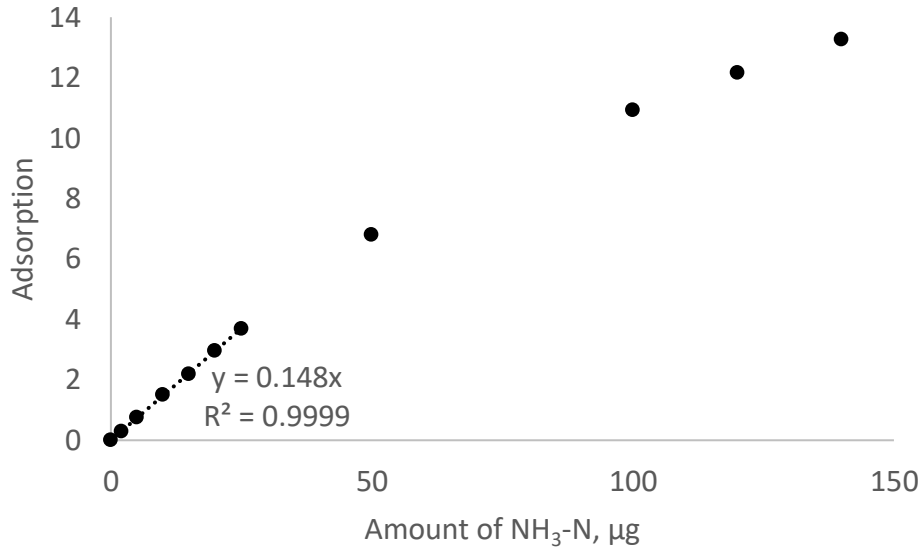

Figure 5-1 UV-Vis calibration curve showing the linear relationship between adsorption and amount of NH3-N

The activity of the urease enzyme was then calculated using the following equation:

$$Urease\ activity\ \left(\frac{Units}{ml\ enzyme}\right) = \frac{m_{NH_3-N} * df * 1000}{t * V_{enzyme} * M_N} \qquad (5)$$

Where: m_{NH_3-N} is the amount of ammonia nitrogen (in µg) produced by the urease which is derived from the calibration curve; df is the dilution factor used to dilute the enzyme so that it produces an amount of NH_3-N within the calibration curve; 1000 is the conversion factor from µl to ml; t is the time of the assay (in minutes); V_{enzyme} is the volume (in µl) of enzyme used; M_N is the molar mass of Nitrogen (in µg/µmole).

Urease activity in a gram of jack bean powder was calculated using the following equation:

$$Urease\ activity\ \left(\frac{Units}{gram\ solid}\right) = \frac{\left(\frac{Units}{ml\ enzyme}\right)}{\left(\frac{gram\ solid}{ml\ enzyme}\right)} \qquad (6)$$

5.2.3 Urease-catalyzed hydrolysis of urea

The urease-catalyzed hydrolysis of urea was studied at 50°C and 70°C. The test procedure is similar to the procedure used in our previous work [36] with some modifications due to the use of ASW. The composition of the ASW is shown in Table *5-1* [18].

Table 5-1 Composition of Artificial Seawater

Chemical	Concentration, wt. %
NaCl	2.629
KCl	0.074
$CaCl_2$	0.099
$MgCl_2$	0.609
$MgSO_4$	0.394
Total	3.805

In our previous work with highly purified commercial urease, we established that urease concentration of 31 U/g of solution was sufficient to effectively hydrolyze 10 wt. % urea solution [36]. Therefore, we used solutions with urease concentration of 31 U/g of solution and 10 wt. % urea in the work reported herein. Solutions containing urea and urease were prepared in DI and ASW. About 20 mL of the prepared solution was loaded in glass vials, sealed and placed in an oven at the designated test temperature. Multiple vials were prepared for each series of kinetics tests. After a designated time interval, one of the vials was removed from the oven and mixed by hand-shaking. Afterward, it was centrifuged at 335 RPM (17.5 x g) for 10 mins and then a sample was collected from the supernatant. The sample was diluted with HPLC grade ACN at a ratio of 9 : 1 w/w. The addition of ACN precipitates out the urease and stops the hydrolysis reaction. The diluted solution was then filtered through a 0.2-micron pore-size syringe filter before analysis. The change in the concentration of urea with time was used to study the kinetics of urea

hydrolysis. The concentration of urea in the solution was determined with HPLC using a UV-vis detector set at 200 nm wavelength [42]. If the concentration of urea in the sample is too high, then the sample is diluted with DI water or ASW before diluting with ACN. Calibration curves were prepared with known concentrations of urea prepared in DI water or ASW and diluted with ACN at 9 : 1 w/w ratio to obtain the final desired urea concentration. The calibration solution was also filtered through a 0.2-micron pore-size syringe filter before HPLC analysis. To separate urea from the salt in ASW, we connected a cation exchange and hydrophilic interaction liquid chromatography (HILIC) column in series with the analyte flowing through the cation exchange column first before flowing through the HILIC column. The column temperature was set at 30°C. The HPLC pumping rate was 1.5 mL/min and the mobile phase was acetonitrile and 0.1 M ammonium acetate in a 94 and 6 volume ratio. The pH of the mobile phase was adjusted to 4.5 using glacial acetic acid. After each run, the columns were flushed with several pore volumes of 30/70 v/v ACN/ammonium acetate followed by 94/6 v/v ACN/ammonium acetate. At least three replicate measurements were taken at each time interval.

5.2.4 Urease adsorption on porous media

The tests to evaluate the adsorption of urease on porous media were performed at room temperature. First, Ottawa sand and crushed Indiana limestone were sieved through ASTM 60 and 140 sieves with opening sizes of 250 and 106 microns respectively. The particles that were collected between the ASTM 60 and 140 sieves were used as the porous media for the test. 31 U/g urease solution was prepared with ASW, and 10 grams of the solution was then loaded into a 20 cc glass vial containing 2 grams of porous media. The sealed vials were then rotated on a rotary mixer with end-over-end rotation at 8 RPM to ensure adequate mixing between the urease

solution and the porous media. A reference solution was prepared by loading urease solution in a glass vial without porous media. After a designated time, a sample was collected from one of the vials to determine the urease activity using the Berthelot method. The sample was filtered through a 0.2 micron pore size syringe filter and diluted with DI water at a weight ratio of 1 : 30 before the activity measurement. A vial was prepared for each time interval tested for the porous media-containing solutions, while one vial was used for the reference solution. The adsorption of urease on the porous media was determined by comparing the activity of urease in the solutions with porous media and in the reference solution, at each time interval. The relative activity of the enzyme in the porous media was calculated by dividing the activity of urease in the porous media by the activity of the urease in the reference solution. A 30 gram/L urea solution prepared in DI water was used for the Berthelot activity measurement. The pH of the urea solution was adjusted to 6.9 to 7.0 with 0.25 M HEPES buffer. At least two replicate measurements were taken at each time interval.

5.2.5 Sand pack flooding

Sand pack flooding was performed to evaluate the oil recovery potential of the urease-catalyzed hydrolysis of urea under low-temperature conditions. The setup for the sand pack flooding is shown in Figure *4-1* and ASW was used instead of DI water. Tests were carried out at 50 $\pm$ 1 °C and 70 $\pm$ 1 °C and operating pressure of 1500 psi, using the general procedure in our previous work [36]. First, the porous media was prepared using a procedure similar to the approach used to prepare the porous media in the adsorption tests described in the previous section. Then, the sand pack was prepared by loading a specified amount of the sieved Ottawa sand or crushed and sieved Indiana limestone into a steel pressure vessel. Afterward, the sand pack was saturated

with crude oil and aged in an oven at 80 °C for 1 week. After the aging period, the sand pack was placed in an oven set at the test temperature and connected to an ISCO 500D syringe pump and back-pressure regulator. Water flooding was then initiated by injecting ASW at a flow rate of 0.3 ml/min and 1500 psi pressure until the oil cut dropped to zero. Once the residual oil saturation was established, 1 pore volume (PV) of treatment fluid was injected after compensating for the dead volume of the sand pack, followed by a 72-hour shut-in period. The purpose of the shut-in period was to provide sufficient time for urea hydrolysis and mass transfer of CO_2 from the aqueous phase to the oil phase. The syringe pump and back pressure regulator were used to maintain the pore pressure at 1500 psi throughout the shut-in period. After the shut-in period, the water flooding was resumed until all the mobilized oil was collected. The tertiary oil recovery (Etr) was calculated using the following equation:

$$Etr = \frac{So_i - So_f}{So_i} \times 100 \qquad (7)$$

Where So_i is the oil saturation after water flooding and So_f is the oil saturation after *in situ* CO_2 treatment.

5.3 Results and Discussion

5.3.1 Urease characterization

The first step in characterizing the enzyme was to determine its activity. This will determine the effectiveness of the enzyme extraction method used in our studies. We determined the urease activity in the jack bean extract with the Berthelot method. The average activity of the extracts was calculated from Equation 5 and was 706 ± 52 U/ml extract. The unit yield of the jack bean was calculated from Equation 6 and was 2211 ± 163 U/g jack bean powder. Tirkolaei, et al. [33]

obtained urease activity value of about 2600 U/g for their crude urease extracts from sword jack beans (*Canavalia gladiate*) in water. In their extraction process, the jack bean was first dehusked and then soaked overnight in DI at 4 °C. Afterwards, the solutions containing the beans were homogenized in a kitchen blender and filtered through a fabric to separate the enzyme-containing solution from the solids. This was followed by centrifugation and the removal of excess fat from the supernatant. The removal of the husk from the beans before extracting the urease could explain the increased urease activity observed in their experiments. The husk accounts for about 14 % of the mass of the beans [33], so taking this into account will yield an activity value of about 2570 U/g for our extracts, which is in close agreement with their value. Therefore, the simple and cost-efficient extraction method used in our study effectively extracts urease from jack beans and can easily scale-up for field application.

5.3.2 Urea hydrolysis

We studied urease-catalyzed hydrolysis of urea to understand the reaction rate and efficiency of the enzyme to convert urea to CO_2 and NH_3 under different test conditions. We did not introduce any buffers to control the pH of the system to replicate practical field applications where the use of buffers will add extra cost to the ICE process.

Figure *5-2* shows the results of the urease-catalyzed urea hydrolysis reaction kinetics in DI water. The result of the hydrolysis kinetics test from our previous work with high-purity commercial urease is also shown on the plot for comparison purposes [36]. The urea conversion ratio for the 50 °C test was over 95 % after 753 minutes of reaction time. This was higher than the 58 % conversion ratio we obtained after 753 minutes in our previous tests with high-purity commercial urease. The final urea conversion ratio in that test was 68.7 % after 2200 minutes. The higher

hydrolysis rate obtained with the crude urease extracts can be attributed to the presence of other jack bean proteins in the crude urease extract that protect the urease enzyme from rapid denaturalization due to changes in environmental conditions [33,43]. The urea hydrolysis rate was slower for the 70 °C test compared to the 50 °C test. The concentration of urea decreased rapidly and then remained fairly constant after 759 minutes, indicating that the urease was completely denatured at this point. The urea conversion ratio after 2220 minutes was 76.2 % for the 70 °C test. The lower hydrolysis rate and urea conversion ratio is due to the thermal denaturation of urease. The optimum temperature range for urease has been reported to occur in the temperature range 45 – 65 °C [44]; however, urease denatures over time at high temperatures [45,46]. Therefore, the reaction rate will initially increase with the increase in temperature and then slow down as the urease denatures. For all three tests, the pH of the solution increased rapidly and then plateaued at 9.99, 9.87 and 9.55 for the crude urease 50 °C test, 70 °C test and commercial urease 50 °C test, respectively.

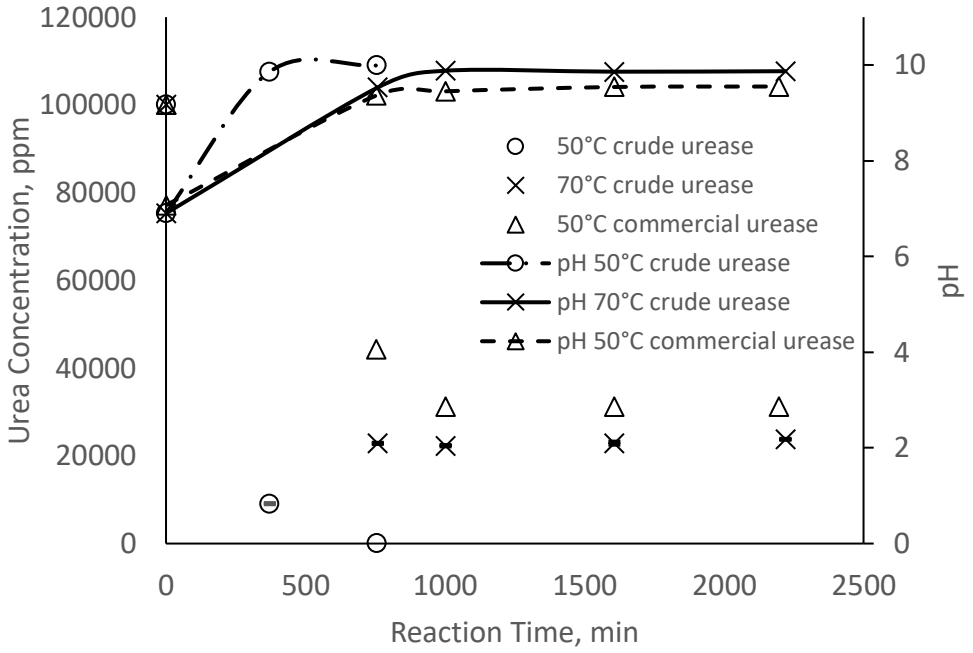

Figure 5-2 Urea concentration change of the jack bean urease catalyzed hydrolysis at different temperatures in DI

Figure *5-3* shows the results of the urease-catalyzed urea hydrolysis reaction kinetics in ASW. Similar to the DI case, the rate of hydrolysis and urea conversion was higher for the 50 °C test, which can be attributed to the denaturation of urease at higher temperatures. The use of ASW in the fluid system slowed the hydrolysis rate. The urea conversion ratio for the 50 °C test after 375 minutes was 84.5 %, which is lower than the 90.9 % obtained in the DI test. However, the urea conversion ratio for the 50 °C test after 764 minutes was over 95 %, which is similar to the DI test. The final urea conversion ratio for the 70 °C test after 2220 minutes was 64.8 %, lower than the 76.2 % obtained in the DI test. The influence of ASW on the hydrolysis rate and conversion ratio is attributed to two factors: the increase in ionic strength compared to the DI water case and the presence of divalent ions in ASW. Both factors can negatively impact the stability of urease. This effect seems more pronounced for the higher temperature test at 70 °C.

The concentration of urea is stable after 765 minutes indicating complete denaturation of urease, similar to the DI case. The pH of the system increased from 6.71 and plateaued at 9.73 and 9.57 for the 50 °C and 70 °C tests, respectively, which is slightly lower than the DI case.

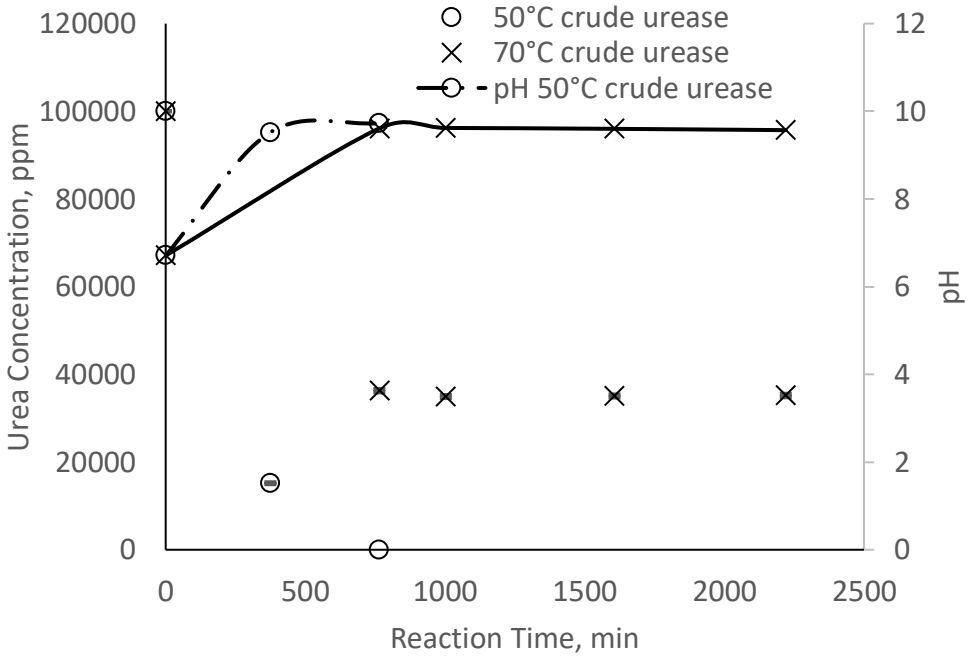

Figure 5-3 Urea concentration change of the jack bean urease catalyzed hydrolysis at different temperatures in ASW

5.3.3 Urease adsorption on porous media

The adsorption of urease on porous media was tested to understand the interaction between the enzyme and porous media and what role this might play in EOR. High adsorption of urease on porous media could lead to a loss of the enzyme near the wellbore, thereby reducing the amount of enzyme available for urea hydrolysis at the targeted oil-producing zone. While

immobilizing urease on solid surfaces through adsorption or other techniques enhances the stability of the enzyme, particularly in terms of thermal and low pH conditions, it generally leads to a decrease in enzyme activity [44,47]. Pinto Vilar and Ikuma [48,49] studied the adsorption of urease, as part of a total bacterial protein extract, onto soils. Their results showed preferential adsorption of the larger proteins in the extract onto the soils. Additionally, a smaller amount of urease was adsorbed onto the sand-only soils (98.7% silica) compared to sand-silt mixtures. This was attributed to differences in the electrostatic affinities between negatively charged urease and negatively charged sand compared to urease and positively charged patches on the silt surfaces in the sand-silt mixtures. Although the urease that was adsorbed on the solid surface maintained some activity, an overall loss of activity was observed due to the adsorption of urease on the soil surfaces. Pisani, et al. [50] also used density functional theory (DFT) to investigate the binding ability of urease enzyme on quartz and other minerals. They simulated amino acids comprising at least 5% of the urease enzyme and observed a low preference for the binding of the amino acids on quartz. In general, protein adsorption behavior is a multifaceted process governed by multiple parameters such as temperature, pH, ionic strength, and buffer composition. In our experiment, we did not use a buffer to control the solution pH in order to replicate actual reservoir conditions. The isoelectric points of crystalline urease from jack bean, of quartz, and of calcite are at pH 5.0 to 5.1, 2 to 3 and 8 to 9.5, respectively [37,51]. Therefore, we will expect the enzyme to interact differently with silica and limestone. The adsorption of urease on sandstone and limestone is shown in Figure *5-4*. The plot also shows the pH of the solution, starting from the moment the urease solution was introduced to the porous media up until the 24-hour mark. There was no significant change in the solution pH throughout the course

of the experiment for each of the porous media. The pH of the solutions with sandstone and limestone ranged from 5.4 to 5.6 and 6.9 to 7.6 respectively. The pH of the reference urease solution without porous media ranged from 5.3 to 5.4 for the 24-hour period. The slight increase in the pH of the solutions with limestone is due to the dissolution of limestone in the ASW [52].

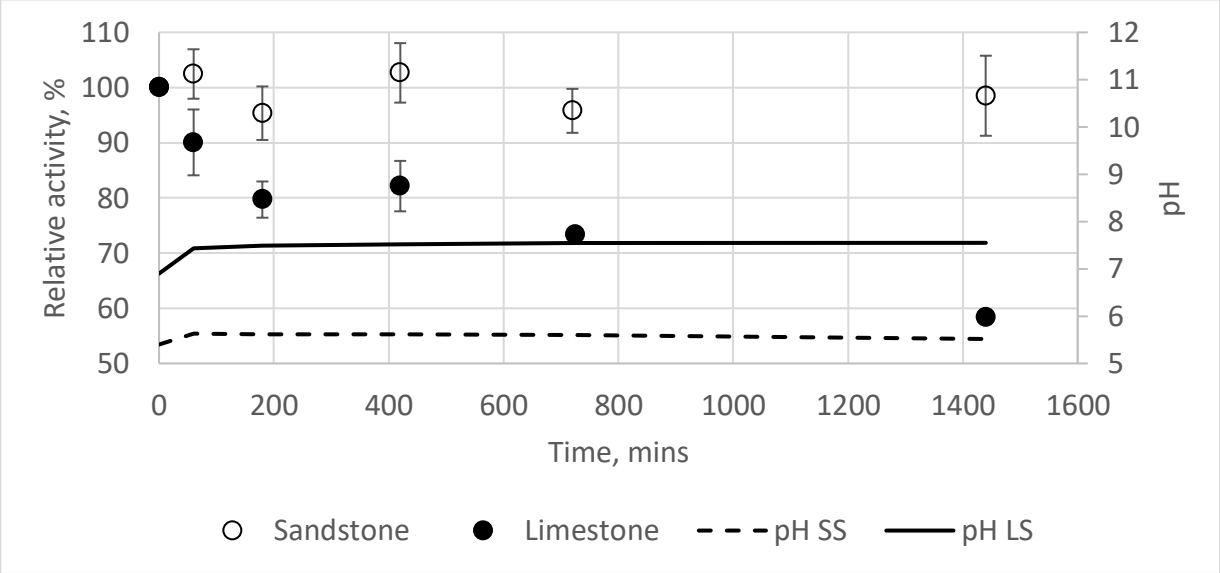

Figure 5-4 Adsorption of urease on porous media

We observed no adsorption of urease on silica within the 24-hour test period. This could be attributed to the lack of charge affinities of the urease molecule for sandstone. The pH of the solutions with sandstone was slightly above the isoelectric point of urease, therefore we will expect the urease molecule to be negatively charged. The surface of sandstone will also be negatively charged under these pH conditions. Therefore, there will be repulsive electrostatic interactions between the sandstone and urease molecule, which will hinder adsorption [53]. Another factor that could hinder the adsorption of urease on sandstone could be the presence of some larger proteins in the crude urease extract. Pinto Vilar and Ikuma [48] observed that larger proteins in a complex protein mixture of bacterial urease are preferentially adsorbed on

sand surfaces. Urease is adsorbed on limestone as shown in Figure *5-4*. Similar to the sandstone case, this could be attributed to the charge affinities of the urease molecule for limestone. We expect the surface of the limestone grains to be positively charged under the pH conditions of the solution. Therefore, there will be attractive electrostatic interactions between the limestone grains and urease molecules. Based on the adsorption kinetics study, we will expect the crude urease to retain more net activity in sandstone porous media than limestone.

5.3.4 Low-temperature ICE sand pack flooding

Sand pack flooding tests were conducted to determine the effectiveness of the crude urease extracts in a low-temperature ICE system. In our previous study [36], we used high-purity commercially available urease from jack bean (*Canavalia ensiformis*) to study the feasibility of the urease-catalyzed ICE system at 50 °C and DI water was used instead of brine. In this study we expanded the temperature envelope to include 70 °C and ASW was used as the brine. Moreover, the oil-saturated sand pack was aged for 7 days in this study while the aging time in our previous feasibility study was 1 day. The parameters for the sand pack studies are summarized in Table *5-2*.

Table 5-2 Summary of the sand pack flooding experiments

Test #	Temperature, °C	Chemical Slug Type	Porous Media Type	Residual Oil Saturation, %	Permeability, mD	Porosity, %
1	50	Low T ICE	Ottawa Sand	52.6	3937	33.09
2	70	Low T ICE	Ottawa Sand	47.7	3697	32.68
3	50	3.7 wt. % NH_3	Ottawa Sand	52.3	3533	32.39
4	50	Low T ICE	Crushed Indiana Limestone	57.7	4953	38.55
5	70	Low T ICE	Crushed Indiana Limestone	57.3	4656	38.47
6	50	3.0 wt. % NH_3	Crushed Indiana Limestone	56.7	4903	38.93

* Note: In all tests, sand pack aging time was 7 days (80 °C), the injection rate was 0.3 mL/min, ASW was used in water flooding, back pressure was 1500 psi, and the oil type was middle-east oil.

Figure *5-5* shows the tertiary recoveries of the sand pack flooding for sandstone at 50 °C and 70 °C. Around 8.5 and 9 PV was applied to reach residual oil saturation for the 50 °C and 70 °C tests, respectively. The 50 °C test reached a residual oil saturation of 52.6 % and the residual oil saturation of the 70 °C test was 47.7 %. The dashed line shown in Figure *5-5* indicates the injection of the chemical slug. The tertiary recovery factor was 10.6 % and 8.6 % for the tests at 50 °C and 70 °C, respectively. The higher recovery at the lower temperature is expected due to the increased solubility of CO_2 in oil at lower temperatures. Based on the CO_2 solubility model proposed by Emera and Sarma [54], CO_2 solubility in oil would increase by about 14% when the temperature is reduced from 70 °C to 50 °C, while keeping other parameters constant. The oil recovery for the 50 °C test in this work is lower compared to the 50 °C test with sandstone in our previous work [36]. In our previous work, we used DI water as the base fluid and the oil-saturated sand pack was aged for 1 day before running the sand pack flooding. Zhou, et al. [55] showed that the water wetness and the oil recovery by water flooding for sandstone cores decreased with an increase in the time the cores were aged in crude oil from 1 to 240 hours. Moreover, there was a period of more than one year between the time we ran the tests in our previous work and the tests reported in this work. Within that period, the acid number of the crude oil changed while in storage from 0.19 mg KOH/g to < 0.05 mg KOH/g. In our previous work [56], we established that the oil recovery of crude oil-aged sandstone porous media, increases with an increase in crude oil acid number. Therefore, the reduction in oil recovery could be due to the longer aging time and the change in the acid number of the crude oil.

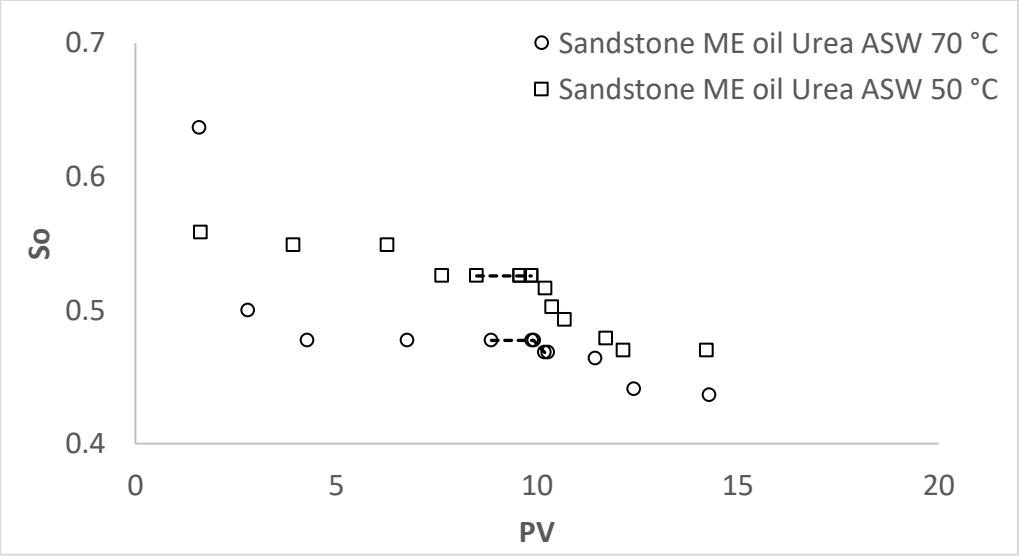

Figure 5-5 The effect of temperature in low-temperature ICE system for sandstone

Sand pack flooding with NH_3(aq) was performed to compare with the urea flooding case at 50 °C. The NH_3(aq) flooding will help isolate the contributions of NH_3 and CO_2-related mechanisms on the tertiary recovery. The conversion ratio for the urea in the 50 °C sandstone test was 65.7 %, corresponding to 3.7 wt. % NH_3(aq.). Figure *5-6* shows the result of the NH_3(aq) flooding compared to the urea flooding at 50 °C. About 9.5 PV of ASW was injected through the sand pack to achieve a residual oil saturation of 52.3 % for the NH_3(aq) flooding case. This is in good agreement with the residual oil saturation for the urea flooding case and shows consistency in the porous media structure. The tertiary oil recovery for the NH_3 flooding was 2.6 %. The NH_3-related tertiary recovery is mainly due to the elevated alkalinity of the aqueous phase and the water wetness improvement caused by the ammonium hydroxide. The NH_3(aq) flooding recovery is about 25 % of the tertiary recovery for the urea flooding case at 50 °C. This implies that 75 % of the tertiary recovery in the urea flooding case is due to CO_2-related oil recovery mechanism

and 25 % is due to NH_3-related mechanisms. This is in good agreement with the tertiary recovery from the NH_3(aq) and urea flooding in our previous low-temperature tests with DI water as the brine [36]. In those tests, we obtained 31.3 % and 7.4 % tertiary oil recovery for the urea and NH_3(aq) flooding, respectively. Thus, the NH_3 flooding oil recovery was about 24 % of the urea flooding oil recovery, which is in good agreement with the 25 % obtained in our current tests with ASW as the base fluid. In our previous high-temperature tests with sand at 120 °C [56], we obtained 26.1 % and 11.1 % tertiary oil recovery for the urea and NH_3(aq) flooding, respectively. This implies that about 43 % of the tertiary oil recovery was due to the NH_3-related oil recovery mechanisms and 57 % was due to CO_2-related mechanisms. It is evident that CO_2 contributes more to the tertiary oil recovery as the test temperature decreases from 120 °C to 50 °C. This is reasonable since the solubility of CO_2 in oil is higher at lower temperatures, hence CO_2 will contribute more to the total oil recovery compared to the higher temperature tests. However, in the high-temperature tests, the urea and ammonia concentrations were higher at 35 wt % and 15 wt % respectively, which could also impact the oil recovery.

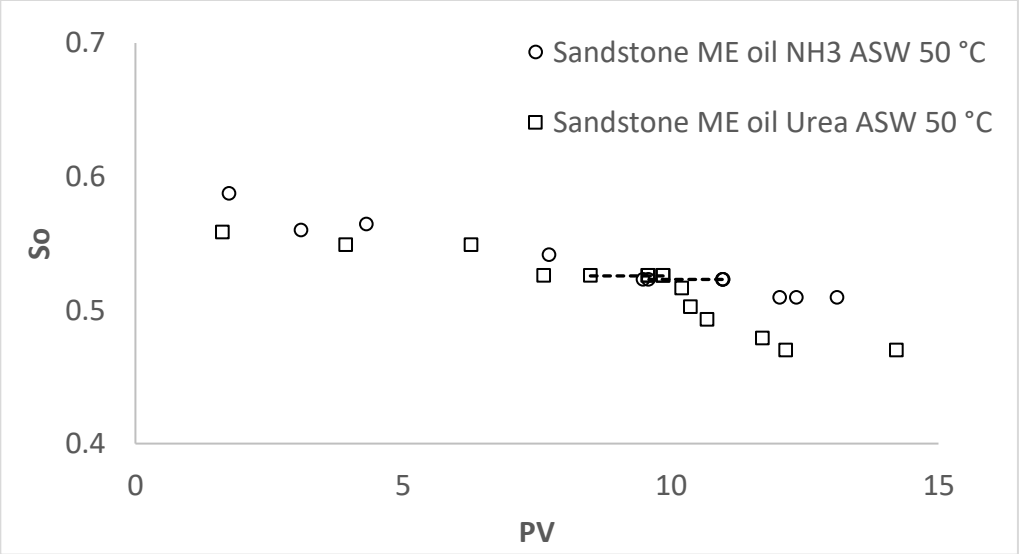

Figure 5-6 The effect of CO_2 in low-temperature ICE system for sandstone

Figure *5-7* shows the tertiary recoveries of the sand pack flooding for limestone at 50 °C and 70 °C. Around 8.8 and 8.6 PV ASW was injected to reach residual oil saturation for the 50 °C and 70 °C tests, respectively. The 50 °C test reached a residual oil saturation of 57.7 % and the residual oil saturation of the 70 °C test was 57.3 %. The dashed line shown in Figure *5-7* indicates the injection of the chemical slug. The tertiary recovery factor was 28.0 % and 22.5 % for the tests at 50 °C and 70 °C respectively. Similar to the sandstone case, the higher recovery at the lower temperature was expected due to the increased solubility of CO_2 in oil at lower temperatures. The oil recovery for the 50 °C test was comparable to the oil recovery for the urea flooding with DI as the brine.

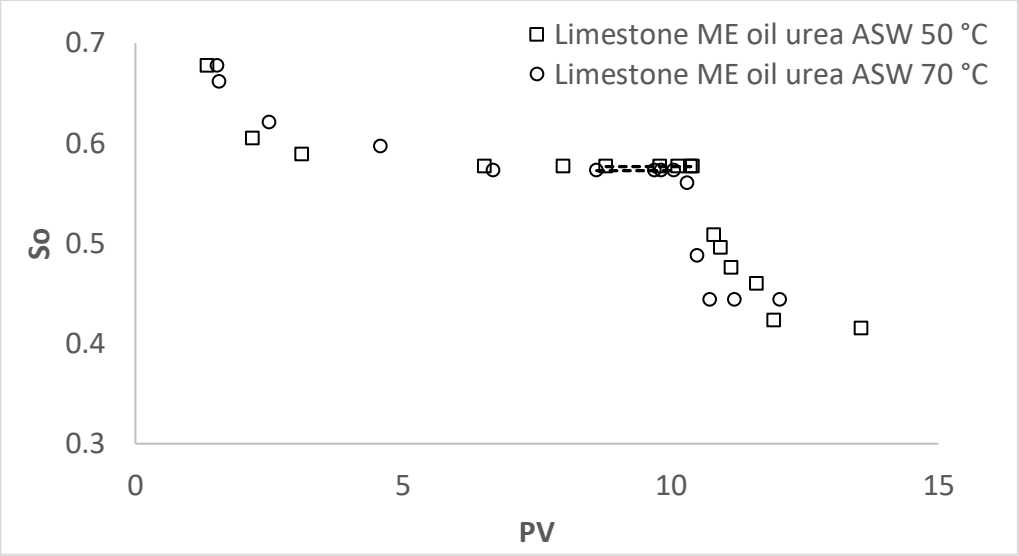

Figure 5-7 The effect of temperature in low-temperature ICE system for limestone

Sand pack flooding with NH_3(aq) was performed to compare with the urea flooding case at 50 °C and help isolate the contributions of NH_3 and CO_2-related mechanisms on the tertiary recovery. The conversion ratio for the urea in the 50 °C limestone test was 53.8 %, corresponding to 3.0 wt. % NH_3(aq). Figure *5-8* shows the result of the NH_3(aq) flooding compared to the urea flooding at 50 °C. About 9.3 PV of ASW was injected through the sand pack to reach a residual oil saturation of 56.7 % for the NH_3(aq) flooding case. The tertiary oil recovery for the NH_3 flooding was 2.9 %. According to research by Wang et al. [56], the impact of NH_3 on carbonate wettability alteration was determined to be insignificant. As a result, the main factor influencing tertiary oil recovery was IFT reduction by the ammonium hydroxide. The NH_3(aq) flooding recovery is about 10 % of the tertiary recovery for the urea flooding case which implies that 90 % of the tertiary recovery in the urea flooding case is due to CO_2-related oil recovery mechanism and 10 % is due to NH_3-related mechanisms. In our previous low-temperature tests with commercially available

urease we obtained 27.5 % and 4.1 % tertiary oil recovery for the urea and NH_3(aq) flooding, respectively [36].

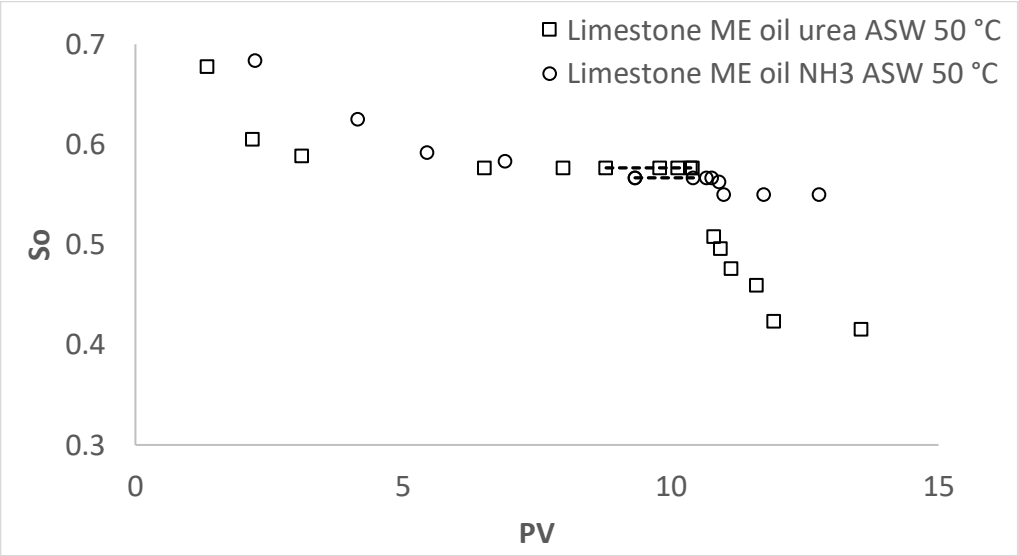

Figure 5-8 The effect of CO_2 in low-temperature ICE system for limestone

This implies that 15 % of the tertiary oil recovery was due to NH_3-related mechanisms and 85.1 % was due to CO_2-related mechanisms, which is similar to the values obtained in this work. Hence, the contribution of NH_3-related mechanism on the tertiary oil recovery is lower for the limestone case compared to sandstone (25 %) and is consistent with our previous work [36,56]. It appears that the longer aging time and change in oil acid number did not affect the tertiary oil recovery for limestone compared to the sandstone case. This could be due to the higher oil wetness of limestone and the reduced contribution of NH_3-related mechanism on limestone oil recovery, compared to sandstone.

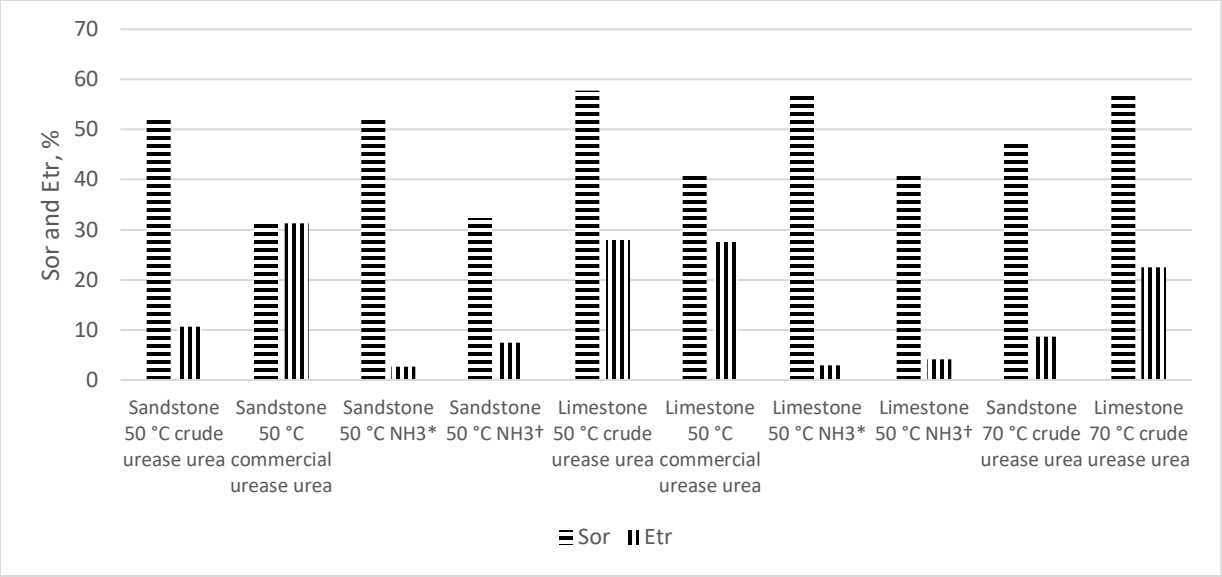

Figure 5-9 Tertiary recovery comparison between crude urease extract and commercial urease *[36]*

*Test was run with the crude urease tests. †Test was run with the commercial urease tests.

5.3.5 Effect of crude oil and porous media on urea hydrolysis

The urea conversion ratio for both sandstone and limestone porous media tests was lower than the batch tests. This can be attributed to the presence of the porous media, crude oil, or both. To investigate the effect of crude oil on the efficiency of urease enzyme to catalyze the hydrolysis of urea, we carried out two sand pack flooding tests at 50 °C with water-saturated sandstone and limestone. The sand packs were prepared similar to the oil saturated sand packs, however we saturated the sand packs with ASW instead of crude oil. The urea conversion ratios for the flowthrough tests are summarized in Table *5-3*. The results show urea conversion ratio of 87.5 % and 84.3 % for the sandstone and limestone, respectively. This is higher than the 65.7 % and 53.8 % urea conversion ratio obtained for the oil-saturated sandstone and limestone porous media, respectively; however, it is lower than the 95 % or greater urea conversion obtained in

the 50 °C batch tests discussed in section 5.3.2. The lower urea conversion ratio for the oil-saturated sand pack compared to the ASW-saturated sand pack could be due to the presence of substances in the crude oil, which potentially inhibit urease activity. It can also be due to crude oil coating the enzyme and potentially obstructing its active sites. The lower urea conversion ratio of the ASW-saturated sand packs compared to the batch tests could be attributed to the presence of the porous media. The relatively high tertiary oil recovery despite the modest urea conversion rate of the oil-saturated sand pack suggests that the system can be further optimized. One optimization strategy will be to reduce the urea concentration, while leaving the urease concentration the same. Lower urea concentration can increase the urea conversion ratio since the activity of urease could be inhibited by higher urea concentrations [27,57,58]. Moreover, the urease active sites to substrate ratio will increase if the urea concentration is reduced while keeping the enzyme concentration constant. Another optimization strategy will be to deliver the urea plus urease slug in two stages, with a shut-in period and water flooding after the first and second stages.

Table 5-3 Urea conversion for the flowthrough tests

Porous media type	Temperature, °C	Pore fluid type	Urea conversion, %
Sandstone	50	Crude oil and ASW	65.7
Sandstone	70	Crude oil and ASW	55.4
Limestone	50	Crude oil and ASW	53.8
Limestone	70	Crude oil and ASW	52.6
Sandstone	50	ASW	87.5
Limestone	50	ASW	84.3

Some of the divalent cations in the ASW combined with the carbonate ion from the generated CO_2 to form insoluble carbonates like calcium carbonate, which precipitate out of the solution.

These precipitates could pose a problem for low permeability reservoirs; however we did not observe any adverse effects in our flowthrough experiments due to the high permeability of our sand packs. Hence, it is worth considering the preparation of the urease plus urea solution with soft water to mitigate any potential issues related to the precipitation of carbonates. Furthermore, if the hardness content in the formation water is high, a preflush may be necessary to separate the reservoir brine from the chemical slug.

5.4 Conclusion

Using crude jack bean urease extracts makes urease-catalyzed *in situ* CO_2 EOR economically viable compared to using high-purity commercially available urease. Urease was successfully extracted with DI water using a simple method without any chemical additives. The extracted urease effectively catalyzed the hydrolysis of urea at reservoir temperatures of 50 °C and 70 °C and pressure of 1500 psi. The hydrolysis rate and conversion ratio of urea was lower at 70 °C compared to 50 °C, due to the denaturation of urease at the higher temperature. Urease was adsorbed on limestone surfaces which resulted in an overall decrease in enzyme activity, whereas the adsorption of urease on sandstone was insignificant. The flowthrough sand pack tests show that the tertiary recovery for the limestone and sandstone tests were lower at 70 °C compared to 50 °C. This is due to the higher solubility of CO_2 in oil at lower temperature conditions. The tertiary recoveries at 50 °C were 28.0 % and 10.6 % for the limestone and sandstone tests, respectively. At 70 °C, the tertiary recoveries were 22.5 % and 8.6 % for the limestone and sandstone tests, respectively. Moreover, the contribution of NH_3-related mechanism on the tertiary oil recovery is lower for the limestone case compared to sandstone.

References

[1] https://jpt.spe.org/author/trent-jacobs. CO2 EOR Could Be Industry's Key to a Sustainable Future or Its Biggest Missed Opportunity. JPT 2020. https://jpt.spe.org/co2-eor-could-be-industrys-key-sustainable-future-or-its-biggest-missed-opportunity (accessed July 4, 2023).

[2] National Energy Technology Laboratory (NETL), https://netl.doe.gov/sites/default/files/2023-04/Program-157.pdf. Enhanced Oil Recovery Programme 157 2022.

[3] https://jpt.spe.org/author/ole-gunnar-tveiten. Recycling CO2 for EOR? Why Not? JPT 2023. https://jpt.spe.org/recycling-co2-for-eor-why-not (accessed July 4, 2023).

[4] Ogbonnaya O, Wang S, Shiau B, Harwell J. Use of In-Situ CO2 Generation in Liquid-Rich Shale, Society of Petroleum Engineers; 2020. https://doi.org/10.2118/200383-MS.

[5] Shu WR. Carbonated waterflooding for viscous oil recovery. United States patent US4441555A, 1984.

[6] Teklu TW, Alameri W, Graves RM, Kazemi H, AlSumaiti AM. Low-salinity water-alternating-CO2 EOR. J Pet Sci Eng 2016;142:101–18. https://doi.org/10.1016/j.petrol.2016.01.031.

[7] Afzali S, Rezaei N, Zendehboudi S. A comprehensive review on Enhanced Oil Recovery by Water Alternating Gas (WAG) injection. Fuel 2018;227:218–46. https://doi.org/10.1016/j.fuel.2018.04.015.

[8] Esene C, Rezaei N, Aborig A, Zendehboudi S. Comprehensive review of carbonated water injection for enhanced oil recovery. Fuel 2019;237:1086–107. https://doi.org/10.1016/j.fuel.2018.08.106.

[9] Al-Shargabi M, Davoodi S, Wood DA, Rukavishnikov VS, Minaev KM. Carbon Dioxide Applications for Enhanced Oil Recovery Assisted by Nanoparticles: Recent Developments. ACS Omega 2022;7:9984–94. https://doi.org/10.1021/acsomega.1c07123.

[10] Raifsnider PJ, Raifsnider DE. In-situ formed CO2 drive for oil recovery. United States patent US3532165A, 1970.

[11] Bayless JH, Williams RE. Recovery of viscous oil from geological reservoirs using hydrogen peroxide. United States patent US4867238A, 1989.

[12] Gumersky KK, Dzhafarov IS, Shakhverdiev AK, Mamedov YG. In-Situ Generation of Carbon Dioxide: New Way To Increase Oil Recovery, OnePetro; 2000. https://doi.org/10.2118/65170-MS.

[13] Altunina L, Kuvshinov V. Improved Oil Recovery of High-Viscosity Oil Pools with Physicochemical Methods and Thermal-Steam Treatments. Oil Gas Sci Technol - Rev IFP 2007;63. https://doi.org/10.2516/ogst:2007075.

[14] Shiau BJ, Hsu T-P, Roberts BL, Harwell JH. Improved Chemical Flood Efficiency by In Situ CO2 Generation, OnePetro; 2010. https://doi.org/10.2118/129893-MS.

[15] Liu P, Li W, Shen D. Experimental study and pilot test of urea- and urea-and-foam-assisted steam flooding in heavy oil reservoirs. J Pet Sci Eng 2015;135:291–8. https://doi.org/10.1016/j.petrol.2015.09.026.

[16] Yang C, Lin Y, Zhang Z, Deng R, Wu X, Niu B, et al. A Study on the Mechanism of Urea-assisted Steam Flooding in Heavy Oil Reservoirs. J Pet Sci Technol 2015;5:36–44. https://doi.org/10.22078/jpst.2015.511.

[17] Wang S, Kadhum M, Yuan Q, Shiau B-J, Harwell JH. Carbon Dioxide in Situ Generation for Enhanced Oil Recovery. Carbon Manag. Technol. Conf., Houston, Texas, USA: Carbon Management Technology Conference; 2017. https://doi.org/10.7122/486365-MS.

[18] Wang S, Chen C, Shiau B, Harwell JH. In-situ CO2 generation for EOR by using urea as a gas generation agent. Fuel 2018;217:499–507. https://doi.org/10.1016/j.fuel.2017.12.103.

[19] Altunina LK, Kuvshinov VA. Evolution Tendencies of Physico-Chemical EOR Methods, OnePetro; 2000. https://doi.org/10.2118/65173-MS.

[20] Altunina LK, Kuvshinov VA. Physicochemical methods for enhancing oil recovery from oil fields. Russ Chem Rev 2007;76:971–87. https://doi.org/10.1070/RC2007v076n10ABEH003723.

[21] Bakhtiyarov SI. Technology of In-Situ Gas Generation to Recover Residual Oil Reserves | netl.doe.gov 2008. https://netl.doe.gov/node/4028 (accessed December 29, 2019).

[22] Yalkowsky SH, He Y, Jain P, He Y, Jain P. Handbook of Aqueous Solubility Data. CRC Press; 2016. https://doi.org/10.1201/EBK1439802458.

[23] Karplus PA, Pearson MA, Hausinger RP. 70 Years of Crystalline Urease: What Have We Learned? Acc Chem Res 1997;30:330–7. https://doi.org/10.1021/ar960022j.

[24] Sigurdarson JJ, Svane S, Karring H. The molecular processes of urea hydrolysis in relation to ammonia emissions from agriculture. Rev Environ Sci Biotechnol 2018;17:241–58. https://doi.org/10.1007/s11157-018-9466-1.

[25] Wang S, Chen C, Li K, Yuan N, Shiau B, Harwell JH. In Situ CO2 Enhanced Oil Recovery: Parameters Affecting Reaction Kinetics and Recovery Performance. Energy Fuels 2019;33:3844–54. https://doi.org/10.1021/acs.energyfuels.8b03734.

[26] Blakeley RL, Zerner B. Jack bean urease: the first nickel enzyme. J Mol Catal 1984;23:263–92. https://doi.org/10.1016/0304-5102(84)80014-0.

[27] Krajewska B. Ureases I. Functional, catalytic and kinetic properties: A review. J Mol Catal B Enzym 2009;59:9–21. https://doi.org/10.1016/j.molcatb.2009.01.003.

[28] Krajewska B, van Eldik R, Brindell M. Temperature- and pressure-dependent stopped-flow kinetic studies of jack bean urease. Implications for the catalytic mechanism. J Biol Inorg Chem 2012;17:1123–34. https://doi.org/10.1007/s00775-012-0926-8.

[29] Van Slyke DD, Cullen GE. The Mode of Action of Urease and of Enzymes in General. JBiol Chem 1914;19:141–80.

[30] Pinto Vilar R, Ikuma K. Adsorption of urease as part of a complex protein mixture onto soil and its implications for enzymatic activity. Biochem Eng J 2021;171:108026. https://doi.org/10.1016/j.bej.2021.108026.

[31] Krajewska B. A combined temperature-pH study of urease kinetics. Assigning pKa values to ionizable groups of the active site involved in the catalytic reaction. J Mol Catal B Enzym 2016;124:70–6. https://doi.org/10.1016/j.molcatb.2015.11.021.

[32] X. Werkmeister F, Koide T, A. Nickel B. Ammonia sensing for enzymatic urea detection using organic field effect transistors and a semipermeable membrane. J Mater Chem B 2016;4:162–8. https://doi.org/10.1039/C5TB02025E.

[33] Khodadadi Tirkolaei H, Javadi N, Krishnan V, Hamdan N, Kavazanjian E. Crude Urease Extract for Biocementation. J Mater Civ Eng 2020;32:04020374. https://doi.org/10.1061/(ASCE)MT.1943-5533.0003466.

[34] Mateer JG, Marshall EK. The Urease Content of Certain Beans, with Special Reference to the Jack Bean. JBiol Chem 1916;25:297–305.

[35] Weber M, Jones MJ, Ulrich J. Optimisation of isolation and purification of the jack bean enzyme urease by extraction and subsequent crystallization. Food Bioprod Process 2008;86:43–52. https://doi.org/10.1016/j.fbp.2007.10.005.

[36] Wang S, Ogbonnaya O, Chen C, Yuan N, Shiau B, Harwell JH. Low-temperature in situ CO2 enhanced oil recovery. Fuel 2022;329:125425. https://doi.org/10.1016/j.fuel.2022.125425.

[37] Sumner JB, Hand DB. THE ISOELECTRIC POINT OF CRYSTALLINE UREASE 1. J Am Chem Soc 1929;51:1255–60. https://doi.org/10.1021/ja01379a039.

[38] Hanabusa K. High-yield crystallization of urease from jack bean. Nature 1961;189:551–3. https://doi.org/10.1038/189551a0.

[39] Weatherburn MW. Phenol-hypochlorite reaction for determination of ammonia. Anal Chem 1967;39:971–4. https://doi.org/10.1021/ac60252a045.

[40] Krajewska B, Zaborska W. The effect of phosphate buffer in the range of pH 5.80–8.07 on jack bean urease activity. J Mol Catal B Enzym 1999;6:75–81. https://doi.org/10.1016/S1381-1177(98)00129-5.

[41] Spinelli JB, Kelley LP, Haigis MC. An LC-MS Approach to Quantitative Measurement of Ammonia Isotopologues. Sci Rep 2017;7:10304. https://doi.org/10.1038/s41598-017-09993-6.

[42] Sahu JN, Mahalik K, Patwardhan AV, Meikap BC. Equilibrium and Kinetic Studies on the Hydrolysis of Urea for Ammonia Generation in a Semibatch Reactor. Ind Eng Chem Res 2008;47:4689–96. https://doi.org/10.1021/ie800481z.

[43] Van Slyke DD, Archibald RM. Manometric, Titrimetric, and Colorimetric Methods For Measurement of Urease Activity. J Biol Chem 1944;154:623–42.

[44] Krajewska B. Ureases. II. Properties and their customizing by enzyme immobilizations: A review. J Mol Catal B Enzym 2009;59:22–40. https://doi.org/10.1016/j.molcatb.2009.01.004.

[45] Chen J-P, Chiu S-H. A poly(N-isopropylacrylamide-co-N-acryloxysuccinimide-co-2-hydroxyethyl methacrylate) composite hydrogel membrane for urease immobilization to enhance urea hydrolysis rate by temperature swing☆. Enzyme Microb Technol 2000;26:359–67. https://doi.org/10.1016/S0141-0229(99)00181-7.

[46] Illeová V, Polakovič M, Štefuca V, Ačai P, Juma M. Experimental modelling of thermal inactivation of urease. J Biotechnol 2003;105:235–43. https://doi.org/10.1016/j.jbiotec.2003.07.005.

[47] Krajewska B, Leszko M, Zaborska W. Urease immobilized on chitosan membrane: Preparation and properties. J Chem Technol Biotechnol 1990;48:337–50. https://doi.org/10.1002/jctb.280480309.

[48] Pinto Vilar R, Ikuma K. Adsorption of urease as part of a complex protein mixture onto soil and its implications for enzymatic activity. Biochem Eng J 2021;171:108026. https://doi.org/10.1016/j.bej.2021.108026.

[49] Pinto Vilar R, Ikuma K. Effects of Soil Surface Chemistry on Adsorption and Activity of Urease from a Crude Protein Extract: Implications for Biocementation Applications. Catalysts 2022;12:230. https://doi.org/10.3390/catal12020230.

[50] Pisani WA, Jenness GR, Schutt TC, Larson SL, Shukla MK. Preferential Adsorption of Prominent Amino Acids in the Urease Enzyme of Sporosarcina pasteurii on Arid Soil Components: A Periodic DFT Study. Langmuir 2022;38:13414–28.

https://doi.org/10.1021/acs.langmuir.2c01854.

[51] Hirasaki GJ. Wettability: Fundamentals and Surface Forces. SPE Form Eval 1991;6:217–26. https://doi.org/10.2118/17367-PA.

[52] Haddad MJ. Modeling of limestone dissolution in packed-bed contactors treating dilute acidic water. Syracuse Univ.,Syracuse, NY, 1986.

[53] Leprince F, Quiquampoix H. Extracellular enzyme activity in soil: effect of pH and ionic strength on the interaction with montmorillonite of two acid phosphatases secreted by the ectomycorrhizal fungus Hebetomu cylindrosporum. Eur J Soil Sci 1996;47:511–22. https://doi.org/10.1111/j.1365-2389.1996.tb01851.x.

[54] Emera MK, Sarma HK. Prediction of CO2 Solubility in Oil and the Effects on the Oil Physical Properties. Energy Sources Part Recovery Util Environ Eff 2007;29:1233–42. https://doi.org/10.1080/00908310500434481.

[55] Zhou X, Morrow NR, Ma S. Interrelationship of Wettability, Initial Water Saturation, Aging Time, and Oil Recovery by Spontaneous Imbibition and Waterflooding. SPE J 2000;5:199–207. https://doi.org/10.2118/62507-PA.

[56] Wang S, Li K, Chen C, Onyekachi O, Shiau B, Harwell JH. Isolated mechanism study on in situ CO2 EOR. Fuel 2019;254:115575. https://doi.org/10.1016/j.fuel.2019.05.158.

[57] Howell F, Sumner B. THE SPECIFIC EFFECTS OF BUFFERS UPON UREASE ACTIVITY. JBiol Chem 1934;104:619–26.

[58] Kistiakowsky GB, Rosenberg AJ. The Kinetics of Urea Hydrolysis by Urease1. J Am Chem Soc 1952;74:5020–5. https://doi.org/10.1021/ja01140a009.

Chapter 6 Conclusions and Recommendations For Future Research

6.1 Conclusions

Chapter 2 focused on the development of effective ICE formulations for liquid-rich shale reservoirs. We used a simple alkane (dodecane) as the oil phase and urea as the gas-generating agent to investigate the applicability of ICE in liquid-rich shale reservoirs. Due to the extremely low permeability of shale, we combined the gas-generating agent with a thermally stable anionic surfactant to facilitate the imbibition of the ICE formulation into the shale matrix and enhance the EOR performance of the formulation. Imbibition tests designed to simulate the huff-n-puff operation were performed with oil-saturated shale samples using four different EOR formulations: brine only, urea in brine, thermally stable anionic surfactant in brine and a mixture of urea and surfactant in brine. The urea-only solution recovered up to 24% of the OOIP, compared to 6% with brine and 21% with surfactant. Interestingly, combining surfactant with urea did not provide additional benefits. This was attributed to the strong water wetness of the dodecane-saturated shale cores. Additionally, there was no benefit to running the ICE operation at conditions above MMP. This work provided a strong proof of concept for the potential of ICE to significantly enhance oil recovery in liquid-rich shale reservoirs.

In Chapter 3 we further investigate the application of ICE in liquid-rich shale reservoirs. In this chapter, we used crude oil instead of dodecane as the oil phase to investigate the applicability of ICE in liquid-rich shale reservoirs. Imbibition tests that mimic the huff-n-puff technique were conducted with oil-saturated shale samples using four different EOR formulations: brine only, urea in brine, thermally stable anionic surfactant in brine and a mixture of urea and surfactant in

brine. The study found that combining urea with the surfactant led to the best oil recovery results. After 14 days of imbibition, this combination recovered 18 % of the OOIP, whereas brine-only, urea in brine and surfactant in brine recovered 7 %, 9 % and 5 % of the OOIP, respectively. Moreover, there was a distinct difference in the oil recoveries for the 3-days and 14-days imbibition periods in the case of the ternary brine/urea/surfactant mixture. This might indicate that the oil recovery process in the shale cores is dependent on the duration of the imbibition period. Contact angle and IFT measurements showed that both wettability alteration and IFT reduction play critical roles in improving oil recovery. The generated ammonia alters the wettability of the shale from an oil-wet state to a more water-wet state while the surfactant reduces the IFT, thereby facilitating the imbibition of the EOR fluid into the shale matrix. The imbibition of the EOR fluid into the shale matrix allows the generated CO_2 to contact more oil and promotes oil recovery through a counter-current flow mechanism. Furthermore, test results show that there is no benefit to operating the ICE at conditions exceeding MMP. Results from this chapter show that the use of in-situ generated CO_2 is a viable EOR option in liquid-rich shale.

In Chapter 4, we investigated the application of ICE in low-temperature oil reservoirs. The rate of spontaneous decomposition of aqueous solutions of urea to release CO_2 and ammonia at temperatures below 80 °C is not high enough for EOR applications. We used an enzyme, urease, to accelerate the hydrolysis of aqueous solutions of urea at low temperature conditions. In this proof-of-concept study we used highly purified commercially available urease and DI water was used as the aqueous phase for all the solutions used in the tests. Moreover, no buffers were used to stabilize the pH of the EOR formulations. The reaction kinetics of the catalyzed urea hydrolysis was studied at different urea concentrations, urease concentrations, and temperatures. The

results show that the hydrolysis reaction rate is not significantly dependent on the temperature for the studied time and temperature range (30 to 50 °C). The denaturation of urease occurred within 2000 mins and the denaturation time was dependent on the urea concentration but not the temperature. Sand pack flowthrough tests showed that low-temperature ICE yields higher oil recovery than the high temperature equivalents due to the higher solubility of CO_2 in oil at lower temperatures. Moreover, flowthrough tests conducted with aqueous ammonia solutions to isolate the contributions of CO_2 and NH3 related mechanisms showed that CO_2-related mechanisms contributed more towards tertiary oil recovery than the NH3-related mechanisms, at low-temperature conditions. Imbibition tests with oil-saturated sandstone and limestone core samples showed that the urease catalyzed ICE system changed the wettability of the cores from oil-wet to water-wet.

In Chapter 5, we investigated the use of crude urease extracts from jack bean, instead of highly purified commercial urease for ICE applications in low-temperature oil reservoirs. Using crude jack bean urease extracts makes urease-catalyzed ICE economically viable compared to using high-purity commercially available urease. Urease was successfully extracted from jack beans using a simple and cost-efficient method without any chemical additives. Batch tests showed that the crude urease extract was effective in generating CO_2 at the test temperatures with urea conversion rate of over 95 % at 50 °C. The hydrolysis rate and conversion ratio of urea was lower at 70 °C compared to 50 °C, due to the denaturation of urease at the higher temperature. Adsorption tests were also performed, demonstrating that urease was significantly adsorbed on limestone surfaces which resulted in an overall decrease in enzyme activity, whereas the adsorption of urease on sandstone was insignificant. Finally, flowthrough sand pack tests showed

that the extracted urease effectively catalyzed the hydrolysis of urea at reservoir temperatures of 50 °C and 70 °C and pressure of 1500 psi. The tertiary recovery for the limestone and sandstone tests were lower at 70 °C compared to 50 °C. This was attributed to the higher solubility of CO_2 in oil at lower temperature conditions. Additionally, the contribution of NH_3-related mechanism on the tertiary oil recovery is lower for the limestone case compared to sandstone. The observations of this work significantly expands the range of reservoir temperatures where ICE can be applied.

6.2 Recommendations For Future Research

The effectiveness of combining ICE with an anionic surfactant was demonstrated using crude oil saturated outcrop shale core samples. Further research should be conducted using field cores from the targeted oil-producing reservoir to improve the reliability of the experimental results. Moreover, additional huff-n-puff experiments should be conducted with shale cores that are confined under pressure within a core holder. The cores can be fractured longitudinally and EOR fluid introduced through one end to simulate flow through fractured shale rock.

The results of this research showed that urease catalyzed ICE could be applied to sandstone and limestone reservoirs at temperatures below 70 °C. Further research can explore the application of urease catalyzed ICE to shale and other tight reservoirs. This will require careful selection of surfactants that can be combined with ICE without denaturing the urease enzyme. Additionally, research can be conducted on the immobilization of urease enzyme on nanoparticles to improve their catalytic activity and increase their stability. Magnetic iron oxide nanoparticles will be good

candidates to investigate for this purpose since the enzyme-loaded nanoparticles can be recovered and reused [1].

References

[1] Valls-Chivas Á, Gómez J, Garcia-Peiro JI, Hornos F, Hueso JL. Enzyme–Iron Oxide Nanoassemblies: A Review of Immobilization and Biocatalytic Applications. Catalysts 2023;13:980. https://doi.org/10.3390/catal13060980.